

SUPPLEMENTARY MATERIALS TO THE CALIFORNIA CURRENT INTEGRATED ECOSYSTEM ASSESSMENT (CCIEA) CALIFORNIA CURRENT ECOSYSTEM STATUS REPORT, 2020

Appendix A LIST OF CONTRIBUTORS TO THIS REPORT, BY AFFILIATION

NWFSC, NOAA Fisheries

Mr. Kelly Andrews
Ms. Katie Barnas
Dr. Richard Brodeur
Dr. Brian Burke
Dr. Jason Cope
Dr. Correigh Greene
Dr. Thomas Good
Dr. Chris Harvey (co-lead editor)
Dr. Daniel Holland
Dr. Kym Jacobson
Dr. Stephanie Moore
Dr. Stuart Munsch
Dr. Karma Norman
Dr. Jameal Samhour
Dr. Nick Tolimieri (co-editor)
Ms. Margaret Williams
Dr. Jeannette Zamon

Pacific States Marine Fishery Commission

Ms. Amanda Phillips
Mr. Gregory Williams (co-editor)

Oregon State University

Ms. Jennifer Fisher
Ms. Cheryl Morgan
Ms. Samantha Zeman

AFSC, NOAA Fisheries

Dr. Stephen Kasperski
Dr. Sharon Melin

NOAA Fisheries West Coast Region

Mr. Dan Lawson

Farallon Institute

Dr. William Sydeman

Point Blue Conservation Science

Dr. Jaime Jahncke

University of Washington

Dr. Julia Parrish

Scripps Institute of Oceanography

Dr. Dan Rudnick

SWFSC, NOAA Fisheries

Dr. Eric Bjorkstedt
Dr. Steven Bograd
Ms. Lynn deWitt
Dr. John Field
Dr. Newell (Toby) Garfield (co-lead editor)
Dr. Elliott Hazen
Dr. Michael Jacox
Dr. Andrew Leising
Dr. Nate Mantua
Mr. Keith Sakuma
Dr. Jarrod Santora
Dr. Andrew Thompson
Dr. Brian Wells
Dr. Thomas Williams

University of California-Santa Cruz

Ms. Rebecca Miller
Dr. Barbara Muhling
Dr. Isaac Schroeder

Humboldt State University

Ms. Roxanne Robertson

California Department of Public Health

Ms. Christina Grant
Mr. Duy Trong
Ms. Vanessa Zubkousky-White

California Department of Fish and Wildlife

Ms. Christy Juhasz

CA Office of Env. Health Hazard Assessment

Dr. Rebecca Stanton

Oregon Department of Fish and Wildlife

Dr. Caren Braby
Mr. Matthew Hunter

Oregon Department of Agriculture

Mr. Alex Manderson

Washington Department of Health

Mr. Jerry Borchert
Ms. Audrey Coyne

Appendix B LIST OF FIGURE AND DATA SOURCES FOR THE MAIN REPORT

Figure 3.1.1: Oceanic Niño Index data are from the NOAA Climate Prediction Center (http://www.cpc.ncep.noaa.gov/products/analysis_monitoring/ensostuff/ONI_change.shtml). PDO data are from N. Mantua, NMFS/SWFSC, derived from the University of Washington Joint Institute for the Study of the Atmosphere and Ocean (JISAO; <http://research.jisao.washington.edu/pdo/>). North Pacific Gyre Oscillation data are from E. Di Lorenzo, Georgia Institute of Technology (<http://www.o3d.org/npgo/>).

Figure 3.1.2: Sea surface temperature maps are optimally interpolated remotely-sensed temperatures (Reynolds et al. 2007). The daily optimal interpolated AVHRR SST can be downloaded using ERDDAP (<http://upwell.pfeg.noaa.gov/erddap/griddap/ncdcOisst2Agg.html>).

Figure 3.1.3: Newport Hydrographic (NH) line temperature data from J. Fisher, NMFS/NWFSC, OSU. CalCOFI data from <https://calcofi.org>. CalCOFI data before 2019 are from the bottle data database, while 2019 data are preliminary from the recent conductivity, temperature, and depth (CTD) database.

Figure 3.2.1: Daily 2019 values of BEUTI and CUTI are provided by M. Jacox, NMFS/SWFSC; detailed information about these indices can be found at <https://mjacox.com/upwelling-indices/>.

Figure 3.3.1: Newport Hydrographic (NH) line dissolved oxygen data are from J. Fisher, NMFS/NWFSC, OSU. CalCOFI data from <https://calcofi.org>. CalCOFI data before 2019 are from the bottle data database, while 2019 data are preliminary from the recent CTD database.

Figure 3.4.1: Domoic acid concentrations in razor clams and Dungeness crab from Washington are compiled by the Washington State Department of Health from tests conducted by tribal, state, and county partners on Washington beaches. Oregon domoic acid data are compiled by Oregon Department of Fish and Wildlife (ODFW) from samples collected from sites across the Oregon coast by Oregon Department of Agriculture and ODFW staff. California data are compiled by the California Department of Public Health from samples collected by local, tribal, and state partners.

Figure 3.5.1: Snow-water equivalent data were derived from the California Department of Water Resources snow survey (<http://cdec.water.ca.gov/>) and the Natural Resources Conservation Service's SNOTEL sites in WA, OR, CA and ID (<http://www.wcc.nrcs.usda.gov/snow/>).

Figure 3.5.2: Minimum and maximum streamflow data were provided by the US Geological Survey (<http://waterdata.usgs.gov/nwis/sw>).

Figure 4.1.1: Copepod biomass anomaly data were provided by J. Fisher, NMFS/NWFSC, OSU.

Figure 4.1.2: Krill data were provided by E. Bjorkstedt, NMFS/SWFSC and Humboldt State University (HSU), and R. Robertson, Cooperative Institute for Marine Ecosystems and Climate (CIMEC) at HSU.

Figure 4.2.1: Pelagic forage data from the Northern CCE from B. Burke, NMFS/NWFSC and C. Morgan, OSU/CIMRS. Data are derived from surface trawls taken during the NWFSC Juvenile Salmon & Ocean Ecosystem Survey (JSOES; <https://www.nwfsc.noaa.gov/research/divisions/fe/estuarine/oeip/kb-juvenile-salmon-sampling.cfm>).

Figure 4.2.2: Pelagic forage data from the Central CCE were provided by J. Field and K. Sakuma, NMFS/SWFSC, from the SWFSC Rockfish Recruitment and Ecosystem Assessment Survey (<https://swfsc.noaa.gov/textblock.aspx?Division=FED&ParentMenuId=54&id=20615>).

Figure 4.2.3: Pelagic forage larvae data from the Southern CCE were provided by A. Thompson, NMFS/SWFSC, and derived from spring CalCOFI surveys (<https://calcofi.org/>).

Figure 4.3.1: Chinook salmon escapement data were derived from the California Department of Fish and Wildlife (<https://www.dfg.ca.gov/fish/Resources/Chinook/CValleyAssessment.asp>), PFMC pre-season reports (<https://www.pcouncil.org/salmon/stock-assessment-and-fishery-evaluation-safe-documents/review-of-2018-ocean-salmon-fisheries/>), and the NOAA NWFSC's "Salmon Population Summary" database (<https://www.webapps.nwfsc.noaa.gov/sps>), with data provided directly from the Nez Perce Tribe, the Yakama Nation Tribe, and from Streamnet's Coordinated Assessments database (cax.streamnet.org), with data provided by the Oregon Department of Fish and Wildlife, Washington Department of Fish and Wildlife, Idaho Department of Fish and Game, Confederated Tribes and Bands of the Colville Reservation, Shoshone-Bannock Tribes, Confederated Tribes of the Umatilla Indian Reservation, and U.S. Fish and Wildlife Service.

Figure 4.3.2: Data for at sea juvenile salmon provided by B. Burke, NMFS/NWFSC, with additional calculations by C. Morgan, OSU/CIMRS. Derived from surface trawls taken during the NWFSC Juvenile Salmon and Ocean Ecosystem Survey (JSOES) cruises.

Figure 4.4.1: Groundfish stock status data provided by J. Cope, NMFS/NWFSC, derived from NOAA Fisheries stock assessments.

Figure 4.6.1: California sea lion data provided by S. Melin, NMFS/AFSC.

Figure 4.6.2: Whale entanglement data provided by D. Lawson, NMFS/WCR.

Figure 4.7.1: Seabird fledgling production data at nesting colonies on Southeast Farallon provided by J. Jahncke, Point Blue Conservation Science.

Figure 5.1.1: Data for commercial landings are from PacFIN (<http://pacfin.psmfc.org>). Data for recreational landings are from RecFIN (<http://www.recfin.org/>).

Figure 5.2.1: Data for total distance trawled by federally managed bottom-trawl fisheries were provided by J. McVeigh, NMFS/NWFSC, West Coast Groundfish Observer Program. Figures created by K. Andrews, NMFS/NWFSC.

Figure 6.1.1: Community social vulnerability index (CSVI) and commercial fishery reliance data provided by K. Norman, NMFS/NWFSC, and A. Phillips, PSMFC, with data derived from the US Census Bureau's American Community Survey (ACS; <https://www.census.gov/programs-surveys/acs/>) and PacFIN (<http://pacfin.psmfc.org>), respectively.

Figure 6.2.1: Fishery diversification estimates were provided by D. Holland, NMFS/NWFSC, and S. Kasperski, NMFS/AFSC.

Figure 6.3.1: Commercial revenue data compiled by A. Phillips and K. Norman, NMFS/NWFSC, and derived from PacFIN (<http://pacfin.psmfc.org>).

Figure 7.2.1.: Standardized SSTa plots were created by A. Leising, NMFS/SWFSC, using SST data from NOAA's Optimum interpolation Sea Surface Temperature analysis (OISST; <https://www.ncdc.noaa.gov/oisst>), with the SST anomaly calculated using climatology from NOAA's AVHRR-only OISST dataset.

Figure 7.2.2.: Compression index estimates developed and provided by J. Santora, NMFS/SWFSC and I. Schroeder, NMFS/SWFSC, UCSC.

Table 4.3.1: Stoplight table of indicators and projected 2019 salmon returns courtesy of B. Burke and K. Jacobson, NMFS/NWFSC; J. Fisher, C. Morgan, and S. Zeman, OSU/CIMRS.

Table 4.3.2: Table of indicators and qualitative outlook for 2020 Chinook salmon returns to the Central Valley courtesy of N. Mantua, NMFS/SWFSC.

Appendix C CHANGES IN THIS YEAR'S REPORT

Below we summarize major changes and improvements in the 2020 Ecosystem Status Report, in response to the requests and suggestions received from the Council and advisory bodies under FEP Initiative 2, "Coordinated Ecosystem Indicator Review" (March 2015, Agenda Item E.2.b). We also note other new items we have added and information gaps that we have filled since last year's report.

Request/Need	Response/Location in document
Description of marine heatwave and habitat compression along the West Coast, in relation to other basin-scale climate indicators, upwelling, and habitat suitability for key species	Because marine heatwaves have been a recurring feature in the California Current from 2014-2016, 2018, and 2019, we dedicated space in the main body (Section 7.2) and the Supplement (Appendix D.2). These sections feature both analyses of marine heatwave physical characteristics (reviewed previously by the SSC), and of compression of cool-water, upwelled habitat along the coast (Figure 7.2.2).
In 2019, we included harmful algal bloom (HAB) data in the report for the first time, but data were limited to Washington razor clams. Several Council bodies requested coastwide HAB indicator data.	In this year's report, we include domoic acid levels in razor clams and Dungeness crabs from multiple sites in Washington, Oregon and California, as well as spiny lobster and rock crab in southern California. Plots and text are in the main body (Section 3.4) and Supplement (Appendix E).
In 2018, the Ecosystem Advisory Subpanel requested that the IEA team develop indicators of community-level fishery participation and economic status, as related to National Standard 8 (NS-8) under the Magnuson-Stevens Act.	This year we introduce indicators of the proportion of commercial fishing revenue brought in by the top 16 ports in terms of total revenue and FMP-specific revenue. Total revenue is presented in the main body (Section 6.3) and FMP-specific revenue is in the Supplement (Appendix O).
Several Council bodies have requested "stoplight" tables of indicators related to returns of salmon from central California, similar to the table for salmon returns to the Columbia River and Oregon coast.	This year we introduce a fairly simple indicator summary table that relates ecosystem indicators to Central Valley fall Chinook salmon returns. The table is in the main body (Section 4.3).
In 2019, the Coastal Pelagic Species Advisory Subpanel requested that dissolved oxygen and ocean acidification data broadly reflect conditions from different regions of the West Coast	<p>In the main body, Figure 3.3.1, we now include dissolved oxygen time series from both Newport, Oregon and CalCOFI line 93 in Southern California, with additional time series from both sites and broader dissolved oxygen maps in the Supplement (Appendix D.3). We are unaware of time series of dissolved oxygen transects in the region from Cape Mendocino to Point Conception.</p> <p>In this year's report, we put all ocean acidification information in Appendix D.3, for space considerations and lack of clear mechanistic links to broad ecosystem impacts at this time. All data are from off Newport, Oregon; we are unaware of other time series of aragonite saturation state along the coast.</p>

Request/Need	Response/Location in document
<p>In 2019, the Ecosystem Workgroup requested additional indicators of krill from the northern portion of the system</p>	<p>In the Supplement (Appendix G.1), we add maps of krill densities from spring surveys over most of the past decade, off the coast of Oregon and Washington. We will work to identify additional time series from this portion of the coast.</p>
<p>In 2019, the Habitat Committee recommended that the Gear Contact with Seafloor indicator be reviewed by the SSC-ES, to ensure the analytical methods were supported and that the indicator would be suitable for capturing changes in bottom trawling activity related to Groundfish FMP Amendment 28.</p>	<p>The SSC-ES reviewed this analysis in September 2019, and the plots shown in the main body (Section 5.2) (Appendix L) incorporate recommendations from that review. Specifically: in Figure 5.2.1, we replaced the 5-year mean panel with a panel showing the raw, annual data, which shows the magnitude of bottom contact occurring most recently, while retaining an indicator of the historical status (anomaly panel) and trend (5-yr trend). The new raw, annual data panel should provide a rapid assessment of changes in bottom trawl gear contact in the newly opened and closed areas associated with Amendment 28.</p> <p>The SSC-ES suggested that we incorporate VMS data into this indicator in order to capture the path of the trawling vessel in between the set and haul-back coordinates more accurately. We have not incorporated this yet as we are waiting for the development of a "Best Practices Methodology" for processing, standardizing, matching to fish ticket data and increased accessibility that is being funded by the Fisheries Information System Program and carried out by researchers across the U.S. West Coast in 2020.</p>
<p>In March 2019, the SSC stated, "For the first time there are numerical forecasts of salmon returns included in the Status Report...These forecasts are not comparable to the forecasts used by the Salmon Technical Team (STT) for salmon management. The SSC will work with the CCIEA team to review these forecasts and determine how best to communicate this information in future CCIEA reports."</p>	<p>In September 2019, the SSC-ES reviewed the approaches used in the figures in question in a pre-Council advisory body meeting with IEA scientists. The general approach was acceptable but the SSC-ES made some recommendations, including that the term "forecasts" not be used to avoid confusion; we have taken this guidance where these figures and text are presented in this year's Supplement (Appendix H.3).</p> <p>The SSC-ES recommended that we expand the approach to stocks over which the Council has greater management responsibility. This recommendation will require additional research and staff time that we currently do not have, but will look to address in future years.</p> <p>Finally, unlike last year the projections in Figure H.3.2 this year do not include a coho projection, due to poor model performance and lack of staff time.</p>

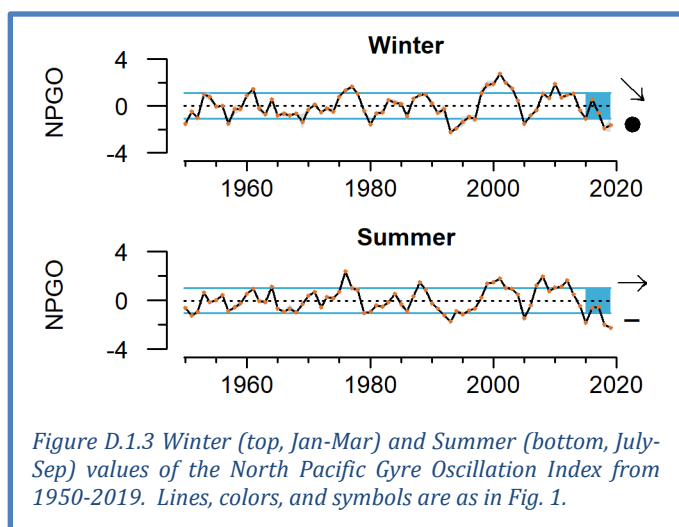
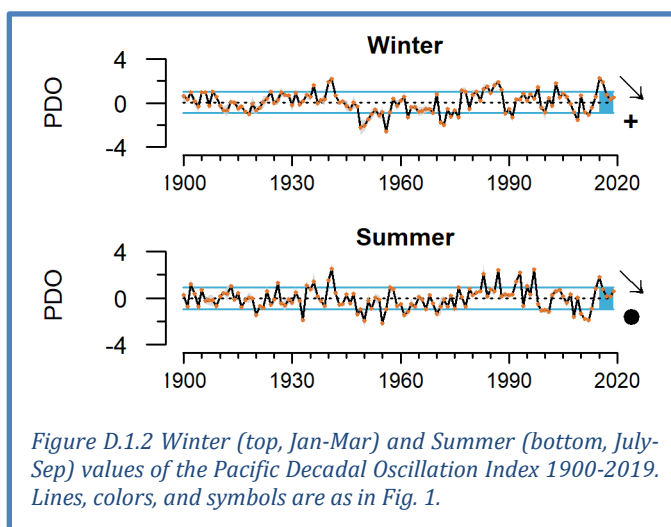
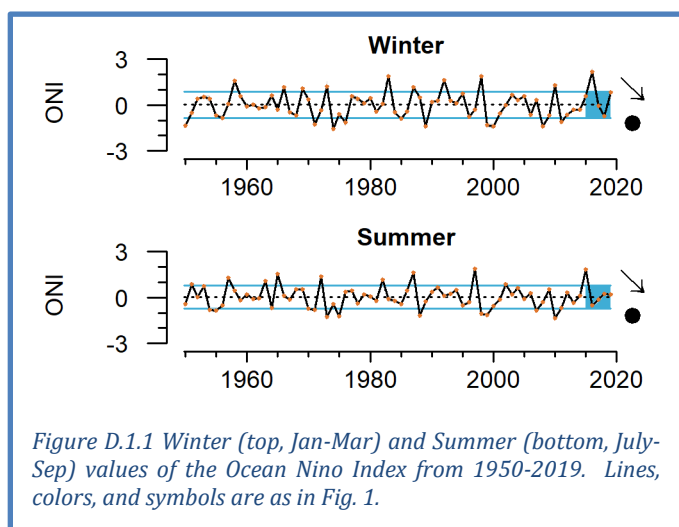
Request/Need	Response/Location in document
Including recreational fishing reliance and engagement in Human Wellbeing section	At the request of various advisory bodies, last year we introduced community-level estimates of recreational fishing reliance and engagement into the Human Wellbeing section (Section 7 of the main document and Appendix M of the Supplement). Those data have not been updated since last year's report and the most recent data go back to 2016; thus, we have not repeated them in this year's report, for space considerations.
At the 2019 March Council meeting, we received feedback that the seabird indicators in the main body of the report (i.e., indicators of at-sea density of birds) were not particularly relevant to foraging conditions in the different regions.	In this year's report, we put indicators of seabird colony production (species-specific fledgling production) in the main report (Section 4.7). Productivity measures like these connect more closely to other indicators of regional forage availability. At-sea densities of seabirds and other seabird indicators are in the Supplement, Appendix J.

Appendix D CLIMATE AND OCEAN INDICATORS

Section 3 of the Main Body describes indicators of basin-scale and region-scale climate and ocean drivers. Here we present additional plots to allow a more complete picture of these indicators.

D.1 BASIN-SCALE CLIMATE/OCEAN INDICATORS AT SEASONAL TIME SCALES

These plots show seasonal averages, short-term trends, and short-term averages of the three basin-scale climate forcing indicators shown in the main report in Figure 3.1.1. Notable outcomes include: both winter and summer Ocean Niño Index (ONI) have declining trends, illustrating the strength of the 2016 El Niño (and the relative weakness of the 2019 El Niño, shown in Figure D.1.1, top); summer and winter PDO have negative trends since 2015 (Figure D.1.2), illustrating the strength of the 2013-2016 marine heatwave (the “Blob”); winter PDO has been above average over the past 5 years (Figure D.1.2, top), illustrating that the system continues to be warmer than normal in the aftermath of the Blob; winter NPGO has a decreasing 5-year trend (Figure D.1.3, top); and summer NPGO has been below average over the past 5 years, and has the lowest values in the time series (Figure D.1.3, bottom).

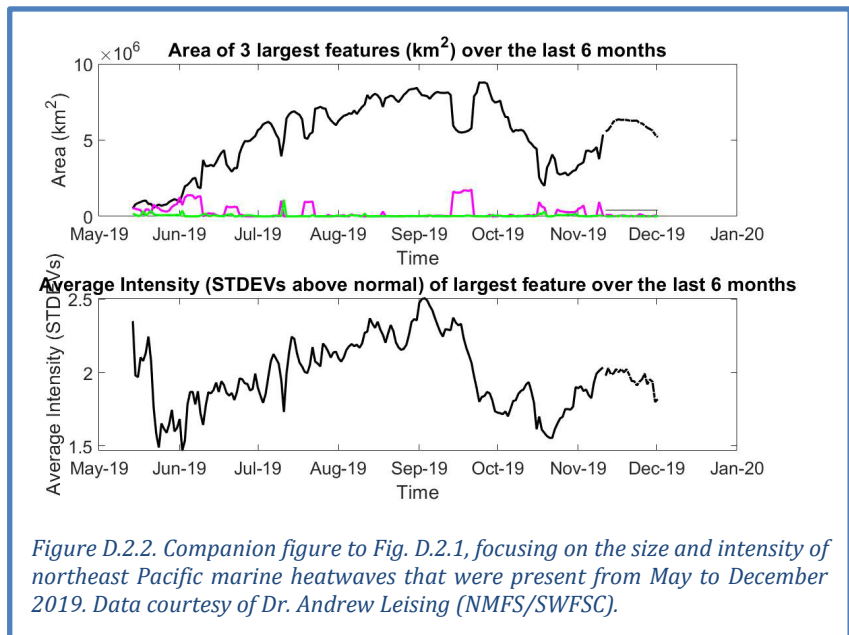
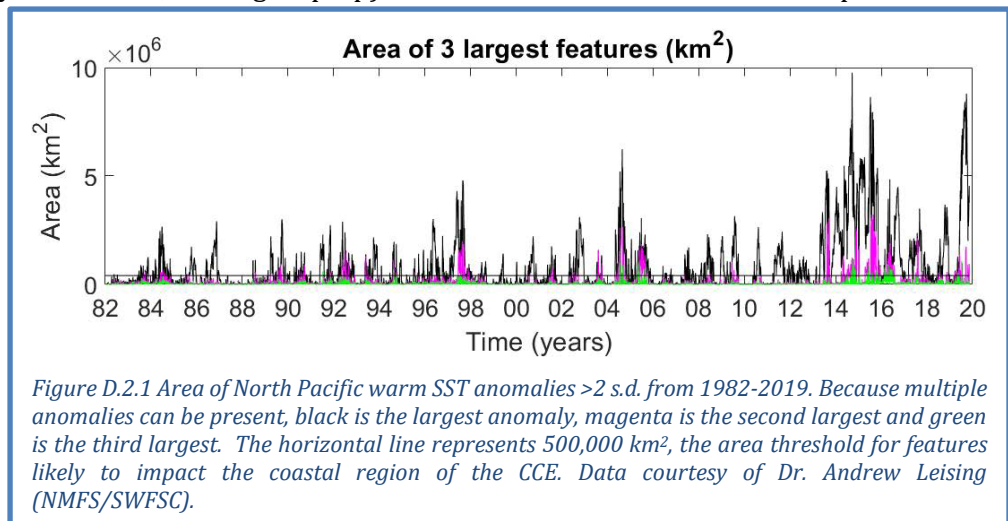


D.2 ASSESSING THE 2019 MARINE HEATWAVE

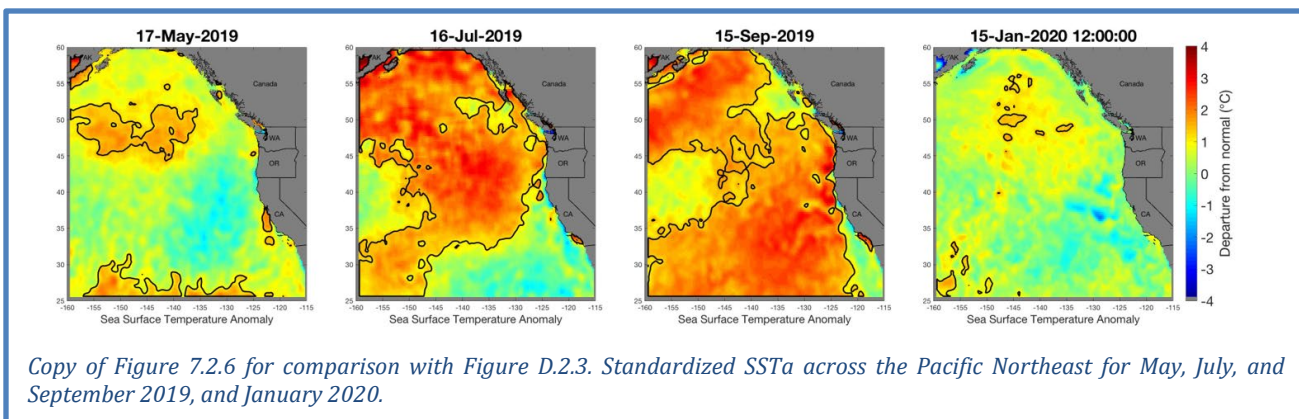
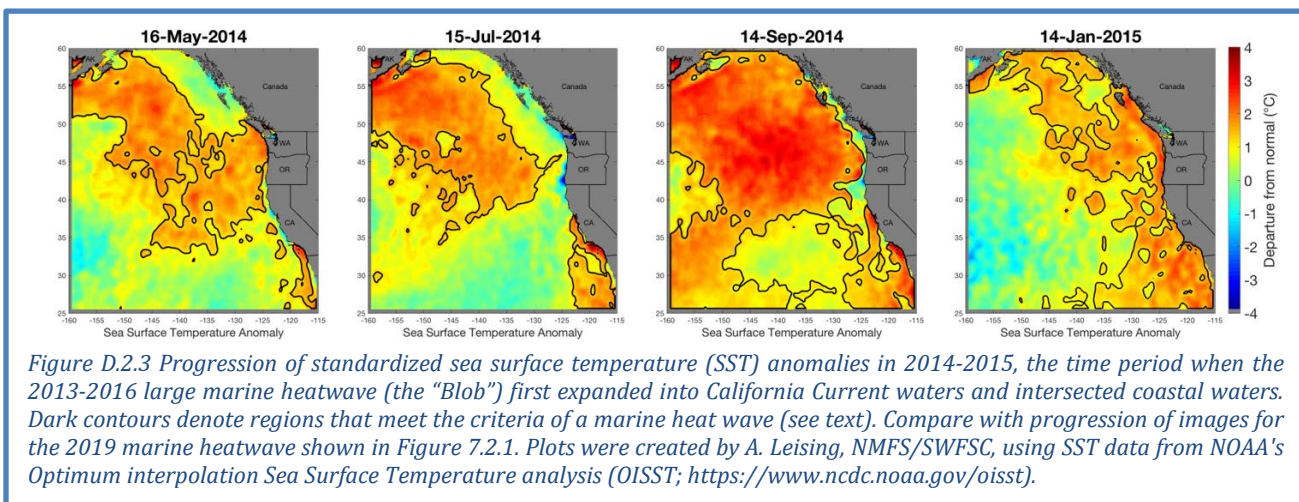
There is increased recognition that marine heatwaves can have immediate short-term impacts on the ecosystem, as well as an indication of stock displacements that may occur with long-term climate warming. For these reasons, monitoring marine heatwaves and developing robust indices of these features are important for management. As noted in Section 3.1 and Section 7.2 of the main body of the report, a large marine heatwave emerged in the northeast Pacific Ocean in the second half of 2019, similar in size and intensity to the 2013–2016 northeast Pacific marine heatwave known as the “Blob.” Here we describe additional analysis related to this event and compare its progression to that of the Blob.

Based on an analysis of sea surface temperature anomalies (SSTa) from 1982–2019, a marine heatwave has the potential to cause impacts in the CCE that are comparable to those from the 2013–2016 event if the anomalous feature: 1) has statistically normalized SSTa >1.29 s.d. (90th percentile) of the long-term SSTa time series at a location; 2) is $\geq 3.5 \times 10^6$ km² in area; 3) lasts for >5 days; and 4) comes within 500 km of the coast (Hobday et al. 2016; Leising in prep). Events in both 2018 and 2019 surpassed these thresholds (Figure D.2.1, Figure D.2.2). In the case of the 2019 event, because it only encroached on coastal waters from July to September, it is too early to determine the impacts of the event on the CCE.

The 2019 heatwave was preceded by a fairly large heatwave during the fall of 2018, which also began during the middle of the year and continued until early December. However, there was no surface expression of a marine heatwave from December 2018 until early May 2019. In May 2019, the new marine heatwave rapidly developed, reaching a peak by August (Figure D.2.2). Its peak conditions rivaled the 2014 event in terms of size and intensity (Figure D.2.1). It is unclear if the 2018 event should be considered a precursor or separate event from the 2019 event, although an ongoing analysis of subsurface temperature anomalies may determine if there was a linkage.



The 2019 heatwave had some similarities, but also some important differences from the 2013-2016 “Blob” event. The Blob began in the far offshore region during mid 2013, grew and moved closer to the coast, showed a slight recession during the winter of 2013-2014, but then steadily gained strength throughout 2014, with a peak intensity that year during September (Figure D.2.3). The anomalous warming persisted into the winter of 2014-2015 (Figure D.2.3, right). The 2019 event (Figure 7.2.1) evolved much more rapidly to its maximum size than the Blob during the similar time period in 2014. By mid October 2019, the recent heatwave showed signs of recession, decreasing in size and intensity, such that by early January 2020, it no longer met the marine heatwave criteria outlined above (Figure 7.2.1). Thus, unlike the Blob, both the 2018 and 2019 events have failed to persist into winter. However, a significant pool of warmer than normal water remained in the far offshore region. Since a similar buildup and then recession occurred during 2013-2014, and we continue to observe anomalously warm water far offshore and retention of heat by deeper waters, it is unclear if we may see a resurgence of another heatwave in the summer of 2020.



The above plots and analyses focus on sea surface temperatures. Subsurface temperature data from autonomous glider transects provide additional information. The northeast Pacific Ocean has remained anomalously warm since the 2014 marine heatwave and 2015 El Niño (Figure D.2.4). Time series of glider data from CalCOFI line 90 (off Dana Point in the Southern California Bight) at 10-m and 50-m depths from the shore to a distance 500 km offshore illustrate the dramatic subsurface temperature change that occurred in 2014 and continues through the end of 2019.

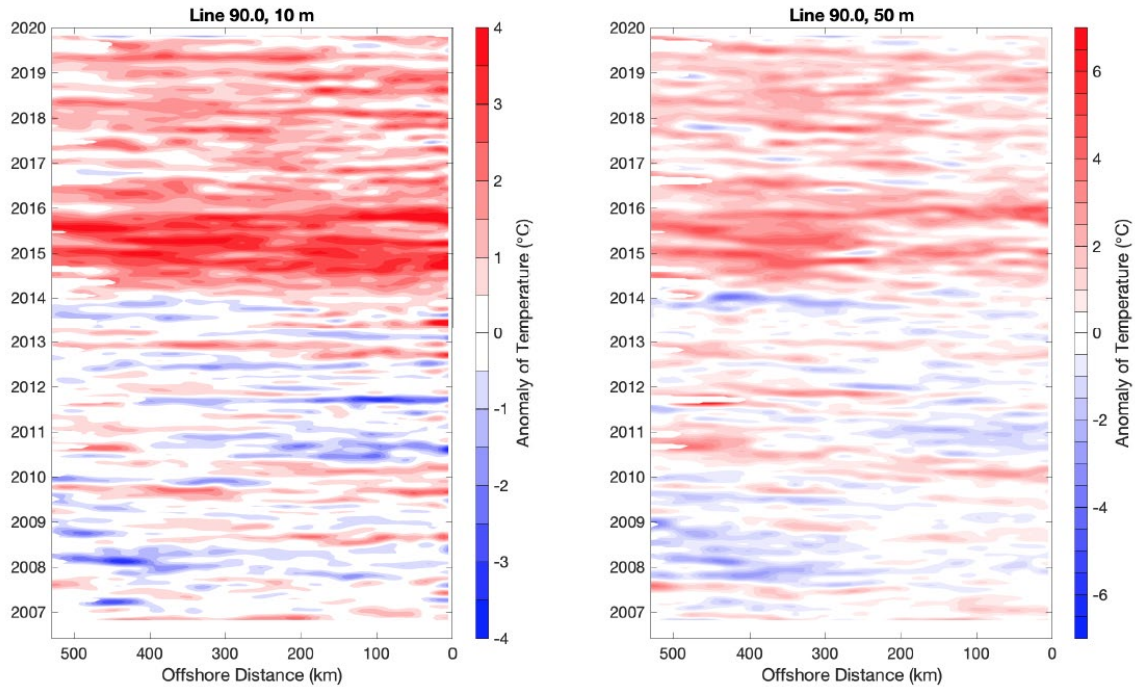


Figure D.2.6 Temperature anomalies at depths of 10 m (left) and 50 m (right) along CalCOFI line 90, extending from the coast to 500 km offshore, 2007-2019. Conditions from 2007 to 2014 oscillated about the mean while from 2014 to the end of 2019, positive temperature anomalies have been consistent. The large anomaly starting in 2014 is the marine heatwave of 2014-2016. Conditions have remained warmer than average ever since. Data from the California Underwater Glider Network are provided by Dr. Dan Rudnick, Scripps Institute of Oceanography Instrument Development Group (doi: 10.21238/S8SPRAY1618).

Note that prior to 2014 the CalCOFI subsurface temperature indices at both 10-m and 50-m depths tracked closely with the ONI index (Figure D.2.5), consistent with the finding that the El Niño Southern Oscillation was the major source of variability in the CCLME for the majority of this time series (Jacox et

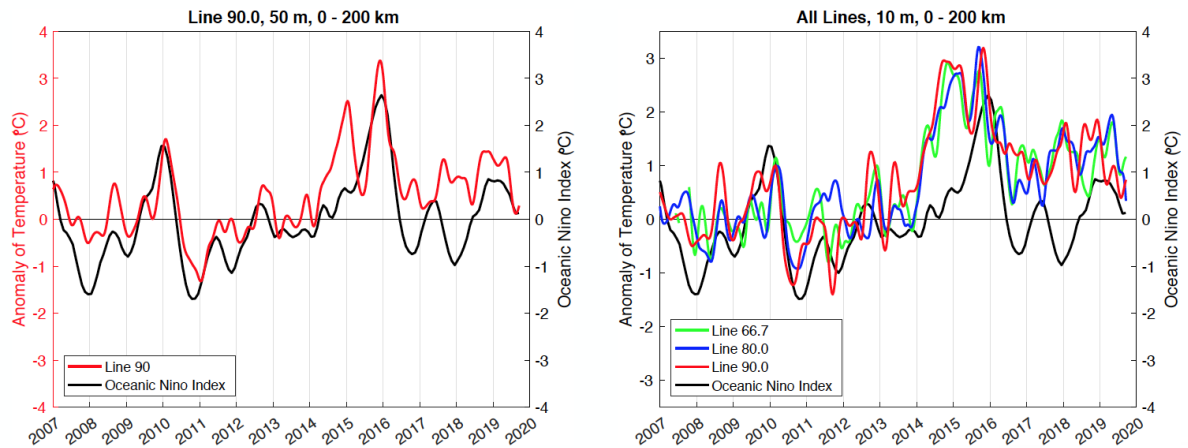
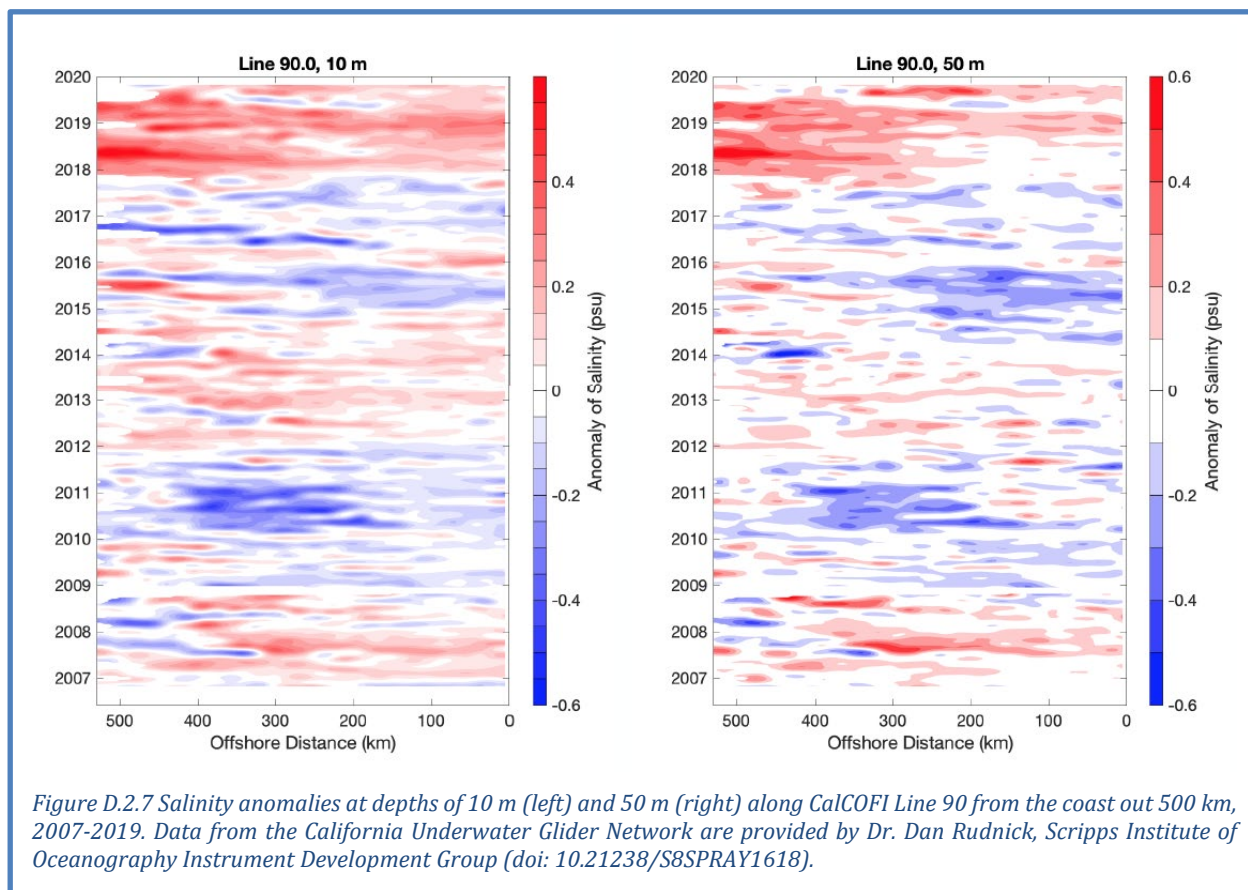


Figure D.2.5 CalCOFI temperature indices for CalCOFI lines 66.7, 80, and 90 (Figure 2.1) compared to the ONI index. The CalCOFI temperature indices are the temperature at the indicated depth averaged from the shore to 500 km offshore. ONI data are from the NOAA Climate Prediction Center. Data from the California Underwater Glider Network are provided by Dr. Dan Rudnick, Scripps Institute of Oceanography Instrument Development Group (doi: 10.21238/S8SPRAY1618).

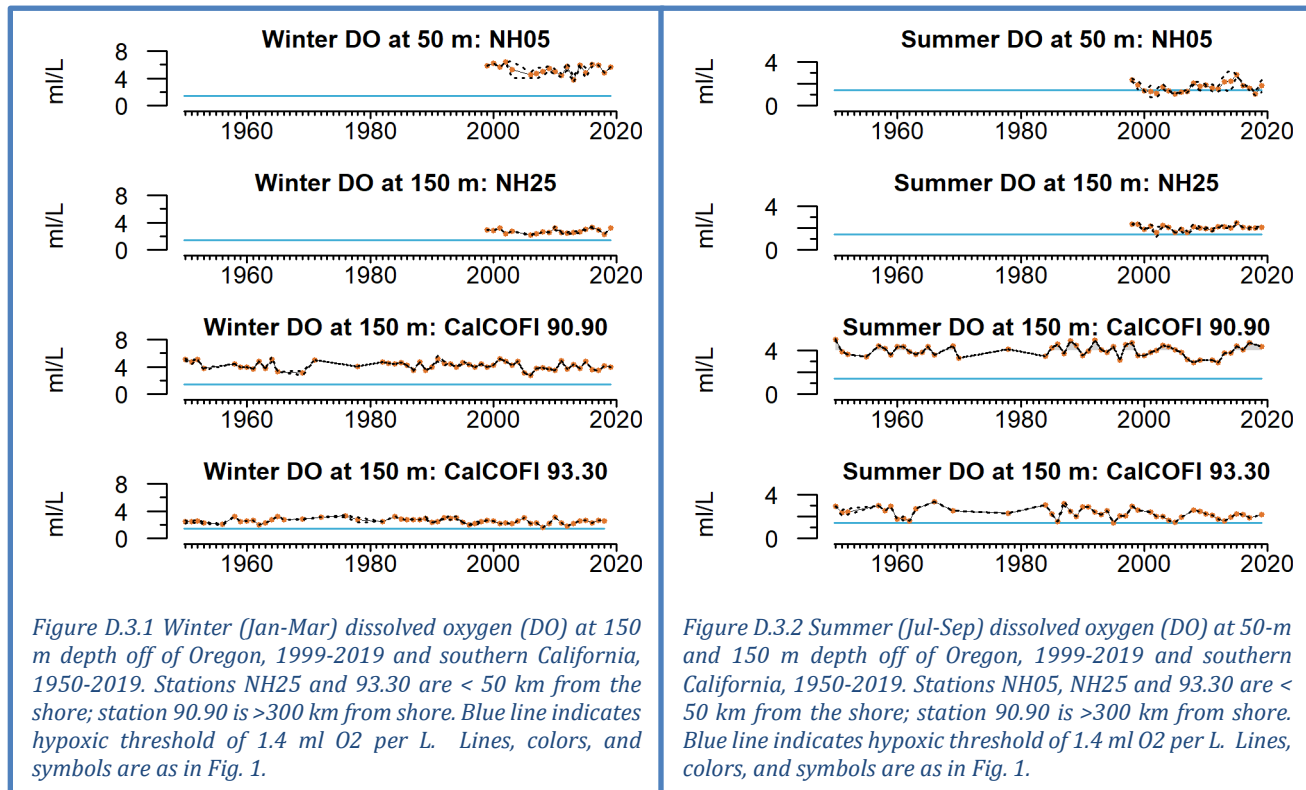
al. 2016). In 2014, the CalCOFI temperature indices on three separate glider lines (Line 67 off Monterey Bay; Line 80 off Point Conception; Line 90 off Dana Point) show the temperature increase began prior to the major 2015-2016 El Niño, but did not return to normal following the end of the El Niño in 2016. The glider trends increase with the mild 2018-2019 El Niño, but still remain anomalously high. These data agree with the anomaly contours of CalCOFI 93.3 in Figure 3.1.3, demonstrating that southern and central California remain warm due to the marine heatwave, and experienced some additional influence from the recent El Niño events.

Data from the glider surveys suggest further changes in the water column, in particular changes in subsurface salinity. A major salinity anomaly can be seen along CalCOFI Line 90 at 10-m and 50-m depths starting in 2018 (Figure D.2.6). These represent some of the largest and most extensive positive anomalies of the available time series. The anomalies suggest that the Southern California Bight temperatures since 2018 may be due to the influx of a warmer, saltier water into the region.

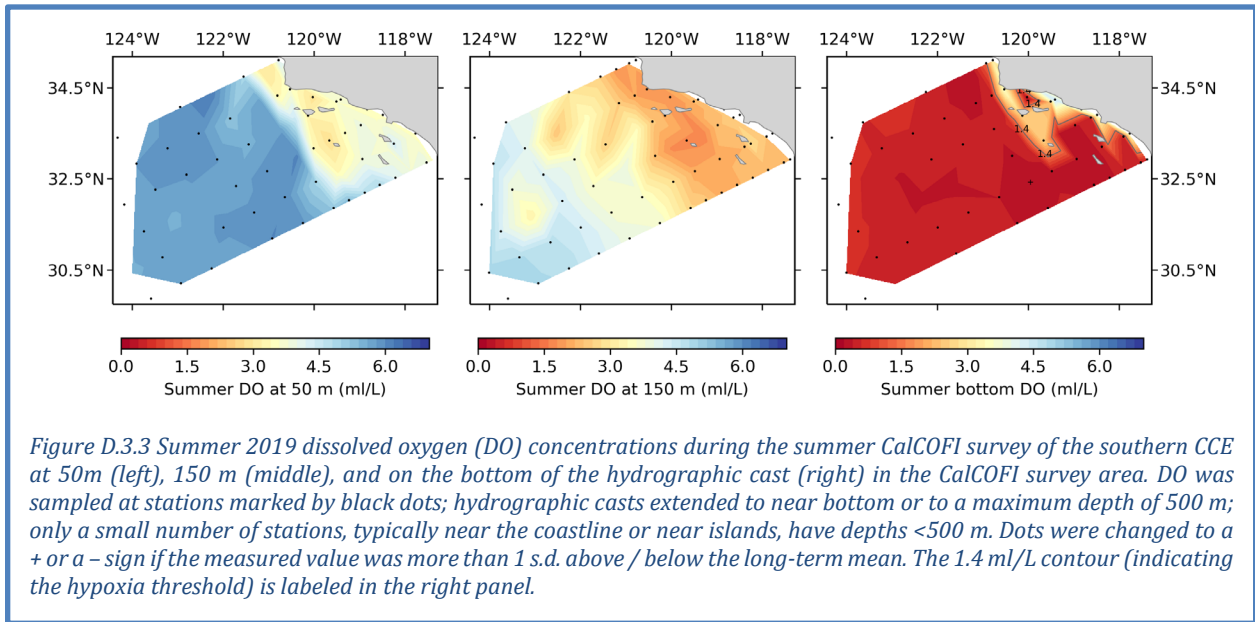


D.3 SEASONAL AND SPATIAL DISSOLVED OXYGEN AND OCEAN ACIDIFICATION INDICATORS

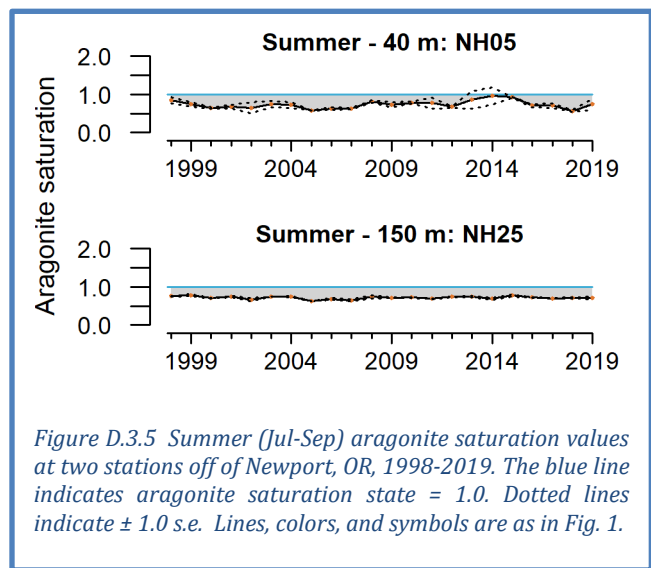
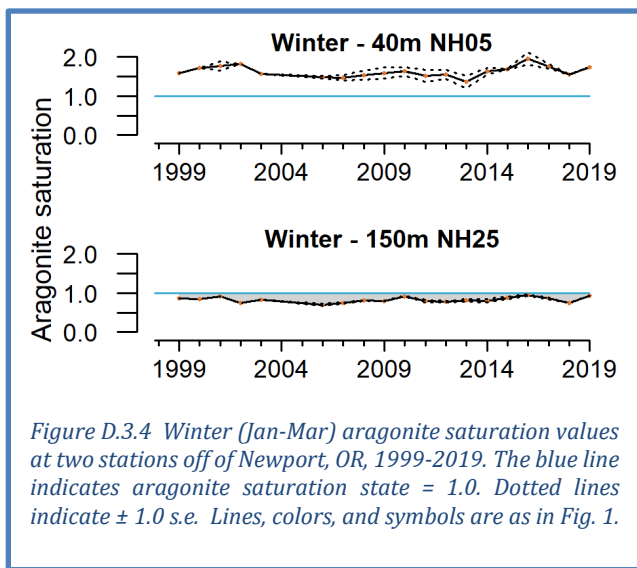
The first series of plots in this section shows summer and winter averages for dissolved oxygen (DO) data off Newport, OR (stations NH05 and NH25, 5 and 25 nautical miles off the coast respectively) and in the Southern California Bight (stations CalCOFI 90.90 and CalCOFI 93.30). In 2019, winter DO concentrations were consistently above the hypoxia threshold (1.4 ml O₂ per L water) at each of the stations, as is typical for the entirety of the winter time series (Figure D.3.1). Summer DO concentrations in 2019 were also above the hypoxia threshold at each station (Figure D.3.2); notable is that DO concentrations in summer 2019 were improved over summer 2018 at station NH05.



The next figure (Figure D.3.3) shows interpolated estimates of DO at different depths from the summer 2019 CalCOFI survey of the Southern California Bight. Summer DO values displayed strong inshore-offshore and depth gradients, with higher values measured farther offshore and lower values measured at depth. The southern CCE DO levels in the upper 150 m measured during the summer 2019 CalCOFI survey had levels above the hypoxic threshold (Figure D.3.3, left and middle). The DO measured during the summer cruise was average, with all stations having DO values near the long-term mean. DO values at 500 m depths were well below the 1.4 ml/L hypoxic threshold, although this is typical. In the area around the Channel Islands and for stations adjacent to shore, DO values near the seafloor were above the hypoxic threshold (Figure D.3.3, right). (We will also hope to have figures of on-bottom DO from the 2019 NMFS groundfish bottom trawl survey by the time of the March PFMC meeting.)



The final set of plots shows aragonite saturation state (an ocean acidification indicator) off Newport, Oregon. First are time series of seasonal aragonite saturation from near bottom at stations NH05 and NH25. Winter saturation state was consistently above the threshold of 1.0 at station NH05, but indicated generally corrosive conditions at station NH25 for most of the time series, including 2019 (Figure D.3.4). Summer aragonite saturation states indicated corrosive waters near bottom at both stations for most of the time series, including 2019 (Figure D.3.5). Saturation horizon depth profiles at NH05 and NH25 are shown in Figure D.3.6. They show that more of the water column was saturated (i.e., aragonite saturation state ≥ 1.0) in 2019 than in 2018, but overall was consistent with long-term expectations.



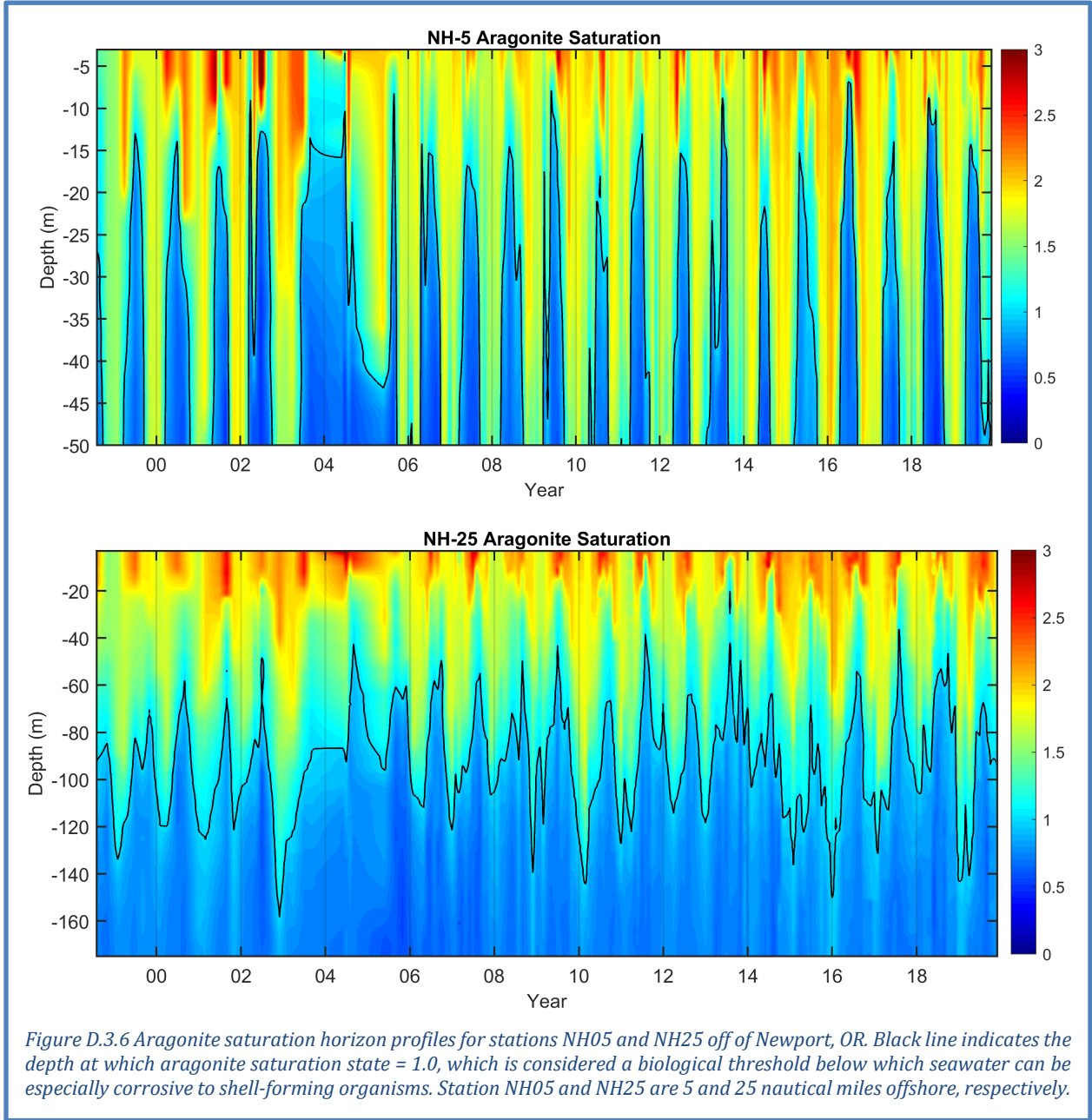


Figure D.3.6 Aragonite saturation horizon profiles for stations NH05 and NH25 off of Newport, OR. Black line indicates the depth at which aragonite saturation state = 1.0, which is considered a biological threshold below which seawater can be especially corrosive to shell-forming organisms. Station NH05 and NH25 are 5 and 25 nautical miles offshore, respectively.

Appendix E DOMOIC ACID ON THE WEST COAST

Harmful algal blooms (HABs) of diatoms in the genus *Pseudo-nitzschia* have been of particular concern along the West Coast in recent years. Certain species of *Pseudo-nitzschia* produce the toxin domoic acid that can accumulate in filter feeders and extend through food webs to cause harmful or lethal effects on people, marine mammals, and seabirds (Lefebvre et al. 2002, McCabe et al. 2016). To protect human health, fisheries that target shellfish (including razor clam, Dungeness crab, rock crab, and spiny lobster) are closed or operate under a health advisory in the recreational sector when concentrations of domoic acid exceed regulatory thresholds for human consumption. Domoic acid levels at or exceeding the Federal Drug Administration (FDA) action level of 20 parts per million (ppm) trigger closures of razor clam harvests. The FDA action level for domoic acid in Dungeness crab is >30 ppm for the viscera and >20 ppm for the meat tissue. In Oregon, Dungeness crab can be landed when the viscera exceeds the FDA alert level but the meat tissue does not if the crab are eviscerated by a licensed processor. In southern California, rock crab and spiny lobster are monitored for domoic acid.

Fishery closures can cause tens of millions of dollars in lost revenue and a range of sociocultural impacts in fishing communities (Dyson and Huppert 2010, NMFS 2016, Ritzman et al. 2018), and can also cause “spillover” of fishing effort into other fisheries. Extremely toxic HABs of *Pseudo-nitzschia* are influenced by ocean conditions and have been documented in 1991, 1998-99, 2002-03, 2005-06, and 2015-19. In the northern CCE, they have been found to coincide with or closely follow El Niño events or positive PDO regimes and track regional anomalies in southern copepod species (McCabe et al. 2016, McKibben et al. 2017). The largest and most toxic HAB of *Pseudo-nitzschia* ever recorded on the West Coast coincided with the 2014-16 Northeast Pacific marine heatwave and caused extensive closures and delays in the opening of crab fisheries, resulting in the appropriation of over \$25M in federal disaster relief funds (McCabe et al. 2016).

In 2019, low levels of domoic acid detected in Washington razor clams and Dungeness crab did not trigger any fisheries closures (Figure E.1).

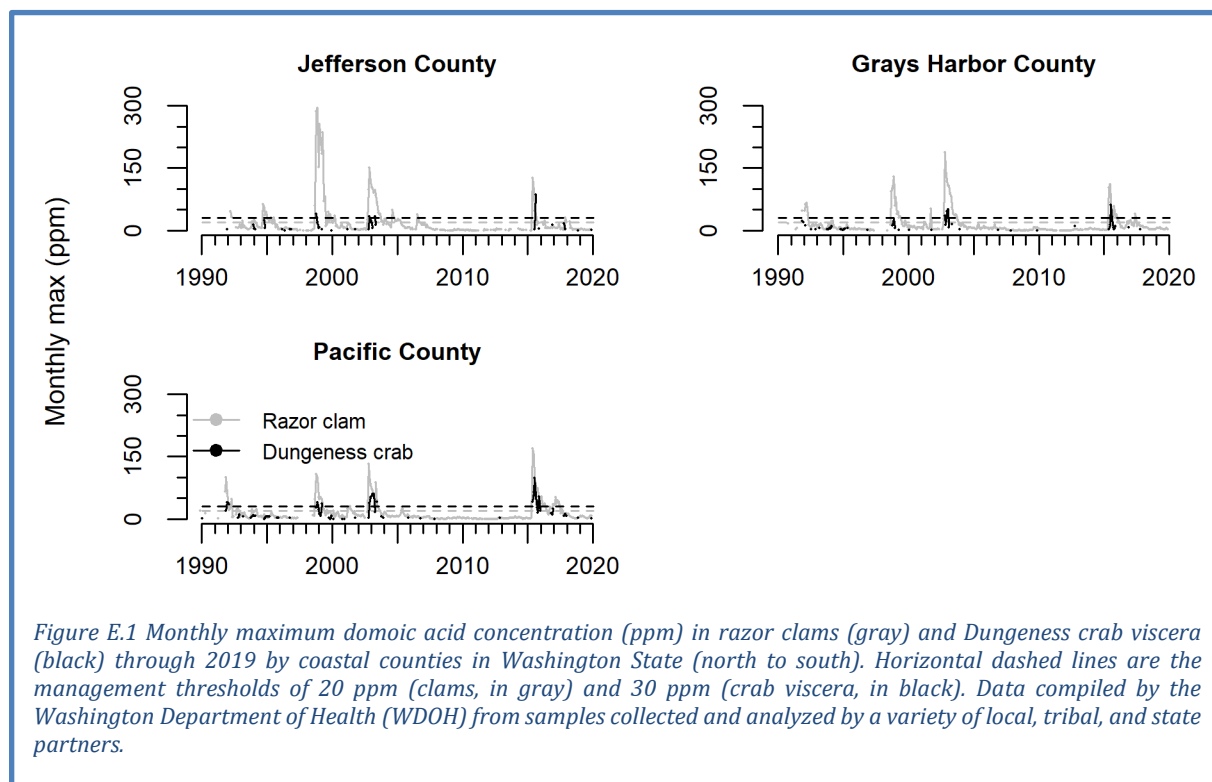
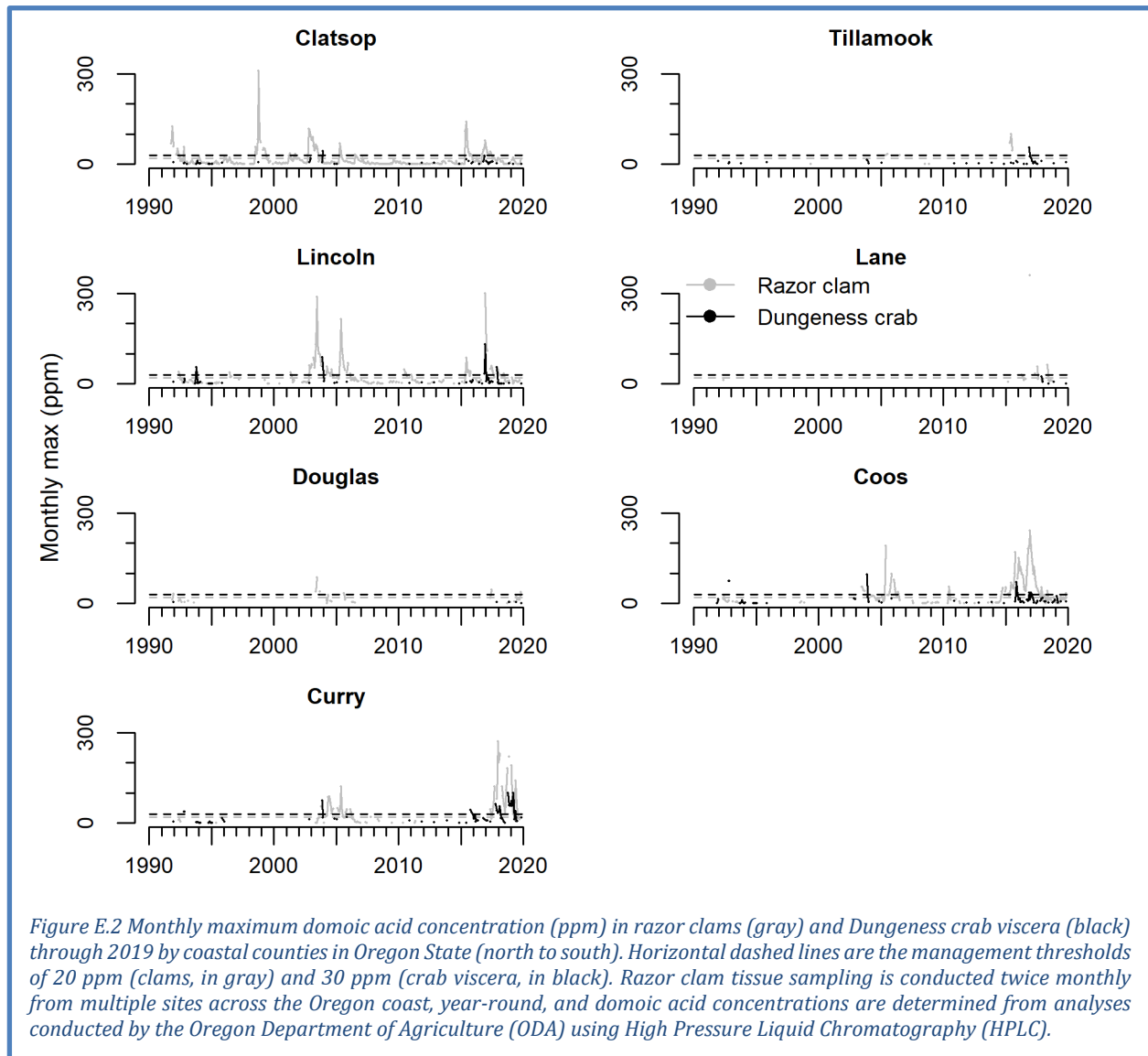


Figure E.1 Monthly maximum domoic acid concentration (ppm) in razor clams (gray) and Dungeness crab viscera (black) through 2019 by coastal counties in Washington State (north to south). Horizontal dashed lines are the management thresholds of 20 ppm (clams, in gray) and 30 ppm (crab viscera, in black). Data compiled by the Washington Department of Health (WDOH) from samples collected and analyzed by a variety of local, tribal, and state partners.

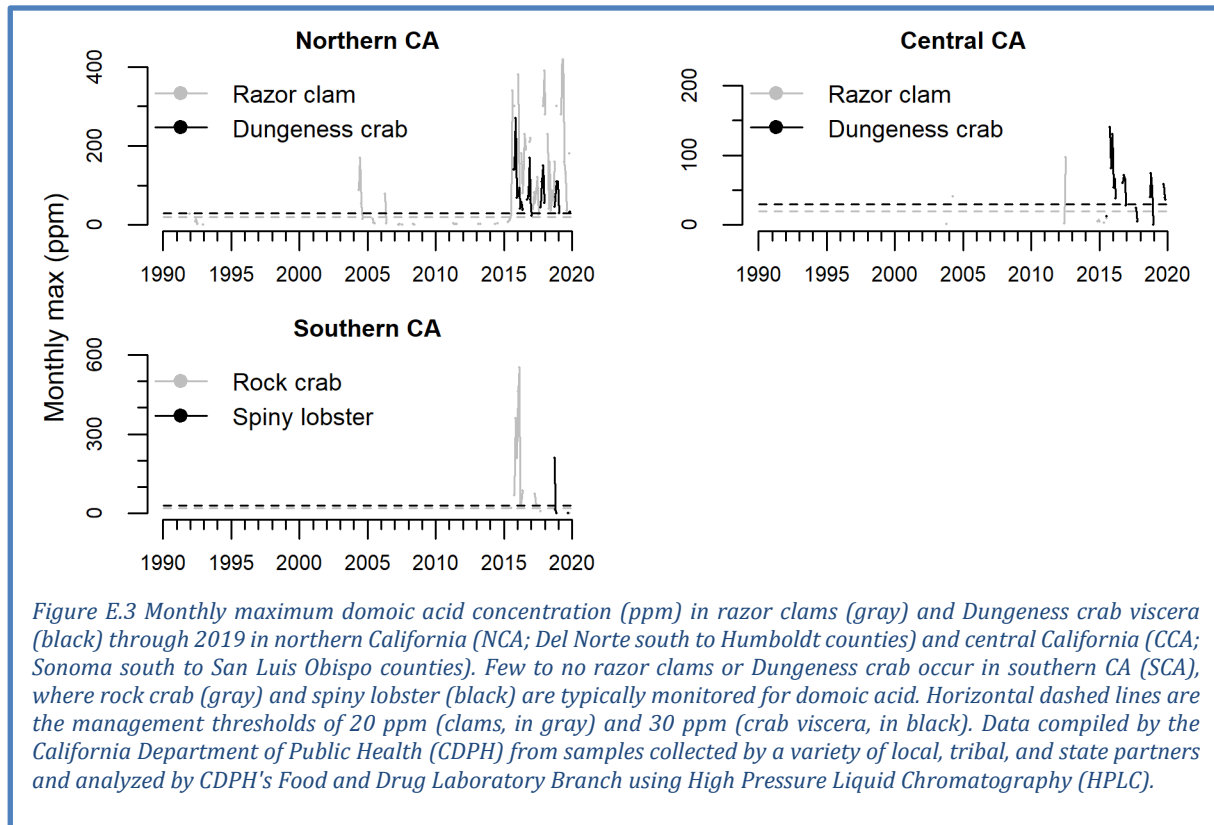
An extended closure of the razor clam fishery due to domoic acid in southern Oregon began in August 2014, but was lifted in September 2019. It was then reinstated in October 2019 (Figure E.2). On December 13, 2019 the entire Oregon coast was closed for razor clams due to domoic acid. A delay in the opening of the 2018-2019 Oregon commercial Dungeness crab fishery due to low meat quality extended into 2019; the fishery opened on January 4, 2019 but was delayed in southern Oregon (Cape Arago to the California border) until January 31, 2019 due to a combination of low meat quality and domoic acid.



In northern California, the razor clam fishery remained closed throughout 2019, extending a closure that began in 2016. Northern California also experienced a delay in the opening of the 2018-2019 commercial Dungeness crab fishery due to low meat quality. Even after the crab filled out, the delay extended until January 25, 2019 for Del Norte and northern Humboldt counties due to domoic acid. Across California, the 2018-2019 commercial Dungeness crab season was closed early on April 15, 2019 to avoid marine life entanglements (Figure E.3). The openings of the 2019-2020 commercial Dungeness crab fisheries were delayed in northern California due to low meat quality, and in central California to avoid marine

life entanglements, respectively; however, exceedances of domoic acid were also observed in Dungeness crab from some regions of California that eventually cleared prior to these delayed start dates.

Domoic acid can also affect California fisheries that target rock crab and spiny lobster. In Southern California, there were no domoic acid-related closures of spiny lobster or rock crab in 2019 (Figure E.3). However, the northern rock crab fishery is still closed in two areas due to domoic acid concerns (data not shown; see <https://wildlife.ca.gov/Fishing/Ocean/Health-Advisories>), and these areas have not been open since November of 2015.



Appendix F SNOW-WATER EQUIVALENT, STREAMFLOW, AND STREAM TEMPERATURE

Development of habitat indicators in the CCIEA has focused on freshwater habitats. All habitat indicators are reported based on a hierarchical spatial framework. This spatial framework facilitates comparisons of data at the right spatial scale for particular users, whether this be the entire California Current, ecoregions within these units, or smaller spatial units. The framework we use divides the region encompassed by the California Current ecosystem into ecoregions (Figure 2.1b), and ecoregions into smaller physiographic units. Freshwater ecoregions are based on the biogeographic delineations in Abell et al. (2008; see also www.feow.org), who define six ecoregions for watersheds entering the California Current, three of which comprise the two largest watersheds directly entering the California Current (the Columbia and the Sacramento-San Joaquin Rivers). Within ecoregions, we summarized data using evolutionary significant units and 8-field hydrologic unit classifications (HUC-8). Status and trends for all freshwater indicators are estimated using space-time models (Lindgren and Rue 2015), which account for temporal and spatial autocorrelation.

Snow-water equivalent (SWE) is measured using two data sources: a California Department of Water Resources snow survey program (data from the California Data Exchange Center <http://cdec.water.ca.gov/>) and The Natural Resources Conservation Service's SNOTEL sites across Washington, Oregon, California and Idaho, <http://www.wcc.nrcs.usda.gov/snow/>). Snow data (Figure F.1) are converted into SWEs based on the weight of samples collected at regular intervals using a standardized protocol. Measurements at April 1 are considered the best indicator of maximum extent of SWE; thereafter snow tends to melt rather than accumulate. Data for each freshwater ecoregion are presented in Section 3.5 of the main report.

The outlook for snowpack in 2020 is limited to examination of current SWE, an imperfect correlate of SWE in April due to variable atmospheric temperature and precipitation patterns. SWE as of February 1, 2020 was below the long-term median throughout much of the region, although parts of eastern Washington, eastern Oregon, northern and southern Idaho, and northeastern California are above the median, as are several individual sites in the Cascades and the Olympic Peninsula (Figure F.1). Stations in interior central California are mostly below the median. The April 1, 2020 SWE measurements will be presented in next year's report.

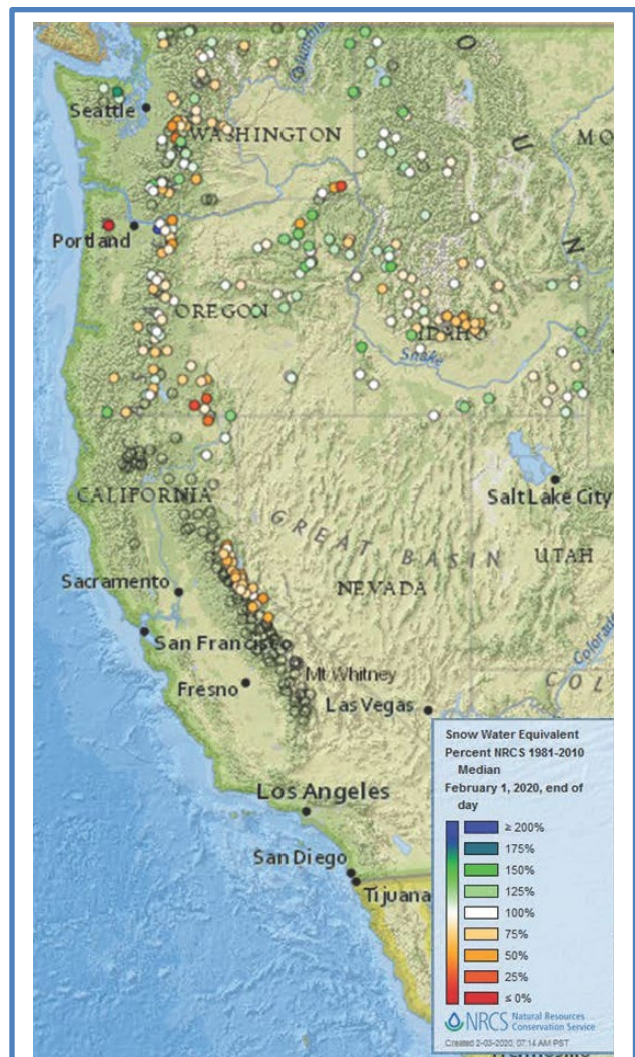


Figure F.1 Snow water equivalent relative to 1981-2010 median value as of February 1, 2020. Data are from the Natural Resource Conservation Service SNOTEL database. Open circles are stations that either lack current data or long-term median data.

Mean maximum temperatures in August were determined from 446 USGS gages with temperature monitoring capability. While these gages did not necessarily operate simultaneously throughout the period of record, at least two gages provided data each year in all ecoregions. Stream temperature records are limited in California, so two ecoregions were combined. Maximum temperatures continued to exhibit strong ecoregional differences (for example, the Salish Sea / Washington Coast streams were much cooler on average than California streams). The most recent 5 years have been marked by largely average values region-wide with the exception of the Salish Sea and Washington Coast, which has much higher temperatures in the last five years compared to the period of record (Figure F.2). Recent trends in maximum August stream temperatures have been relatively stable; the recent decline in Sacramento-San Joaquin and Southern California streams is not statistically significant.

Streamflow is measured using active USGS gages with records that meet or exceed 30 years in duration. Average daily values from 213 gages were used to calculate both annual 1-day maximum and 7-day minimum flows. These indicators correspond to flow parameters to which salmon populations are most sensitive. We use standardized anomalies of streamflow time series from individual gages. Across ecoregions of the California

Current, both minimum and maximum streamflow anomalies have exhibited some variability in the most recent five years. At the ecoregion scale, minimum stream flows were below average with no significant trend over the past 5 years in the two northernmost ecoregions (Figure F.3, see Figure F.5 for flows by ESU). Minimum flow increased over the past 5 years for the Columbia Unglaciaded, Oregon/California Coast and Sacramento/San Joaquin ecoregions, possibly reflecting the 5-year increasing trend in SWE shown in Figure 3.5; correspondingly, central and inland Chinook salmon ESUs also exhibited short-term increases in minimum flow (Figure F.5). Minimum flow in the Southern California Bight was stable over the last 5 years, and has been among the ecoregion’s lowest on record for many years.

Because high rates of maximum late-winter flow are generally beneficial for juvenile salmon in inland regions but detrimental to northern coastal populations, flow conditions during egg incubation (after spawning) may have been good across a wide range of the Pacific Coast. The Salish Sea / WA coast and Columbia Glaciaded ecoregions experienced downturns in maximum flow in 2019, and the Salish Sea /

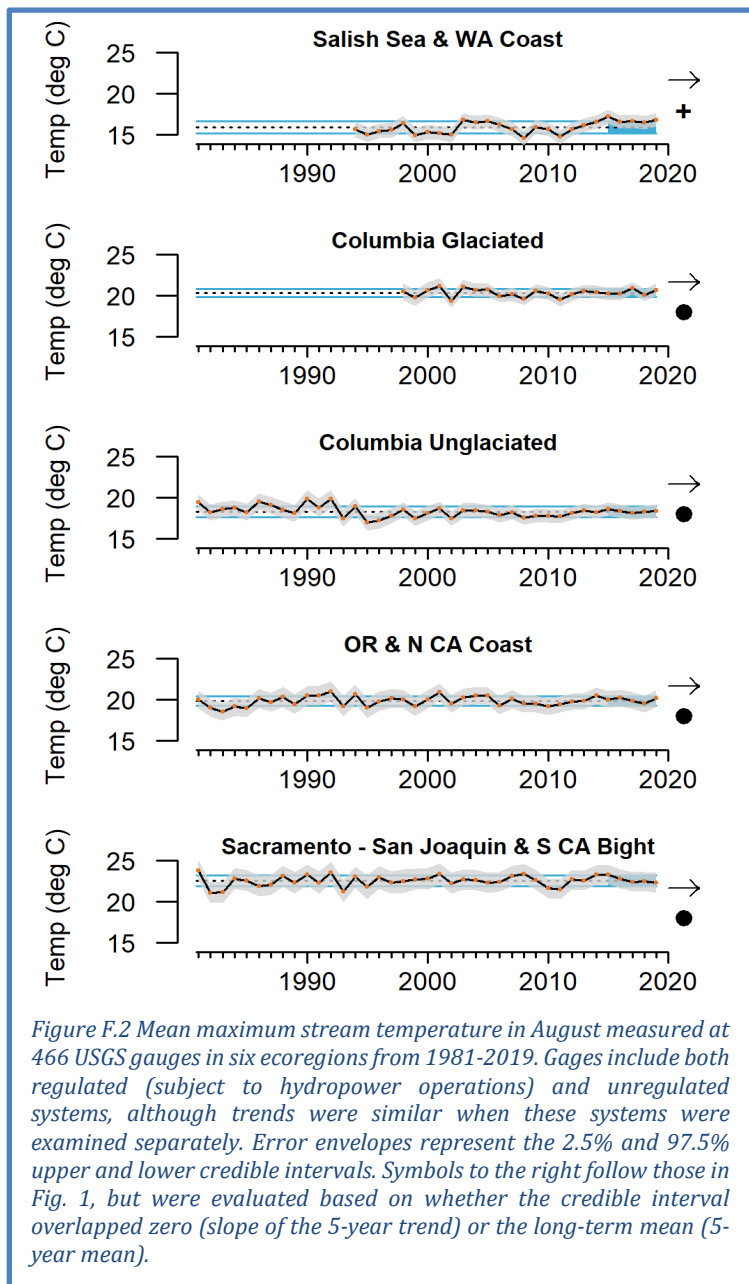
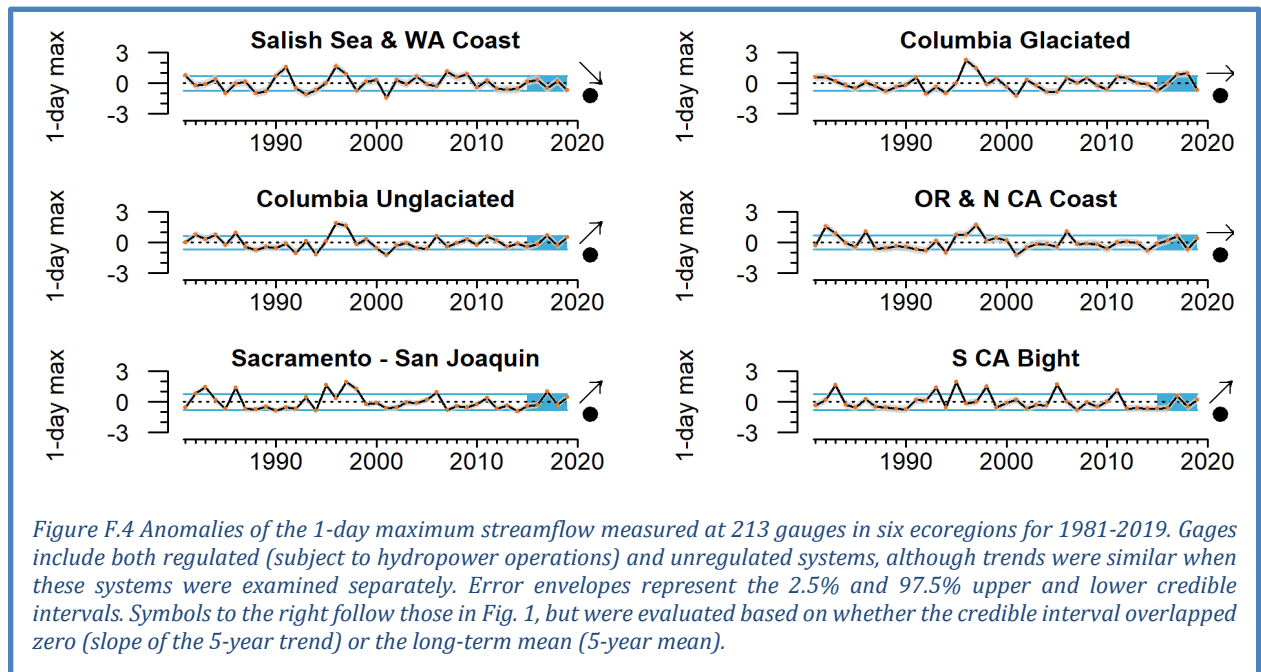
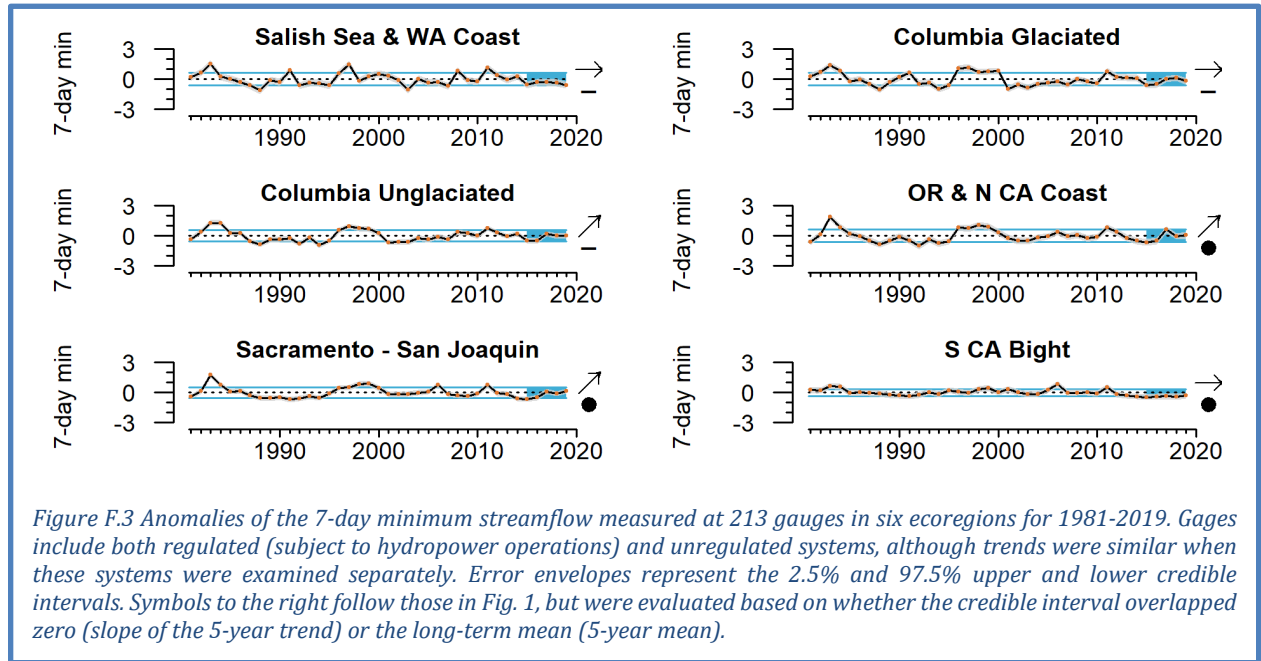


Figure F.2 Mean maximum stream temperature in August measured at 466 USGS gauges in six ecoregions from 1981-2019. Gages include both regulated (subject to hydropower operations) and unregulated systems, although trends were similar when these systems were examined separately. Error envelopes represent the 2.5% and 97.5% upper and lower credible intervals. Symbols to the right follow those in Fig. 1, but were evaluated based on whether the credible interval overlapped zero (slope of the 5-year trend) or the long-term mean (5-year mean).

WA Coast has experienced a negative short-term trend (Figure F.4; see Figure F.6 for flows by ESU). Maximum flow in most other ecoregions has been trending higher since 2015. Recent 5-year averages in maximum flow were not significantly different from long-term averages at the ecoregional level, although several ESUs—most notably Klamath, Sacramento and Central Valley, and Upper Columbia ESUs—exhibited recent 5-year averages that were greater than long-term averages (Figure F.6).



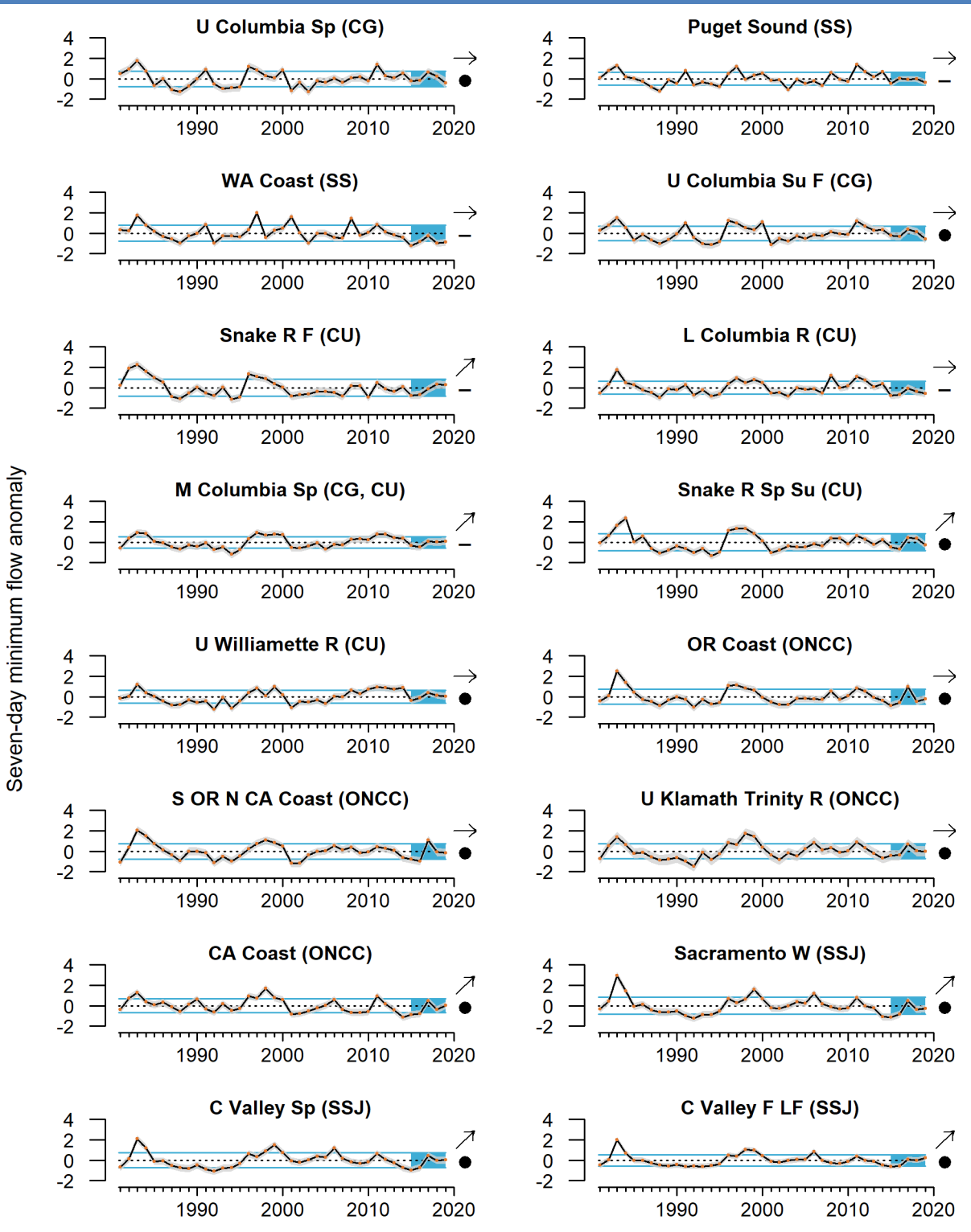


Figure F.5 Anomalies of the 7-day minimum streamflow measured at 213 gauges in 16 Chinook salmon ESUs for 1981-2019. Gages include both regulated (subject to hydropower operations) and unregulated systems, although trends were similar when these systems were examined separately. Error envelopes represent the 2.5% and 97.5% upper and lower credible intervals. Symbols to the right follow those in Fig. 1, but were evaluated based on whether the credible interval overlapped zero (slope of the 5-year trend) or the long-term mean (5-year mean).

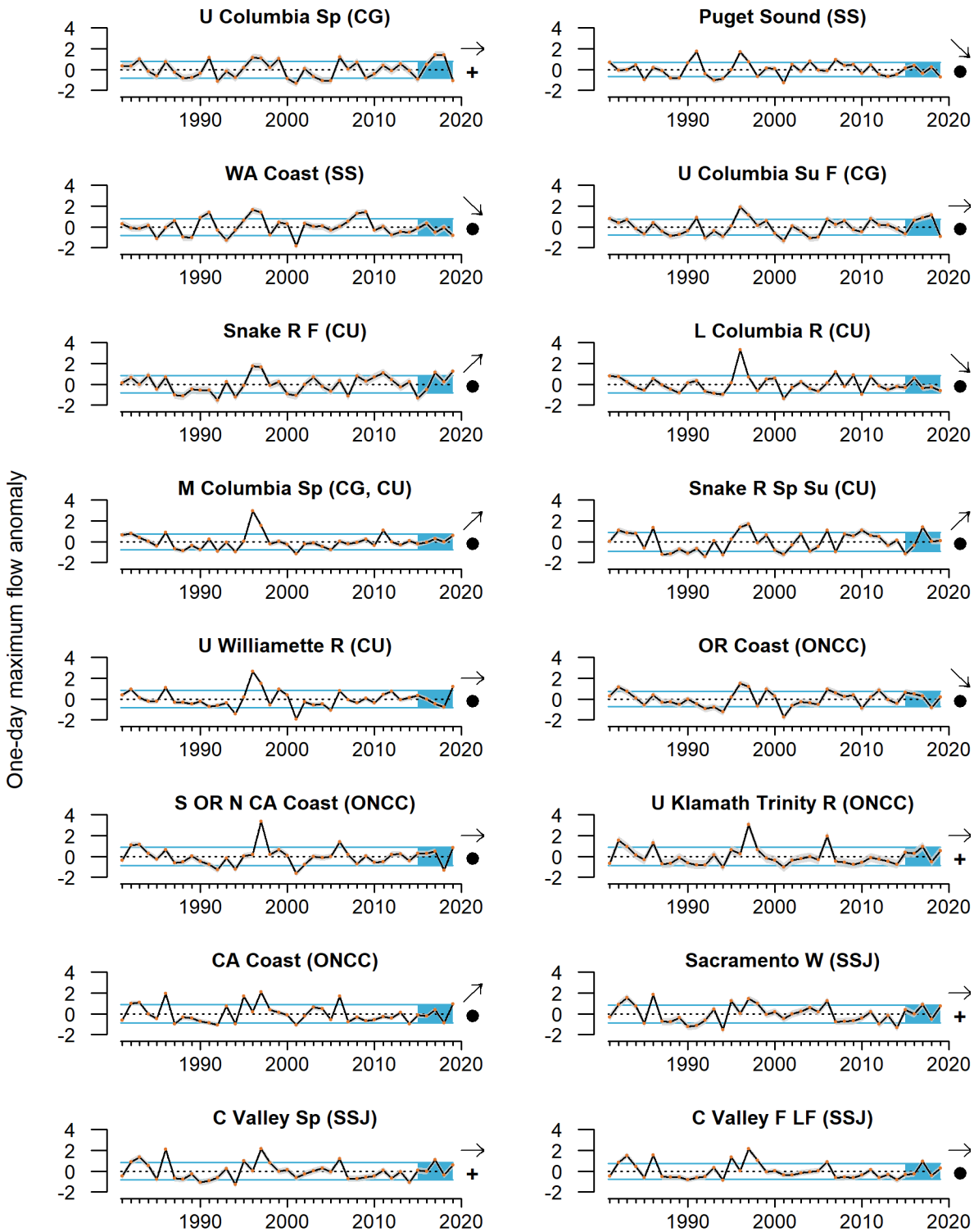


Figure F.6 Anomalies of the 1-day maximum streamflow measured at 213 gauges in 16 Chinook salmon ESUs for 1981-2019. Gauges include both regulated (subject to hydropower operations) and unregulated systems, although trends were similar when these systems were examined separately. Error envelopes represent the 2.5% and 97.5% upper and lower credible intervals. Symbols to the right follow those in Fig. 1, but were evaluated based on whether the credible interval overlapped zero (slope of the 5-year trend) or the long-term mean (5-year mean).

Appendix G REGIONAL FORAGE AVAILABILITY

Regional trends in forage availability are presented in Section 4.2 of the main body, using a cluster analysis method. Here we present the time series that were used in the cluster analyses, along with some additional species that are associated with the forage community.

G.1 NORTHERN CALIFORNIA CURRENT FORAGE

The Northern CCE survey (known as the “Juvenile Salmon Ocean Ecology Survey”) occurs in June and targets juvenile salmon in surface waters off Oregon and Washington, but also collects adult and juvenile (age 1+) pelagic forage fishes, market squid, and gelatinous zooplankton with regularity. The gear is fished during daylight hours in near-surface waters, which is appropriate for targeting juvenile salmon.

In 2019, catches of juvenile Chinook, coho and sockeye salmon were close to average and had non-significant 5-year trends (Figure G.1.1). Chum salmon catches were above average in 2019 and

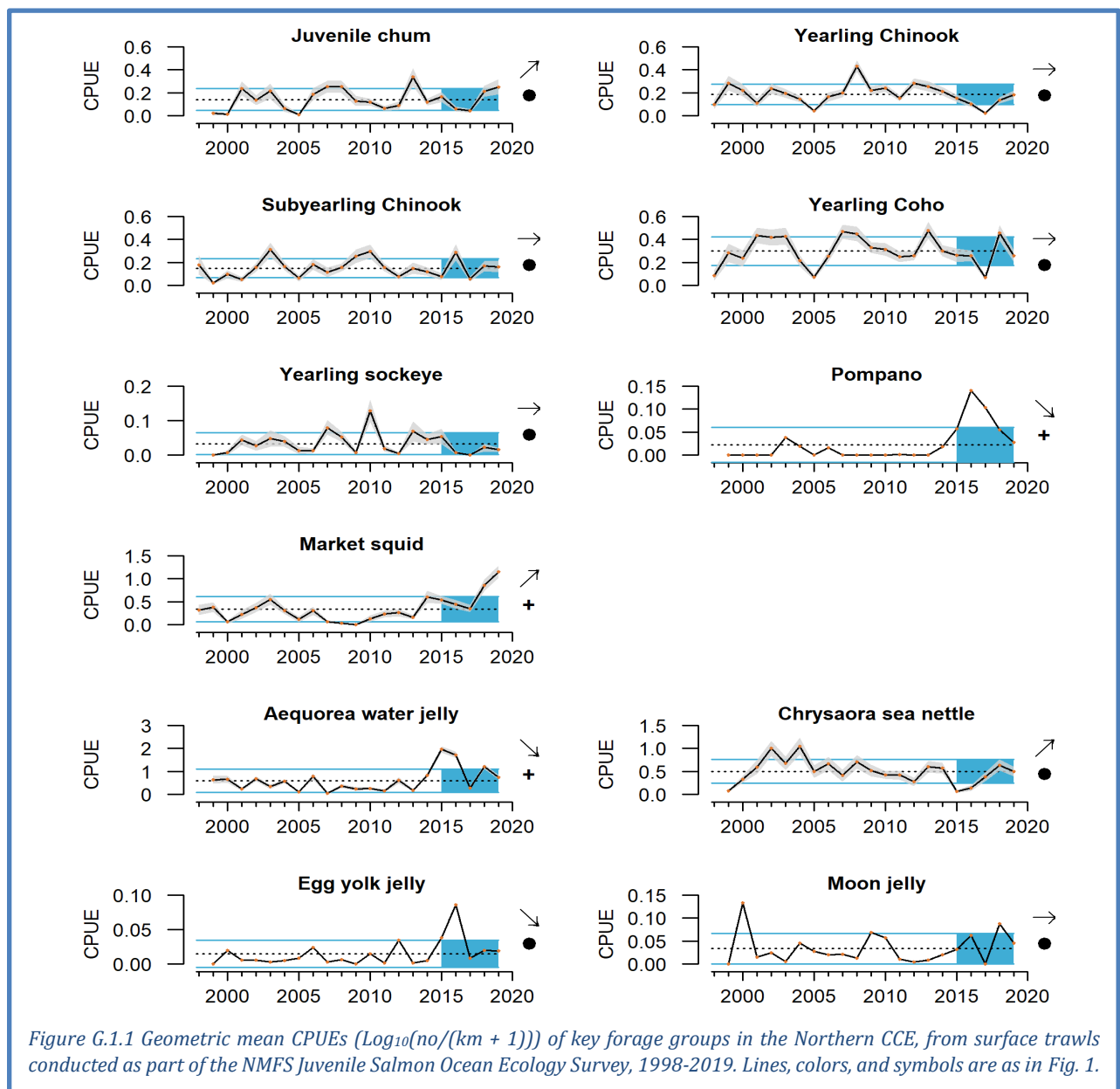
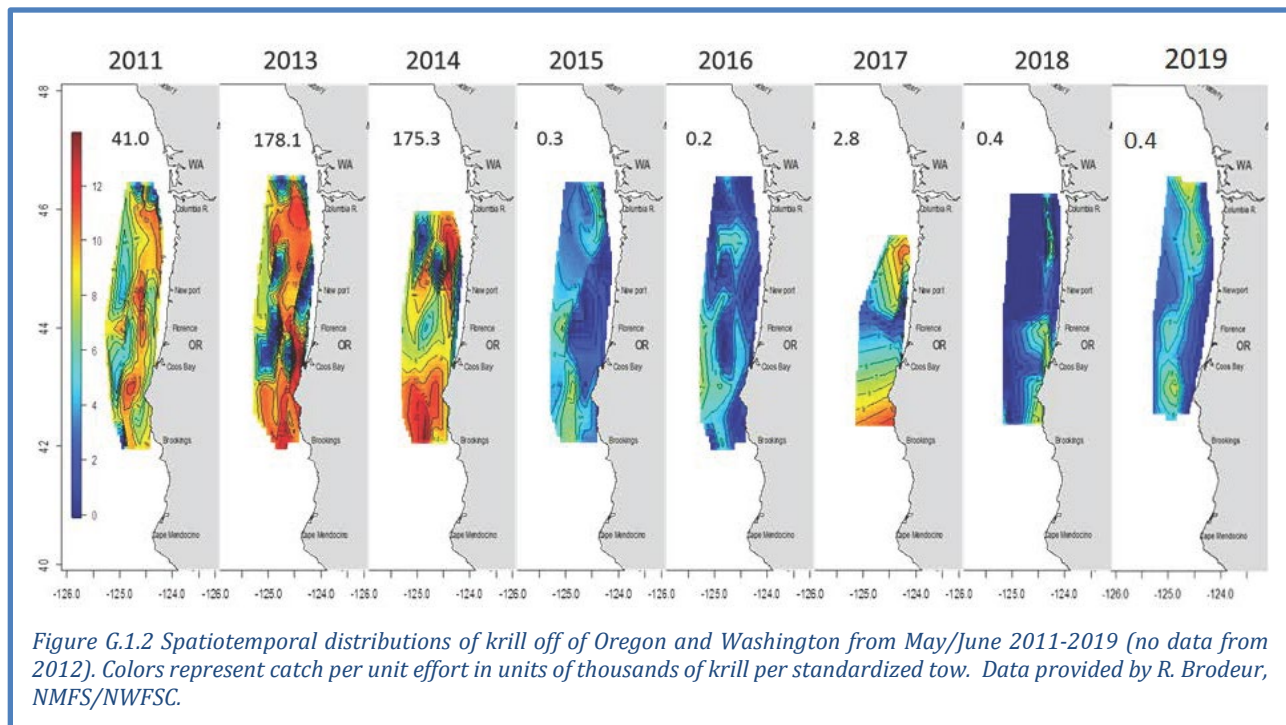


Figure G.1.1 Geometric mean CPUEs ($\text{Log}_{10}(\text{no}/(\text{km} + 1))$) of key forage groups in the Northern CCE, from surface trawls conducted as part of the NMFS Juvenile Salmon Ocean Ecology Survey, 1998-2019. Lines, colors, and symbols are as in Fig. 1.

contributed to a positive 5-year trend. Catches of market squid in 2019 were the highest on record; high catches in both 2018 and 2019 contributed to an increasing trend. Catches of *Chrysaora* jellyfish (sea nettles) have been increasing since the low in 2015 following the marine heatwave, and are near average values. Contrastingly, catches of pompano (butterfish), egg yolk jelly, and water jelly *Aequorea*, all of which peaked during the marine heatwave in 2015 and 2016, have declined.

Some prominent forage species like anchovy, sardine, herring and mackerels are caught by this survey, but not very efficiently because they tend to be deeper in the water column during daylight hours. Thus, we do not report catch-per-unit-effort (CPUE) of such species. However, researchers have tracked the proportion of hauls in which at least one individual of a given species is captured in order to get a general sense of their prevalence (see Thompson et al. 2019b, their Figure 29). In 2018-2019, the prevalence data reflect a community composed of juvenile salmon and market squid, and relatively high occurrence of herring, while warmer-water species like mackerel, water jellies and pyrosomes have declined in occurrence relative to 2015-2017.

Finally, limited krill data are available for the northern CCE from a related survey (which has been operating since 2011 as a northern extension of the forage sampling in the central CCE, described in the next section). This survey covers offshore waters from approximately Willapa Bay, Washington to the Oregon/California border. In 2019, krill densities within the survey area were ~400 individuals per tow (Figure G.1.2). Krill densities within the survey areas have been low since 2015, following the onset of coastal impacts of the 2013-2016 marine heatwave; densities prior to that were several orders of magnitude higher than at present.



G.2 CENTRAL CALIFORNIA CURRENT FORAGE

The Central CCE forage survey (known as the “Rockfish Recruitment and Ecosystem Assessment Survey” or RREAS) samples this region using midwater trawls, which not only collect young-of-the-year (YOY) rockfish species, but also a variety of other YOY and adult forage species, market squid, adult krill, and gelatinous zooplankton. Time series presented here are from the “Core Area” of that survey (see Figure 2.1c in the Main Report). In 2019, catches of adult anchovy increased remarkably for a second straight year, and there were also increases in adult sardine (Figure G.2.2). Market squid catches were above average for a third straight year. In contrast, there were decreases in YOY anchovy, YOY sardine, YOY hake, YOY rockfish, YOY sanddabs, and krill in 2019, and overall over the past 5 years. Krill catches in 2019 were among the lowest of the time series. Catches of jellyfish (*Aurelia* sp., *Chrysaora*) were average, and lower than the dramatic catches in 2018. Pyrosome catches were above average, after dipping to average in 2018.

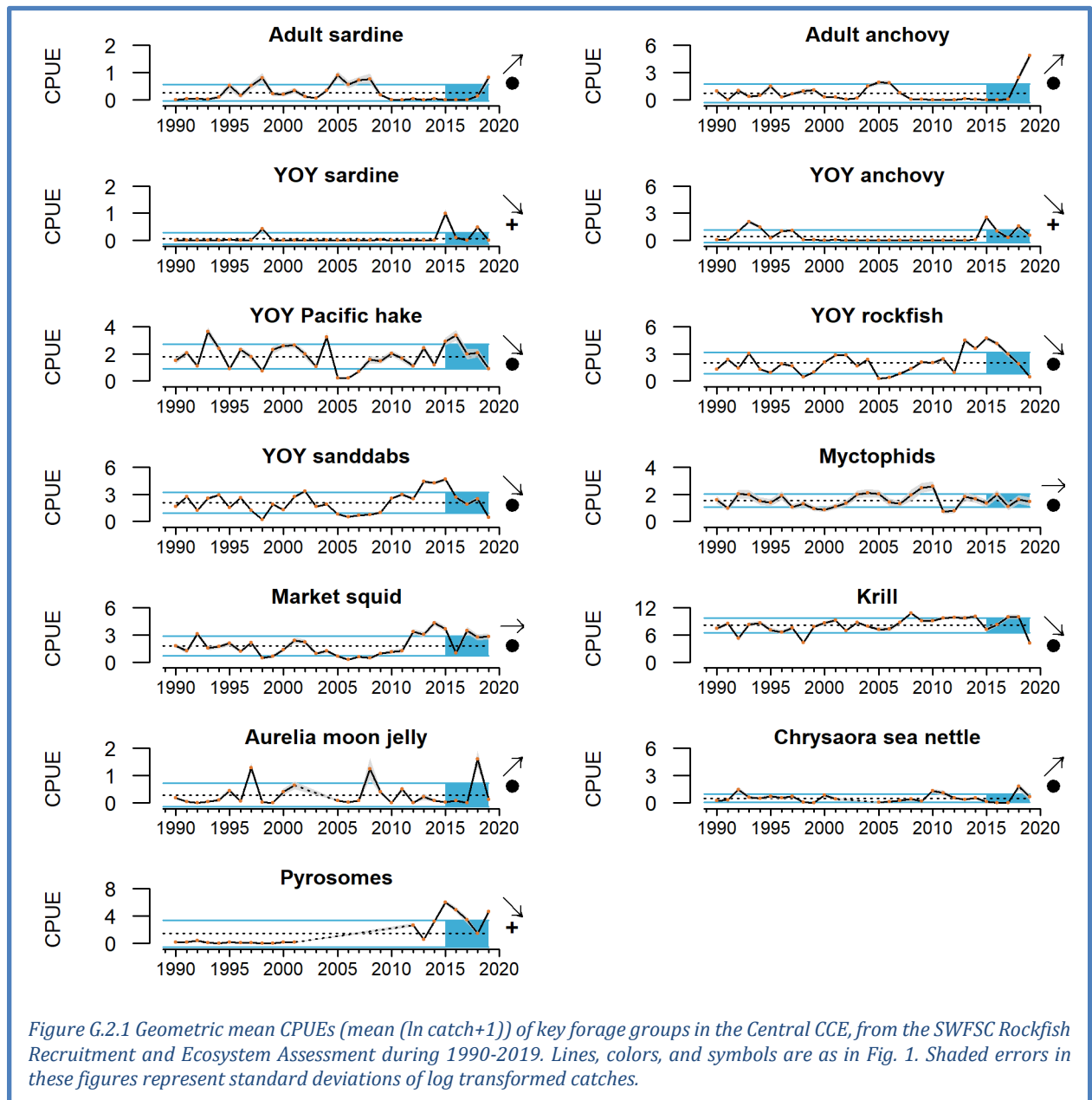
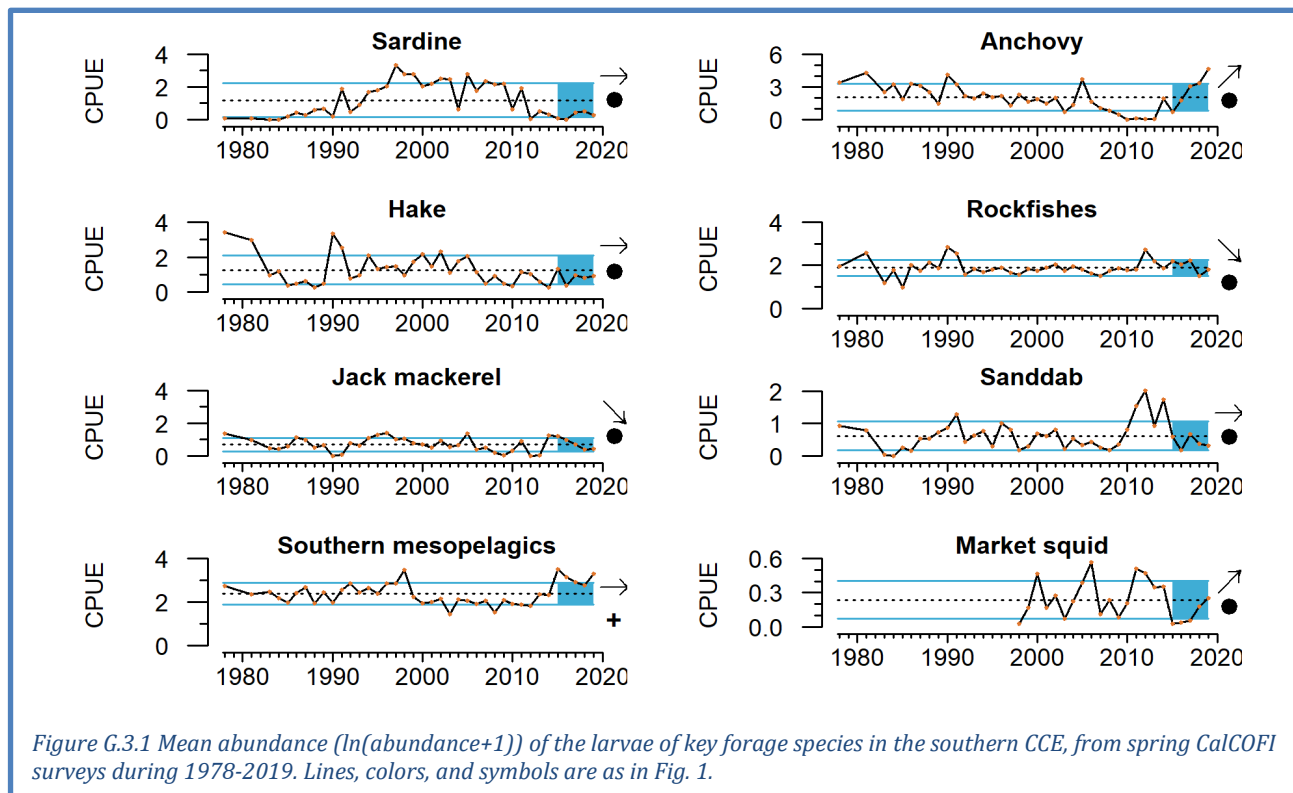


Figure G.2.1 Geometric mean CPUEs (mean (ln catch+1)) of key forage groups in the Central CCE, from the SWFSC Rockfish Recruitment and Ecosystem Assessment during 1990-2019. Lines, colors, and symbols are as in Fig. 1. Shaded errors in these figures represent standard deviations of log transformed catches.

G.3 SOUTHERN CALIFORNIA CURRENT FORAGE

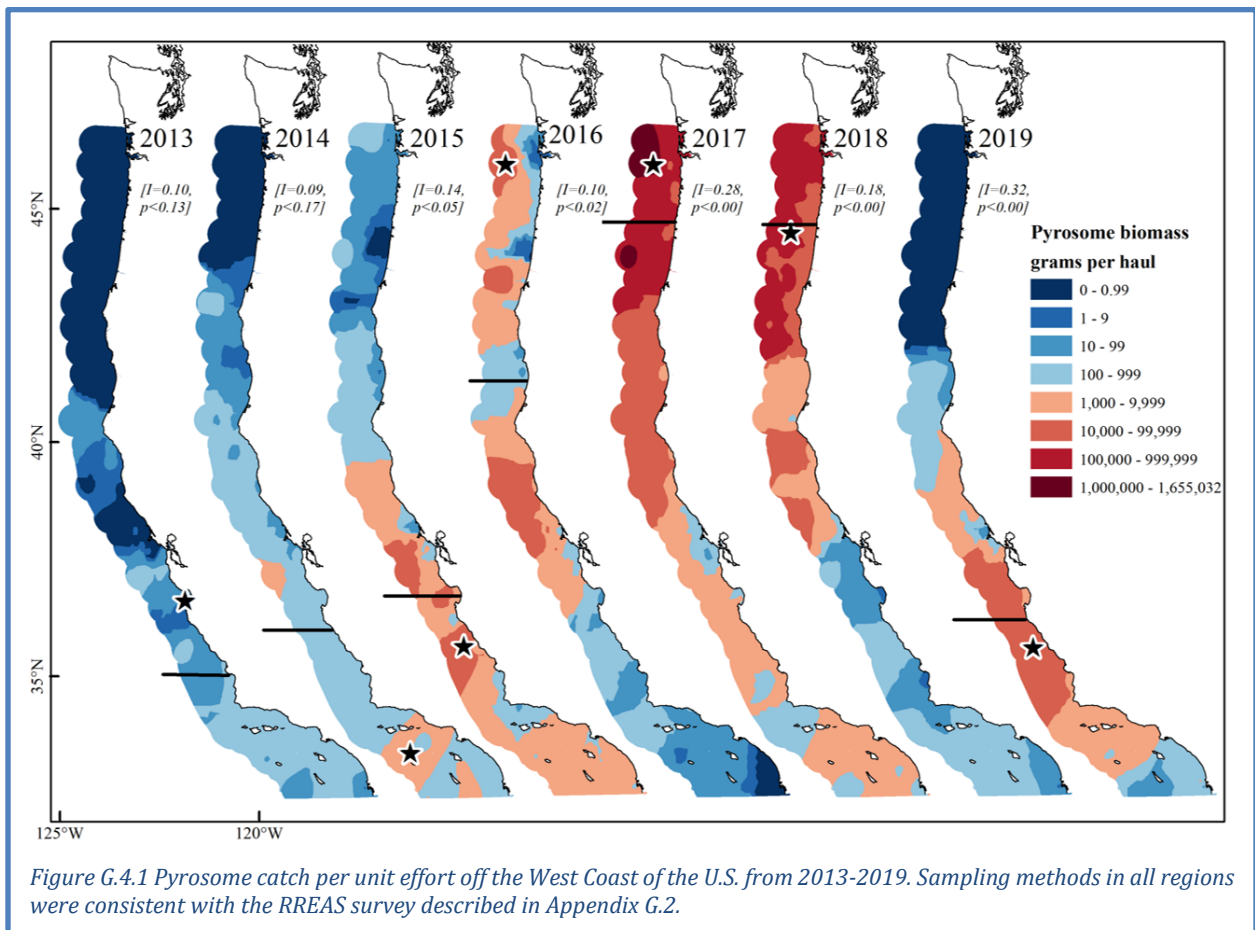
The abundance indicators for forage in the Southern CCE come from fish and squid larvae collected in the spring across all core stations of the CalCOFI survey using oblique vertical tows of fine mesh Bongo nets to 212 m depth. The survey collects a variety of fish and invertebrate larvae (<5 d old) from several taxonomic and functional groups. Larval data are indicators of the relative regional abundances of adult forage fish, such as sardines and anchovy, and other species, including certain groundfish, market squid, and mesopelagic fishes. Noteworthy observations from 2019 surveys include the ongoing increase in relative abundance of anchovy—among the highest catches of the time series—and ongoing high catches of market squid and southern mesopelagic fish larvae (Figure G.3.1). In contrast, several groups experienced low or declining catches, including jack mackerel, sanddab, and sardine. Rockfish catches were average in 2019, but they have declined over the past 5 years.



G.4 PYROSOME BIOMASS

Pyrosomes (*Pyrosoma atlanticum*) are pelagic tunicates known to have a subtropical distribution, and historically have been occasionally observed in southern and central California waters of the CCE; over the past several years they have become far more abundant, and the increases have been attributed to the marine heatwave that affected the CCE from 2014-2016, when anomalously warm ocean conditions may have favored pyrosome feeding and reproduction. Pyrosomes are aggregate filter feeders that consume pico- and microplankton, and in some areas have been shown to cause the depletion of chlorophyll-*a* standing stocks. Mass occurrences of pelagic tunicates have impacts on human activities, such as damaged fishing nets and clogging cooling water intakes of coastal hydropower facilities.

Recent work by Miller et al. (2019) examined the spatial distribution, abundance, and size variability of pyrosomes in the CCE. Pyrosome abundance was significantly greater in 2012–2019 compared to 1983–2001, and recent persistent abundance peaks were unprecedented. Relative biomass trends showed abundance in the CCE shifting from south to north from 2013 to 2018, while in 2019 abundance was vastly reduced in northern regions and predominately located in the central region (Figure G.4.1). In 2014-2015, pyrosome biomass was mostly off California, but spread north in 2016. In 2017 and 2018, pyrosome biomass was greater in the Oregon and Blanco regions, reaching peak relative abundance levels in the waters off of Washington, Oregon, and Northern California. By 2019, a single pyrosome was caught in surveys in the Oregon region, while pyrosome biomass was greatest in the central California region.



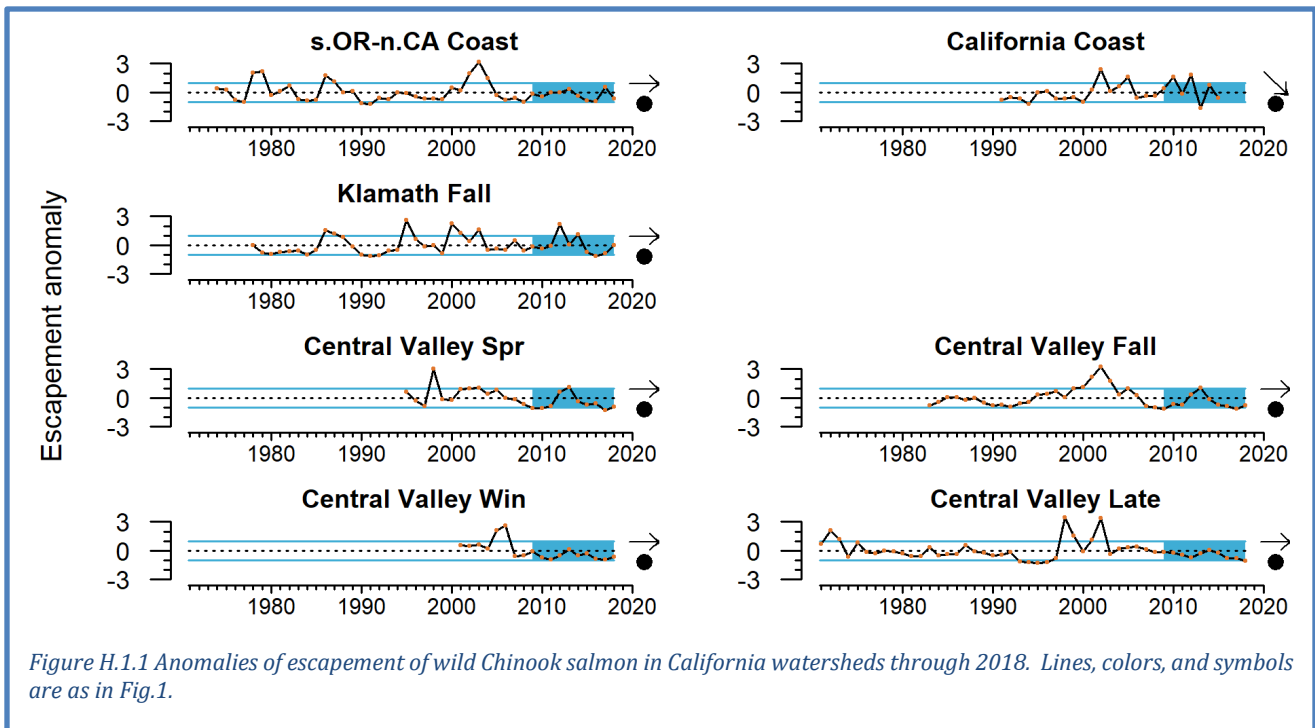
Appendix H CHINOOK SALMON ESCAPEMENT INDICATORS

Salmon escapement data provide indicators of abundance and reproductive potential of naturally spawning salmon stocks. Population-specific status and trends in Chinook salmon escapement are provided in Section 4.3 of the Main Report. Figure 4.3.1 uses a quad plot to summarize recent escapement status and trends relative to full time series. These plots are useful for summarizing large amounts of data, but they may hide informative short-term variability in these dynamic species. The full time series for all populations are therefore presented here. We note again that these are escapement numbers, not run-size estimates, which take many years to develop. Status and trends are estimated for the most recent 10 years of data (unlike 5 years for all other time series in this Report) in order to account for the spatial segregation of successive year classes of salmon.

H.1 CALIFORNIA CHINOOK SALMON ESCAPEMENTS

The Chinook salmon escapement time series from California include data from as recent as 2018 extending back over 20 years, with records for some populations stretching back to the 1970s. No population showed short-term trends over the past 10 years of available data (Figure H.1.1), but escapement estimates in 2018 for two populations (Central Valley Spring, Central Valley Late) were 1 s.d. below the long-term mean for their respective time series, and several others were close to 1 s.d. below the mean. On the other hand, Klamath Fall Chinook were close to the time series average escapement in 2018. Many populations have experienced decreasing escapements from 2013-2018 after some increases in the preceding years.

The California Coast ESU data have not been updated since 2015, so the plot below is likely not representative of recent California Coast ESU escapement levels.



H.2 WASHINGTON/OREGON/IDAHO CHINOOK SALMON ESCAPEMENTS

The escapement time series used for Chinook salmon populations from Washington, Idaho, and Oregon extend back for up to 40+ years, and the most recent data currently available are through 2018 (Figure H.2.1). Stocks are often co-managed and surveyed by a variety of state and tribal agencies. Patterns over the past 10 years were mixed: Snake River Spring-Summer Chinook escapement had a negative trend after declining from peaks earlier in the decade, while Willamette River Spring Chinook had an increasing trend. Snake River Fall Chinook escapement in 2018 was near the long-term mean and have declined over the past few years, but several years of relatively high escapements in the middle of the decade resulted in a 10-year average that is >1 s.d. greater than the long-term mean. Upper Columbia Spring Chinook escapement has been below average for most of the last decade, while Lower Columbia Chinook escapement has been average to below average; both populations' recent averages are within 1 s.d. of the long-term mean, and have neutral escapement trends in the last ten years.

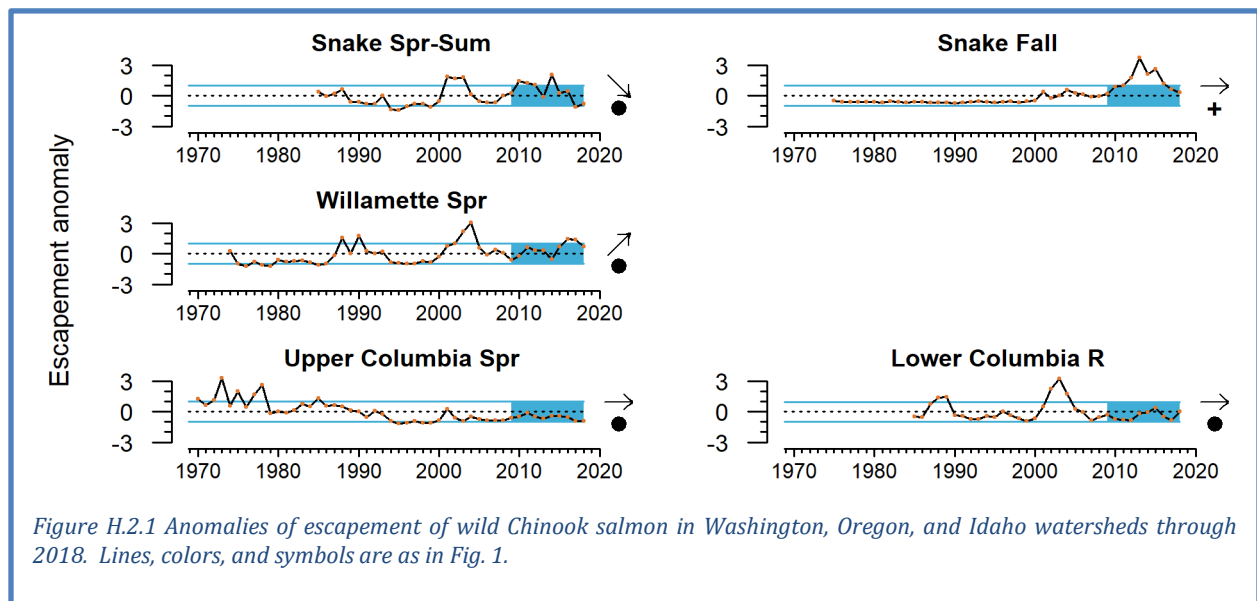
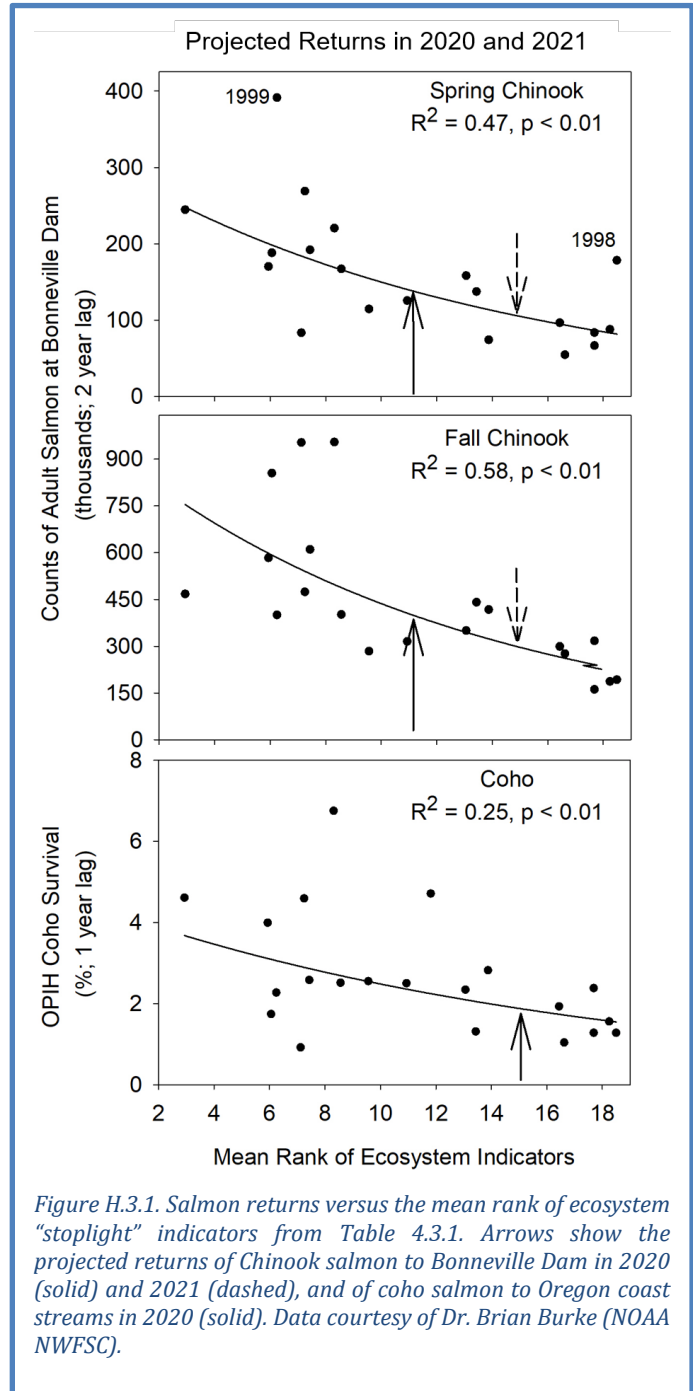


Figure H.2.1 Anomalies of escapement of wild Chinook salmon in Washington, Oregon, and Idaho watersheds through 2018. Lines, colors, and symbols are as in Fig. 1.

H.3 OUTLOOKS FOR 2020 SALMON RETURNS TO THE COLUMBIA RIVER AND OREGON PRODUCTION INDEX AREA

The main body of the report features the “stoplight” table (Table 4.3.1) that shows a ranking of indicators of conditions affecting marine growth and survival of Chinook salmon returning to the Columbia Basin, and coho salmon returning to streams in the Oregon Production Index (OPI) area. The stoplight table provides a qualitative perspective on the likely relative run sizes of salmon in the current year, based on indicator measures in the years since returning salmon originally went to sea as smolts. A somewhat more quantitative analysis based on the stoplight table is depicted at the right. Here, annual Chinook salmon counts at Bonneville Dam (Figure H.3.1, top and middle) and OPI coho smolt-to-adult survival (Figure H.3.1, bottom) over the last two decades are plotted against the aggregate mean ranking of indicators in the stoplight table, with 1-year lag for coho and 2-year lag for Chinook. The highest ranking years at the left tend to produce the highest returns and survival. The 2018 stoplight indicators had a relatively low mean rank of 11.8, for which the model equation projects returns of 131,000 Spring and 379,000 Fall Chinook salmon at Bonneville Dam in 2020 (Figure H.3.1, top and middle panels, solid arrows). The 2019 stoplight indicators had a higher mean rank of 15.1, for which the model projects smolt-to-adult survival of 1.9% for OPI coho in 2019 (Figure H.3.1, bottom, solid arrow). The stoplight indicator ranking of 15.1 in 2019 also corresponds to 2021 Bonneville counts of 104,000 Spring Chinook and 294,000 Fall Chinook (Figure H.3.1, top and middle, dashed arrows). The relationships of past salmon returns to stoplight means explain between 25% (coho) and 58% (Fall Chinook) of variance. This is a fairly simple analysis, however, given that each indicator in the stoplight table is given equal weight.

A more robust quantitative analysis uses an expanded set of ocean indicators plus principal components analysis and dynamic linear modeling to estimate outlooks for salmon returns for the same region. The principal



components analysis essentially is used for weighted averaging of the ocean indicators, reducing the total number of indicators while retaining the bulk of the information from them. The dynamic linear modeling technique relates salmon returns to the principal components of the indicator data, and the approach used here also incorporates dynamic information from sibling regression modeling. The model fits very well to data for Spring Chinook and Fall Chinook at the broad scale of the Columbia River (Figure H.3.2). Model outputs with 95% confidence intervals estimate 2020 Bonneville counts of Spring Chinook salmon that are similar to returns from 2017-2019 (Figure H.3.2, top), and potential increases of Fall Chinook at Bonneville in 2020 relative to 2019, but still well below the returns of 2013-2015 (Figure H.3.2, bottom).

(In past years, a similar model was run for coho salmon returns to the Oregon Production Index region, but that model was not available this year.)

Although these analyses represent a general description of ocean conditions, we must acknowledge that the importance of any particular indicator will vary among salmon species/runs. NOAA scientists and partners are working towards stock-specific salmon projections by using methods that can optimally weight the indicators for each response variable in which we are interested (Burke et al. 2013). We will continue to work with the Council and advisory bodies to identify data sets for Council-relevant stocks for which analyses like these could be possible.

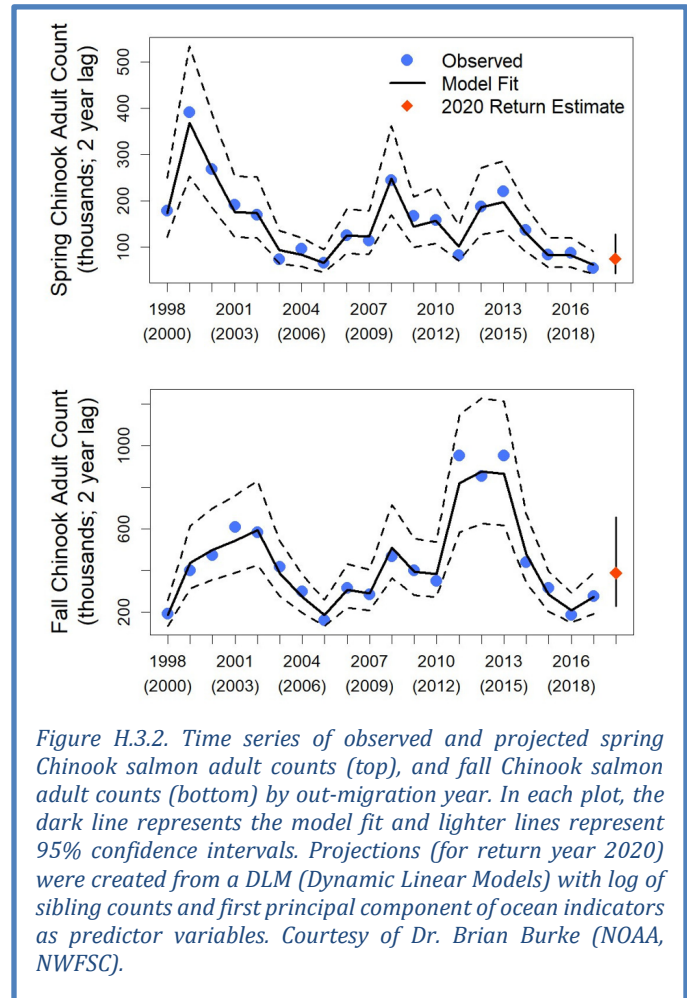
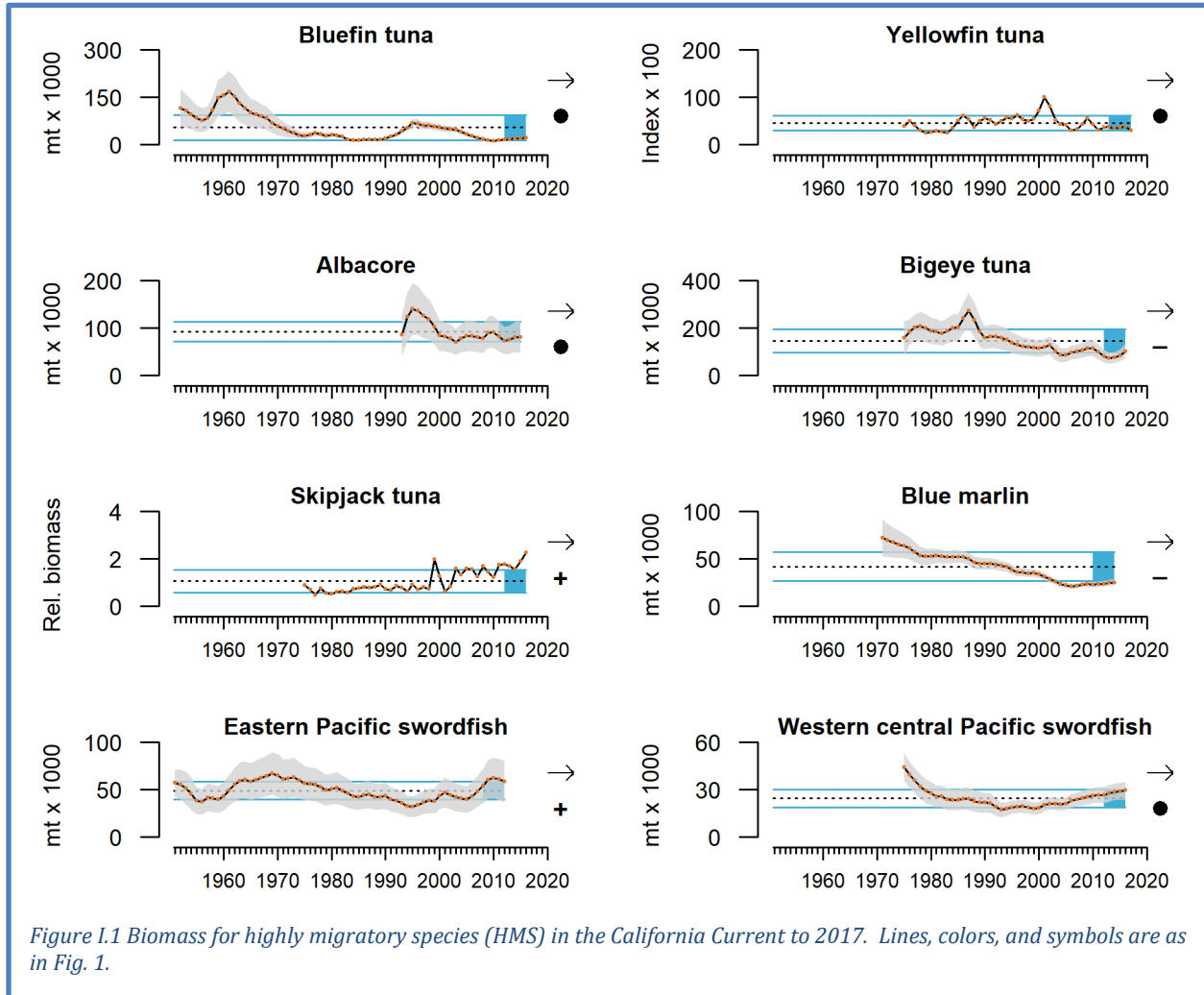
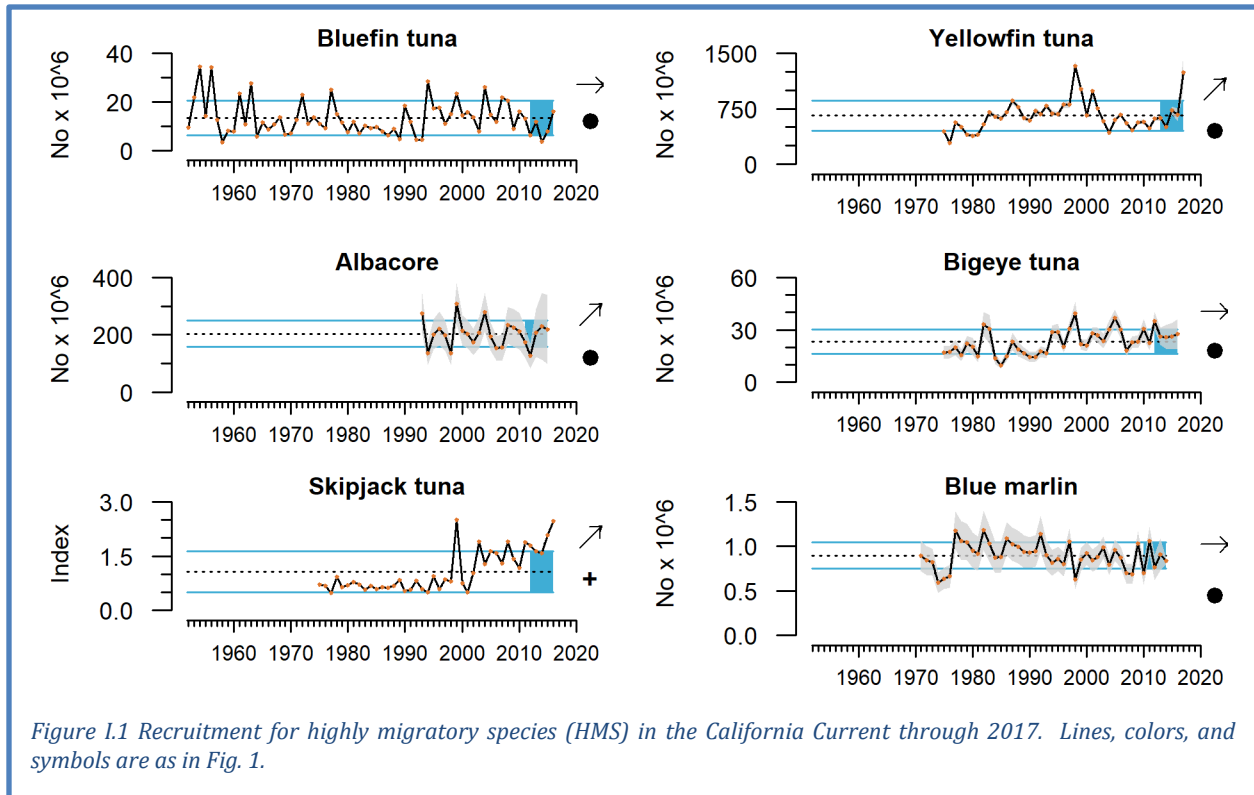


Figure H.3.2. Time series of observed and projected spring Chinook salmon adult counts (top), and fall Chinook salmon adult counts (bottom) by out-migration year. In each plot, the dark line represents the model fit and lighter lines represent 95% confidence intervals. Projections (for return year 2020) were created from a DLM (Dynamic Linear Models) with log of sibling counts and first principal component of ocean indicators as predictor variables. Courtesy of Dr. Brian Burke (NOAA, NWFSC).

Appendix I HIGHLY MIGRATORY SPECIES

Highly migratory species are discussed Section 4 of the main document (Section 4.5). The time series for abundance (Figure I.1) and recruitment (Figure I.2) are plotted here, although these time series have not been updated since our 2019 report and are thus included primarily for reference. We will update these plots in future reports as new information becomes available.





Appendix J SEABIRD DENSITY AND MORTALITY

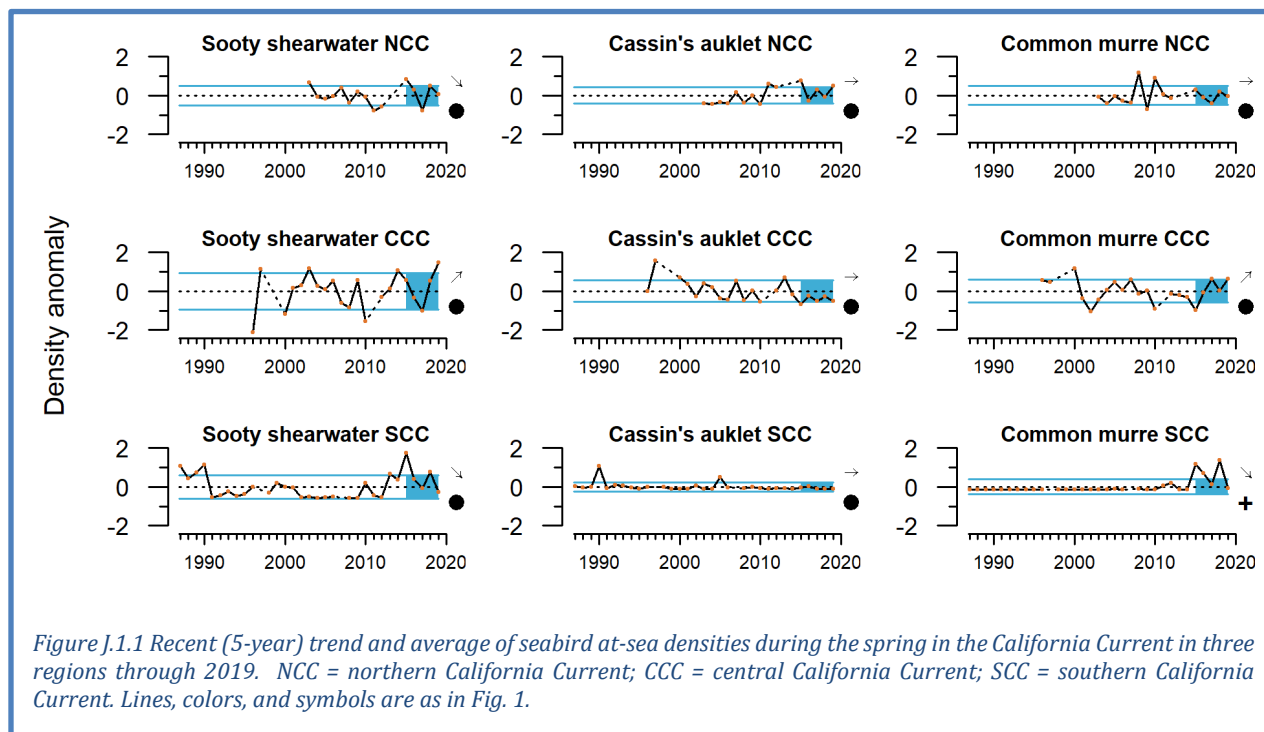
Indicators and other information suggest that seabirds experienced mixed success throughout the California Current in 2019. Seabird indicators (at-sea densities, productivity, diet, and mortality) constitute a portfolio of metrics that reflect population health and condition of seabirds as well as links to lower trophic levels and other conditions in the California Current Ecosystem. To highlight the status of different seabird guilds and relationships to their marine environment, multiple focal species are monitored throughout the CCE. The species we report on in the sections below represent a breadth of foraging strategies, life histories, and spatial ranges.

J.1 SEABIRD AT-SEA DENSITIES

Seabird densities on the water during the breeding season can track marine environmental conditions and may reflect regional production and availability of forage. Data from this indicator type can establish habitat use and may be used to detect and track seabird population movements or increases/declines as they relate to ecosystem change. We monitor and report on at-sea densities of three focal species in the northern, central, and southern regions of the CCE. Sooty shearwaters migrate to the CCE from the southern hemisphere in spring and summer to forage near the shelf break on a variety of small fish, squid and zooplankton. Common murre and Cassin's auklets are resident species that feed primarily over the shelf; Cassin's auklets prey mainly on zooplankton and small fish, while common murre target a variety of pelagic fish (see Appendix J.4).

At-sea density patterns varied within and across seabird species among the three regions of the CCE. Sooty shearwater at-sea density anomalies underwent significant short-term declines in both the northern (NCC) and southern (SCC) regions from 2015–2019 and a significant short-term increase in the central (CCC) region (Figure J.1.1). The negative trends in the northern and southern regions

were driven by steep declines after a peak in 2015, while the 2019 positive anomaly for sooty shearwaters in the central region was the highest in the time series. Cassin’s auklet at-sea density anomalies were high in the northern region 2019 but showed no recent trends in any of the regions, and recent average densities have been within ± 1 s.d. of the long-term regional means. Common murre at-sea density anomaly trends were neutral over the last five years in the northern region, but showed a significant short-term increase in the central region and short-term decrease in the southern region; despite an average anomaly in 2019, recent common murre density anomalies in the south continued to be high relative to the long-term mean. In the northern region, sooty shearwaters and common murres were again aggregated near the Columbia River plume, likely attracted to concentrations of forage fishes, squid, or krill. In the southern region, it appears that recent sooty shearwater and common murre upticks relative to the 1990s and much of the 2000s have subsided.



J.2 SEABIRD PRODUCTIVITY

Seabird population productivity, as measured through variables related to reproductive success, tracks marine environmental conditions and often reflects forage production near breeding colonies. We monitor and report on standardized anomalies of fledgling production per pair of breeding adults for five focal species on Southeast Farallon Island in the central region of the CCE. Data and interpretation are in the main body of the report in Section 4.7.

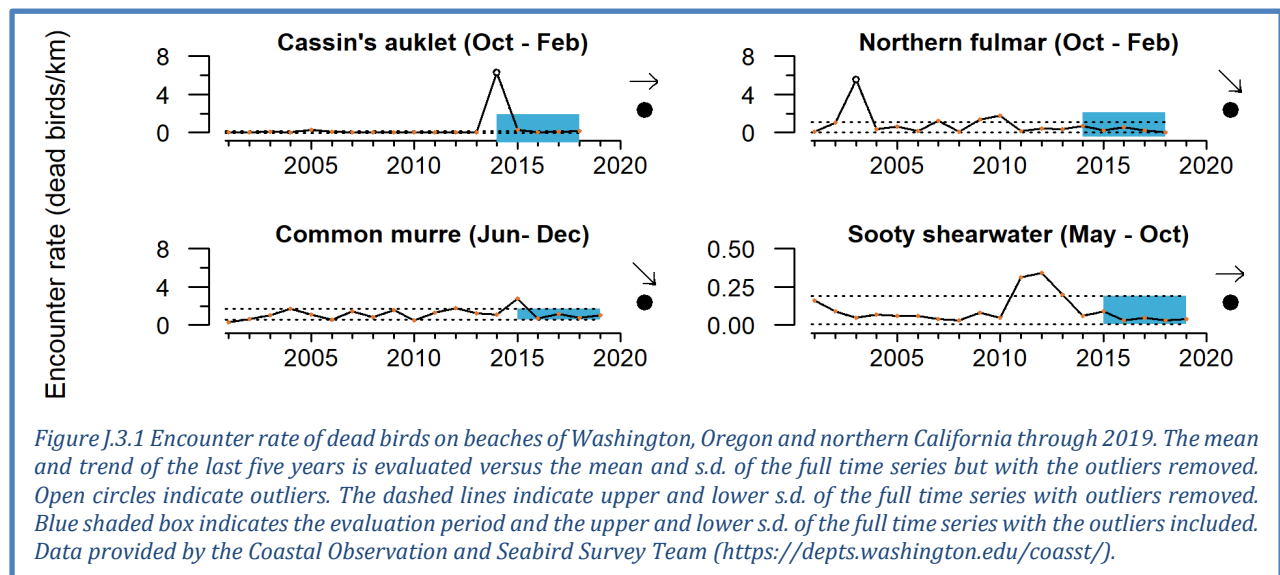
J.3 SEABIRD MORTALITY

Seabird mortality can track seabird populations as well as environmental conditions at regional and larger spatial scales. Monitoring beached birds (often by citizen scientists) provides information on the health of seabird populations, ecosystem health, and unusual mortality events. CCIEA reports from the anomalously warm and unproductive years of 2014–2016 noted major seabird mortality events in each year. These “wrecks”—exceptional numbers of dead birds washing up on widespread beaches—impacted Cassin’s auklets in 2014, common murres in 2015, and rhinoceros auklets in

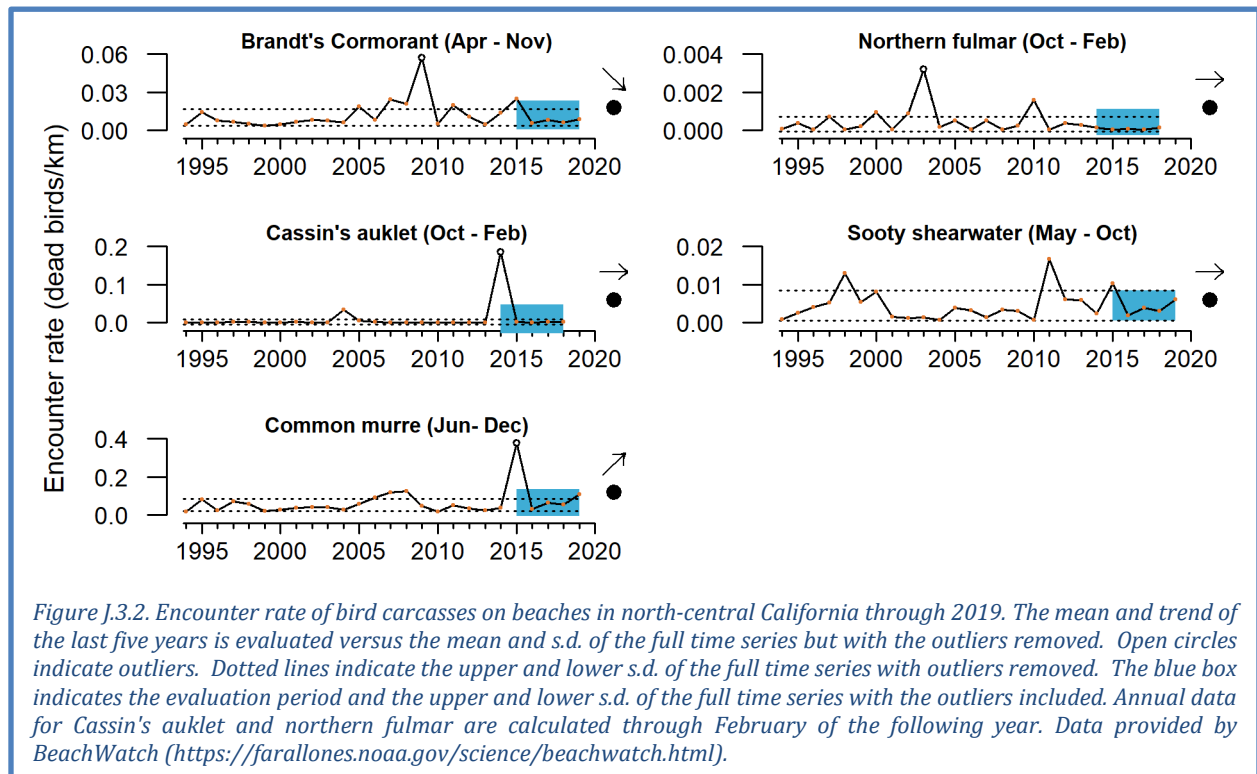
2016. (Note: The most recent wreck data for most species generally lag by one year because data collection is primarily in winter, and thus data for the 2019-2020 winter are still being collected at the briefing book deadline for the March PFMC meeting.)

In the northern CCE (Washington to northern California), the University of Washington-led Coastal Observation And Seabird Survey Team (COASST) documented beached birds at average to below-average levels for four focal species in the winter of 2018-2019 (Figure J.3.1). The Cassin’s auklet encounter rate was at baseline levels in 2018 (the latest year of data), as it has been since its unusual mortality event in 2014. The common murre encounter rate was average in 2019 and showed a significant negative short-term trend since its unusual mortality event in 2015. The northern fulmar encounter rate was just below average in 2018 (the latest year of data) and showed a significant negative short-term trend. The sooty shearwater encounter rate in 2019 was below average, as it has been since a peak from 2011-2013. As mentioned in the main body of the report, preliminary information suggests that an unusual post-breeding mortality event involving rhinoceros auklets was also documented in Washington and Oregon in the fall of 2019, possibly indicating declining foraging conditions for these primarily piscivorous birds in the latter half of 2019 in the northern CCE.

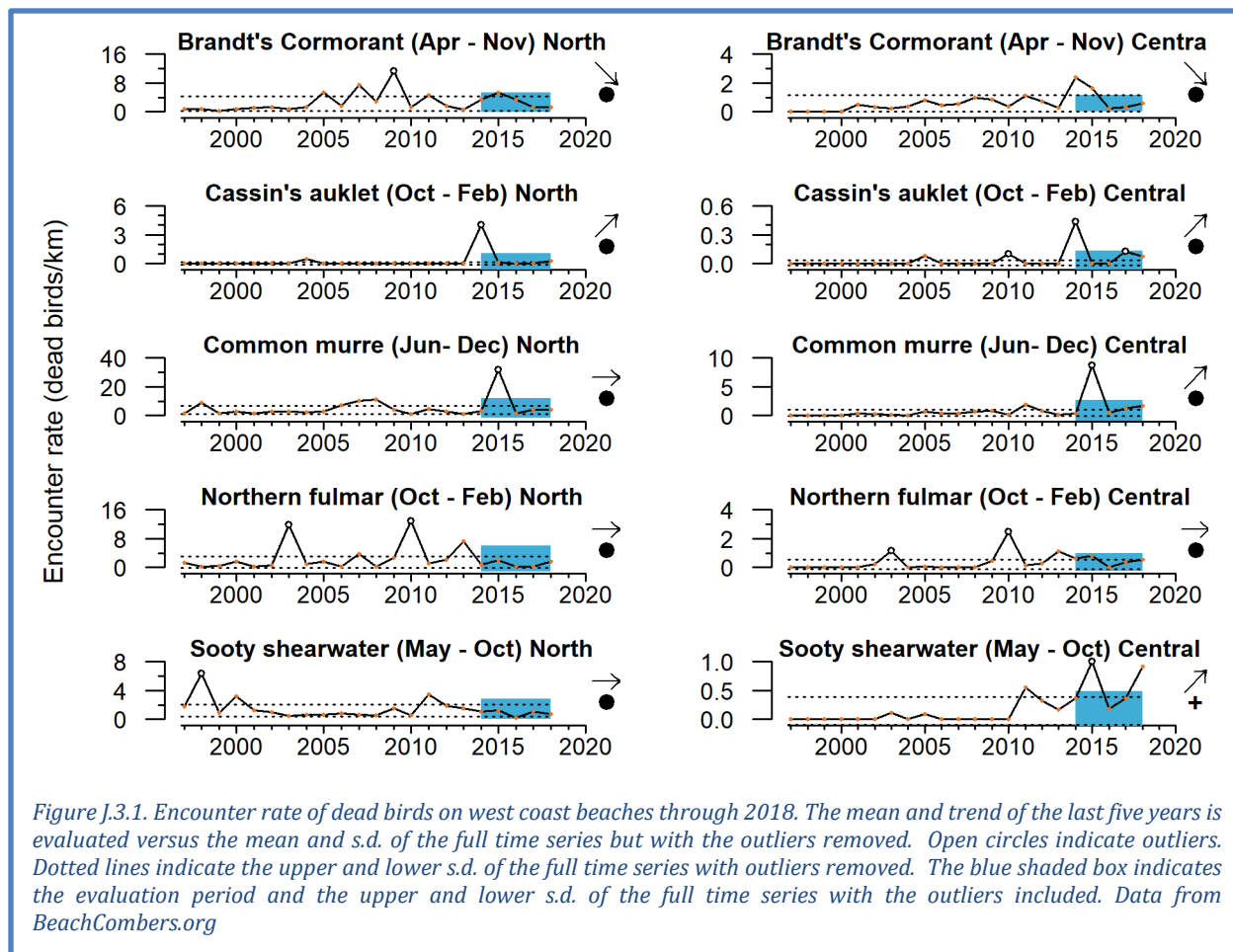
Although encounter rates of indicator species in the COASST survey were near their long-term means in 2019, there was a significant mortality event in COASST’s southern-most regions that is not evident in the spatially aggregated data shown in Figure J.3.1. Elevated numbers of dead adult common murres on beaches were documented during the breeding season in Humboldt and Mendocino counties in northern California. In Mendocino County, spring encounter rates were roughly an order of magnitude above normal (data not shown), and birds appeared emaciated.



In the central region of the CCE (Bodega Bay, CA to Point Año Nuevo, CA), the BeachWatch program documented beached birds at average to below average levels for five focal species in 2018 (Figure J.3.2). The Brandt's cormorant encounter rate was just below average in spring-fall 2019 and showed a significant negative short-term trend following the peak in 2015. The Cassin's auklet encounter rate continued at low baseline levels in 2017-2018 (the most recent year of data), as it has since a peak in 2013-2014. The common murre encounter rate was above average in 2019; common murre encounter rates have been increasing in recent years but remain well below the peak from the wreck in 2014-2015. The sooty shearwater encounter rate was close to average in spring-fall 2019; the peak it also experienced in 2015 was not sharp enough to result in a short-term negative trend. The northern fulmar encounter rate was just below average in 2017-2018, as it has been since a peak in 2009-2010.



Another survey of beached seabirds on California beaches occurs from Point Año Nuevo to Malibu, conducted by the BeachCOMBERS program. In the past, we have reported on two survey regions: north (Point Año Nuevo to Lopez Point, CA) and central (Lopez Point to Rocky Point, CA). These data have not been updated since last year's report, which was current through 2018 and generally found encounter rates at average to below-average levels (Figure J.3.3).



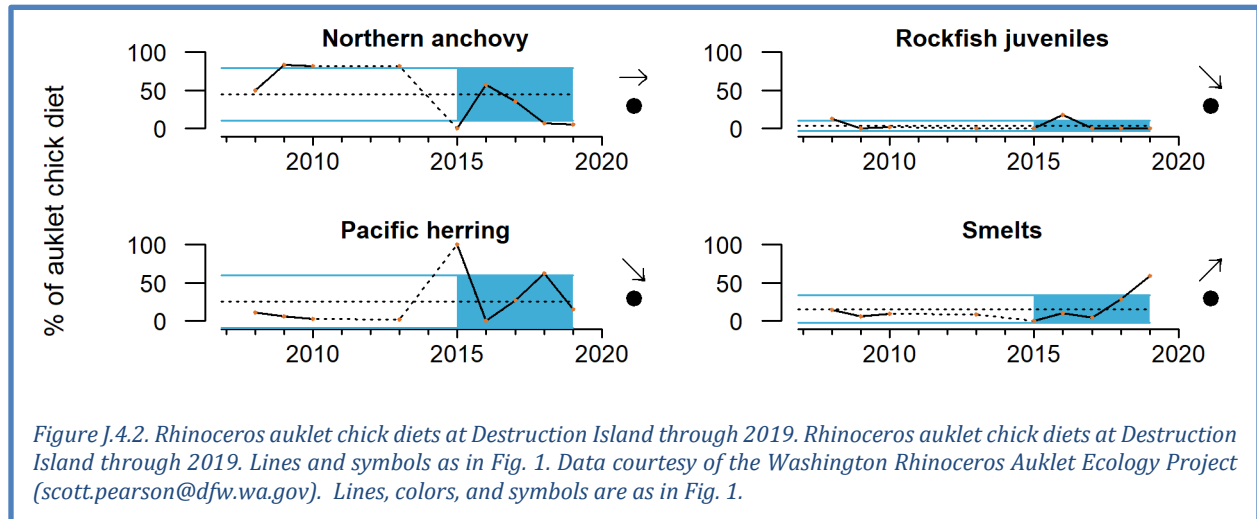
J.4 SEABIRD DIETS

Seabird diet composition during the breeding season tracks marine environmental conditions and often reflects production and availability of forage within regions. Here, we present some seabird diet data that may shed light on foraging conditions along the west coast in 2019. We are working with partner research organizations to better integrate this information into our reporting.

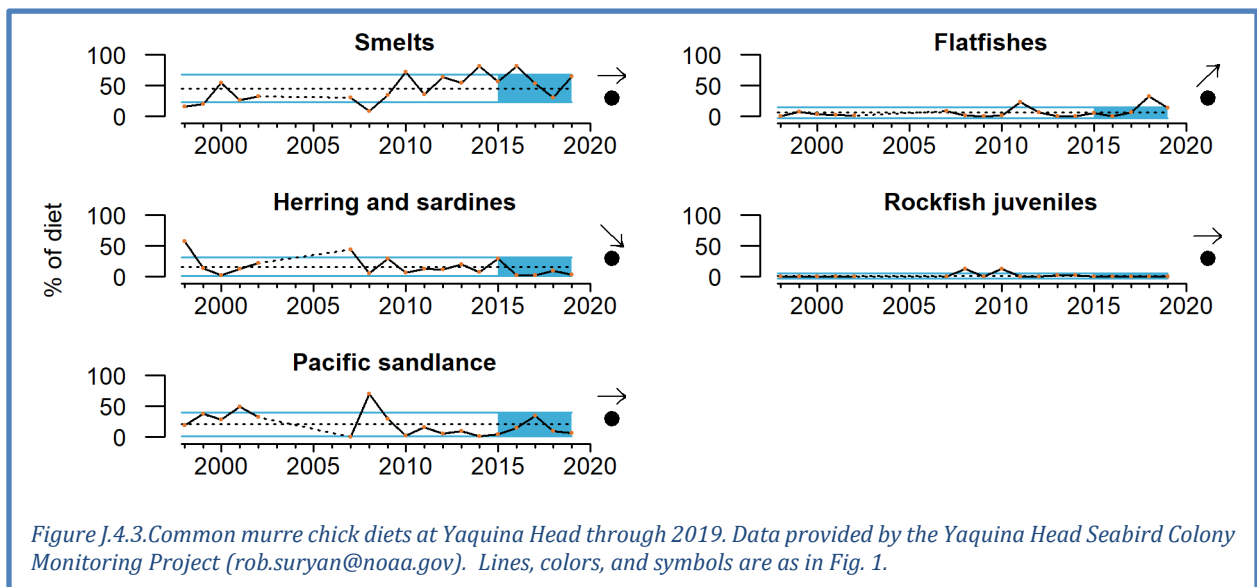
West coast researchers have long-term diet data for five key species in the northern and central CCE. Rhinoceros auklets forage primarily on pelagic fishes in shallow waters over the continental shelf, generally within 50 km of colonies, and they return to the colony after dusk to deliver multiple whole fish to their chicks. Common murres forage primarily on pelagic fishes in deeper waters over the shelf and near the shelf break, generally within 80 km of colonies, and they return to the colony during daylight hours to deliver single whole fish to their chicks. Cassin's auklets forage primarily on zooplankton in shallow water over the shelf break, generally within 30 km of colonies; they forage at day and night and return to the colony at night to feed chicks. Brandt's cormorants forage primarily on pelagic and benthic fishes in waters over the shelf, generally within 20 km of breeding colonies, and they return to the colony during the day to deliver regurgitated fish to their chicks. Pigeon guillemots forage primarily on small benthic and pelagic fish over the shelf, generally within 10 km of colonies, and they return to the colony during the day to deliver a single fish to their chicks.

The first key finding from seabird diet studies pertains to the relatively good production of fledglings at seabird colonies in the northern CCE, such as at Destruction Island, Washington and Yaquina Head, Oregon. Birds at these colonies tend to feed in relatively nearshore waters, where forage species such

as smelts are abundant and may supplement forage from open waters; smelts are not sampled effectively by the forage surveys described elsewhere (Section 4.2, Appendix G), but seabird diets from these colonies suggest that smelt were abundant in 2019 (Figure J.4.1 and Figure J.4.2). At Destruction Island, the proportion of smelts in the diets of rhinoceros auklets provisioning chicks was the highest that has been recorded and showed a significant positive short-term trend (Figure J.4.1). The proportions of anchovies and herring in rhinoceros auklet diets were below average in 2019, and the proportion of juvenile rockfish continued to be low since it peaked in 2016.

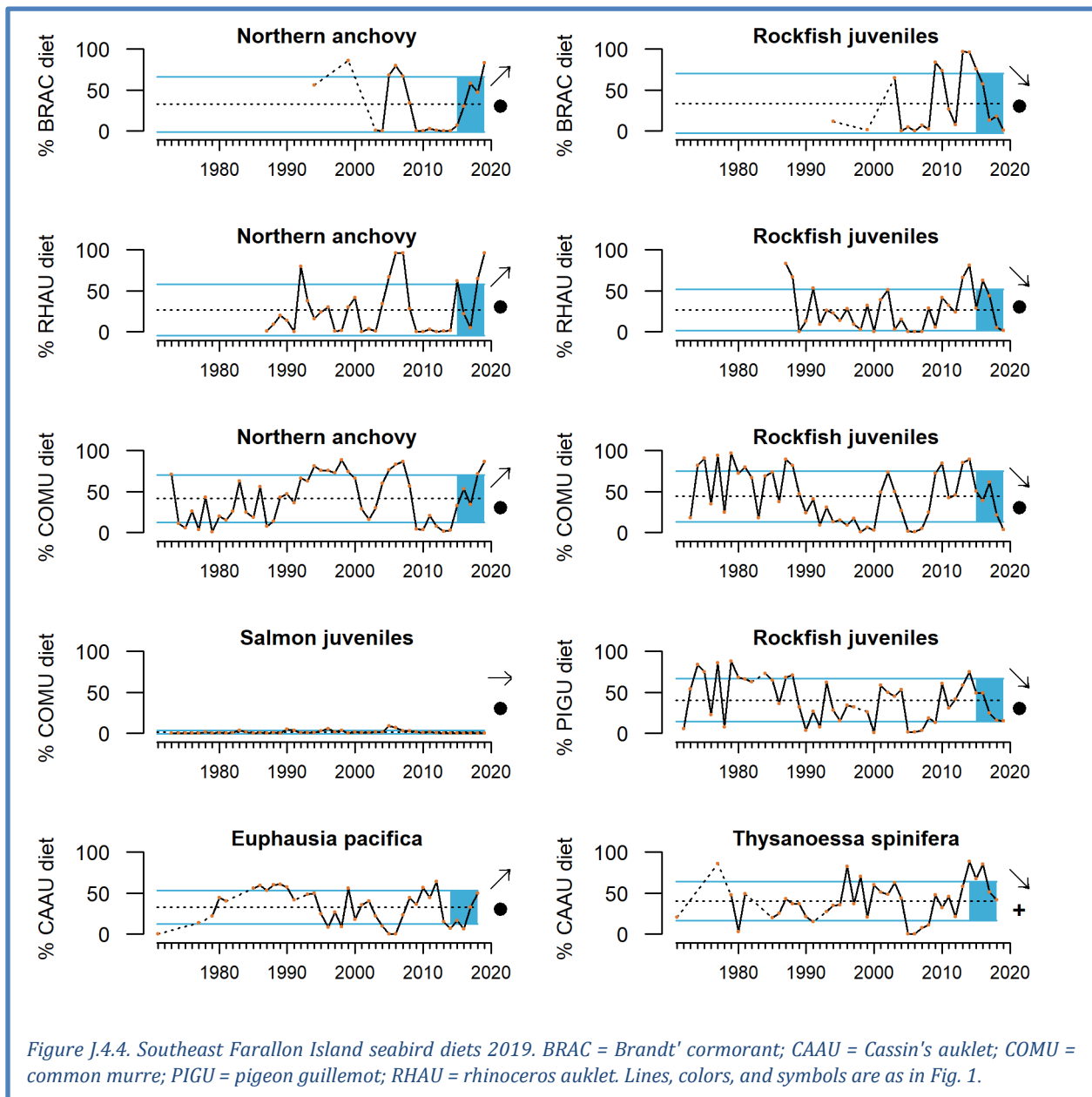


Similarly, at Yaquina Head, the proportion of smelts in the diet of common murres provisioning chicks was above average in 2019, after a below-average value in 2018 (Figure J.4.2). The proportions of herring and sardine in the murre diet were below average in 2019 and showed a significant short-term decline. The proportion of Pacific sandlance in the murre diet was below average in 2019. The proportion of flatfishes in the murre diet was above average for the second straight year and showed a significant positive short-term trend. The proportion of rockfish in the murre diet in was well below average for the fourth straight year, considerably lower than peaks in 2008 and 2010.

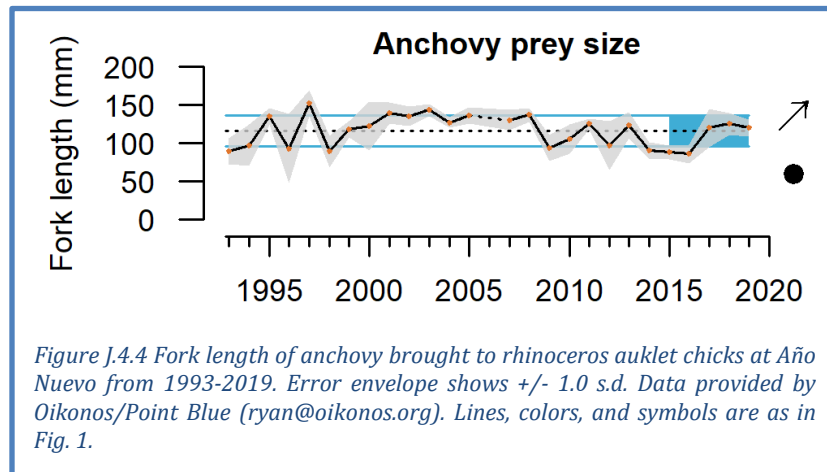


At colonies off central California, there are diet trends available for seabirds from Southeast Farallon Island (SEFI). Among piscivores, there has been increasing reliance on anchovy and decreasing

reliance on juvenile rockfish over the past five years. The proportions of anchovy in the diets of Brandt’s cormorants, rhinoceros auklets and common murre provisioning chicks on SEFI were well above average in 2019 and showed significant positive short-term trends, while the proportions of rockfish in these species’ diets were well below average in 2019 and showed significant negative short-term trends (Figure J.4.3). Pigeon guillemots showed a similar decline in juvenile rockfish. In addition, the proportion of salmonids in common murre diets at SEFI was well below average in 2019. Finally, Cassin’s auklets, which feed heavily on krill, are only current through 2018, prior to the 2019 decline in krill seen off central California (Figure G.2.2). The proportion of *Euphausia pacifica* in the diet of SEFI Cassin’s auklets was above average and showed a significant positive short-term trend, while the proportion of *Thysanoessa spinifera* in the auklet was near average but the recent mean is significantly greater than the long-term mean.



At another central California site, Año Nuevo Island, researchers noted that anchovy accounted for nearly 100% of the diets of rhinoceros auklets provisioning chicks in both 2018 and 2019; other prey resources like rockfish juveniles, market squid and Pacific saury, were very rarely delivered to chicks (data not shown). The size of anchovies returned to chicks on Año Nuevo Island in 2019 was above average and has increased since 2014-2016 (Figure J.4.4). Researchers expressed concern that these anchovy were too large to be ingested by rhinoceros auklet chicks, which may have contributed to the poor fledgling production in central California (e.g., Figure 4.7.1) despite the apparent abundance of anchovy.



Appendix K STATE-BY-STATE FISHERY LANDINGS AND REVENUES

The Council and the EWG have requested information on state-by-state landings and revenues from fisheries; these values are presented here. Data for landings and revenue were available for all states through 2018 at the March 2020 Briefing Book deadline. Fishery landings and revenue data are best summarized by the Pacific Fisheries Information Network (PacFIN, <http://pacfin.psmfc.org>) for commercial landings and by the Recreational Fisheries Information Network (RecFIN, <http://www.recfin.org>) for recreational landings. Landings provide the best long-term indicator of fisheries removals. Revenue was calculated based on consumer price indices for 2018.

K.1 STATE-BY-STATE LANDINGS

Total fisheries landings in California have decreased to the lowest levels of the time series in recent years, primarily due to steep decreases in landings of market squid in 2015, 2016 and 2018 (Figure K.1.1). Commercial landings of CPS finfish were >1 s.d. below long-term averages, while salmon, groundfish (excluding hake) and other species were near the lowest levels observed over the last 5 years. Crab landings have varied within ± 1 s.d. of time series averages over the last 5 years, but were above average in 2017 and 2018. Methods for sampling and calculating total mortality in recreational fisheries changed recently, leading to shorter comparable time series than shown in previous reports. Recreational landings in California (excluding salmon and Pacific halibut) had increased from 2008 to 2015 due to large increases in catches of yellowfin tuna, yellowtail and lingcod, but subsequent decreased landings in these three species are now responsible for the current decreasing trend

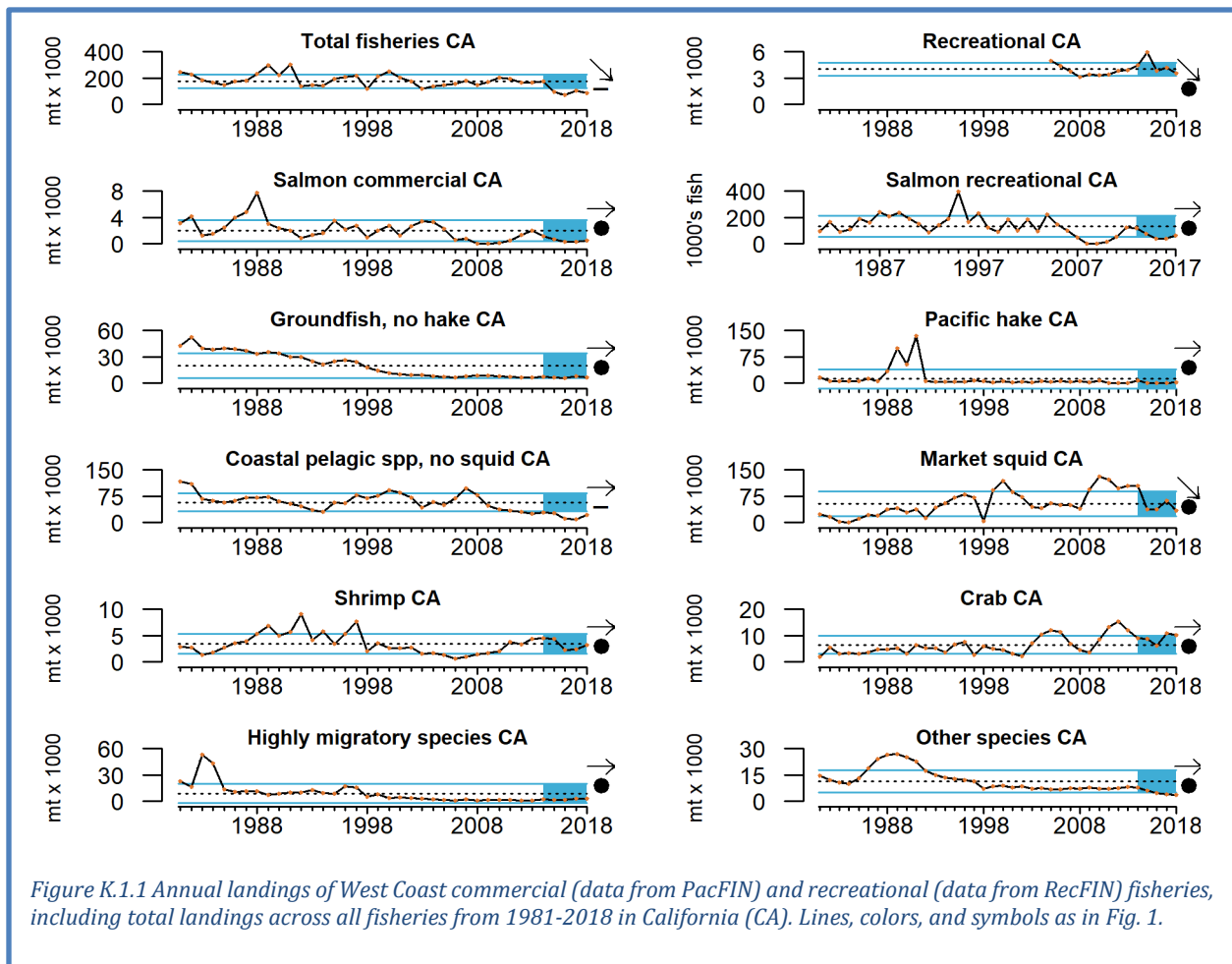
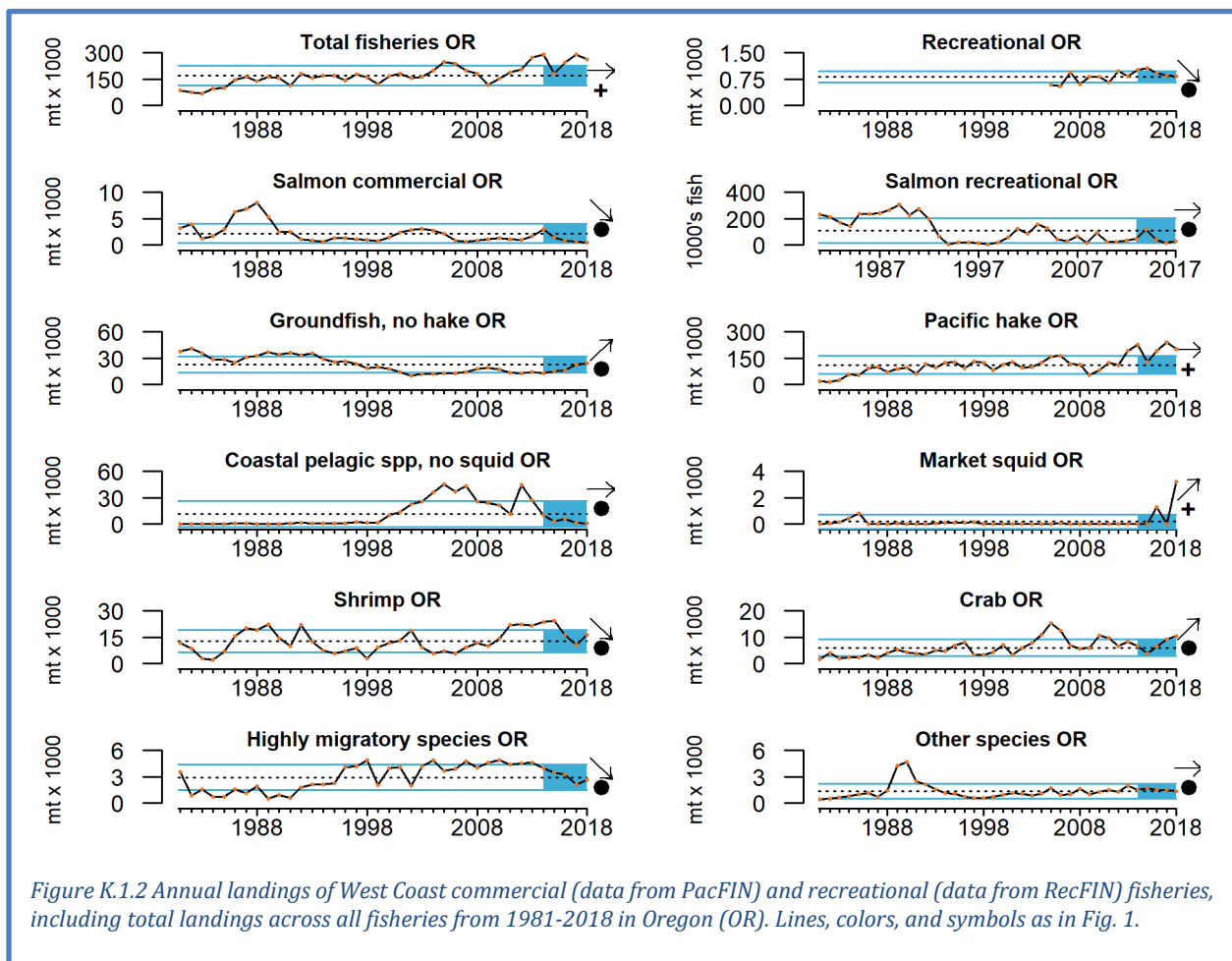


Figure K.1.1 Annual landings of West Coast commercial (data from PacFIN) and recreational (data from RecFIN) fisheries, including total landings across all fisheries from 1981-2018 in California (CA). Lines, colors, and symbols as in Fig. 1.

observed from 2014-2018 (Figure K.1.1). Recreational salmon landings (Chinook and coho) were relatively unchanged and at the lower boundary of the time series from 2014-2018.

Total fisheries landings in Oregon have varied but were above the time series average from 2014-2018 (Figure K.1.2). These patterns were primarily driven by recent landings of hake that were the highest of the time series. Commercial landings of salmon, shrimp and HMS species decreased from 2014-2018. Groundfish (excluding hake) and crab landings increased by >1 s.d. from long-term averages over the last five years. CPS finfish and other species landings were consistently within ± 1 s.d. of time series averages. Landings of market squid in Oregon have been at or near 0 across the time series, but landings over 1200 tons in 2016 and 3200 tons in 2018 suggests the potential for new fishing opportunity.

Methods for sampling and calculating total mortality in recreational fisheries changed recently, leading to shorter comparable time series than shown in previous reports. Recreational fisheries landings (excluding salmon and Pacific halibut) in Oregon showed a decreasing trend from 2014-2018 (Figure K.1.2). This decrease is primarily due to decreases in albacore and black rockfish landings. Chinook and coho salmon recreational landings showed no recent trends but were near the lower limits of the time series observations over the last five years.



Total fisheries landings in Washington increased sharply from 2014–2018, with particularly low landings in 2015 and a large increase in 2017 (Figure K.1.3). These patterns were driven by large increases in hake landings from 2015–2017. Shrimp and HMS landings decreased over the last five years. Landings of groundfish (excluding hake) were consistently below time series averages from 2014–2018, while landings of salmon, CPS finfish, crab and other species showed no current trends and were within ± 1 s.d. of time series averages over the last five years.

Methods for sampling and calculating total mortality in recreational fisheries changed recently, leading to shorter comparable time series than shown in previous reports. Total landings of recreational catch (excluding salmon and halibut) in Washington state decreased from 2014–2018, but remained within ± 1 s.d. of the full time series average (Figure K.1.3). The decrease is primarily due to decreases in albacore and black rockfish landings since 2016. Recreational landings of Chinook and coho salmon were highly variable, but within ± 1 s.d. of time series averages over the last five years.

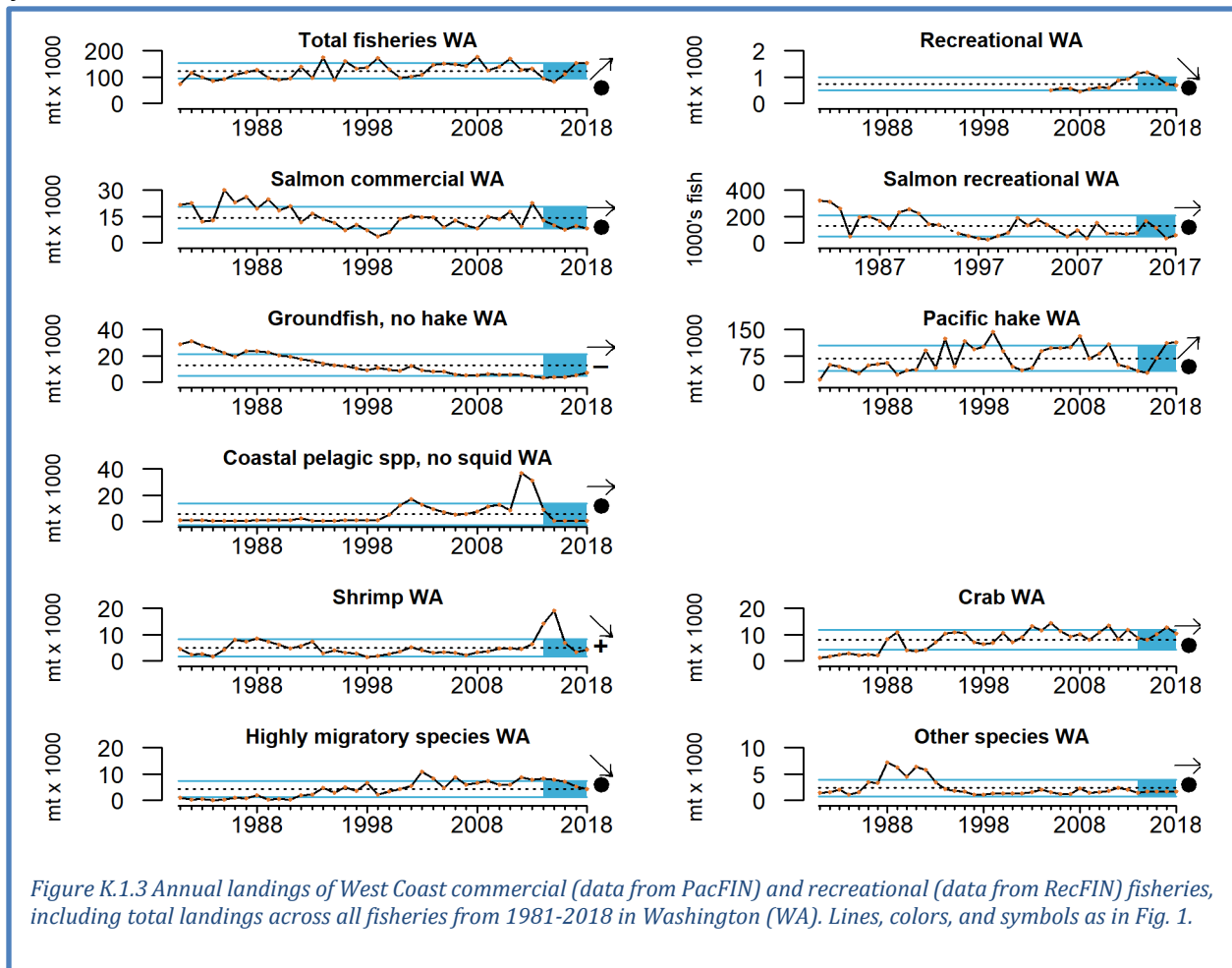
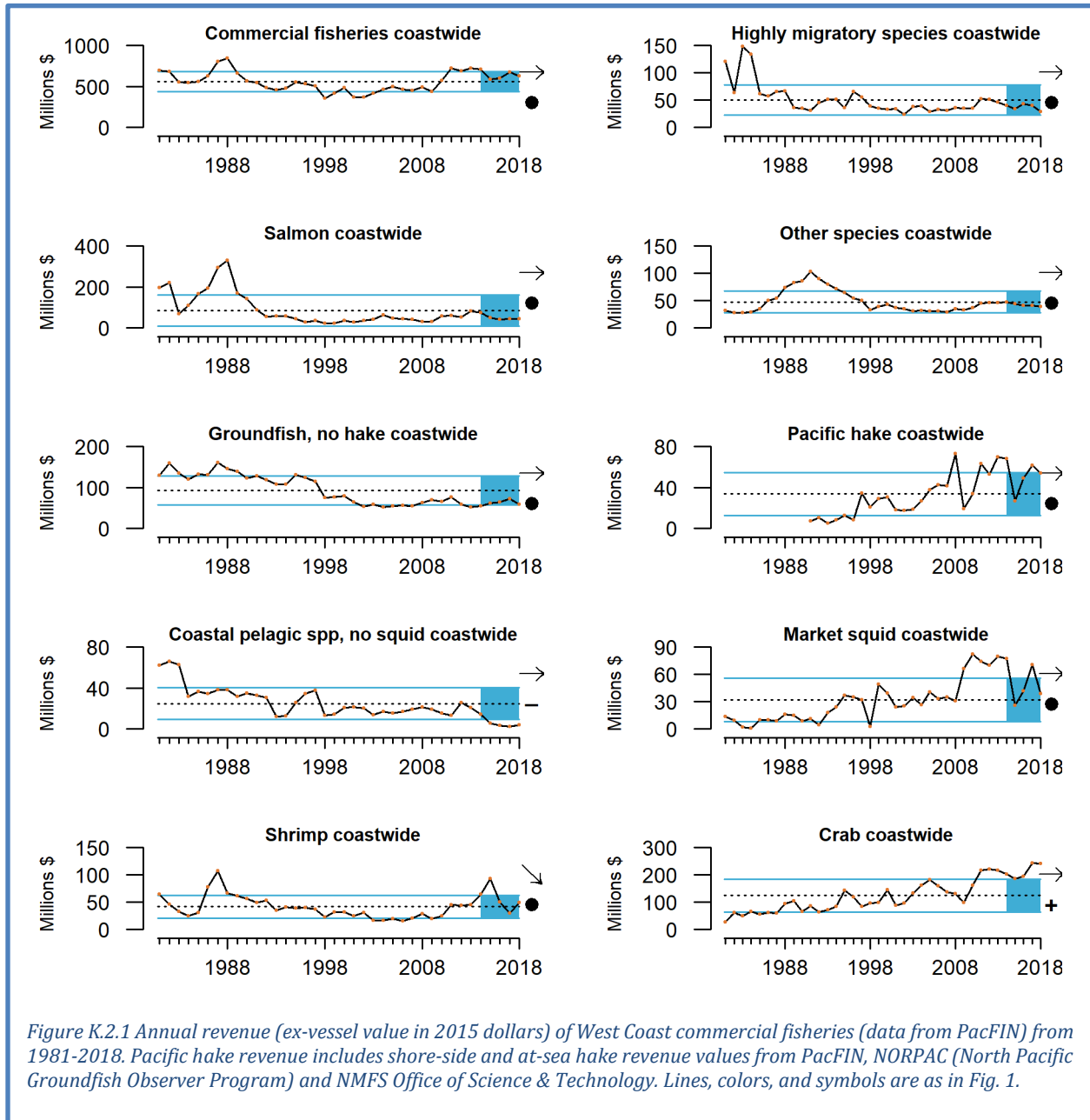


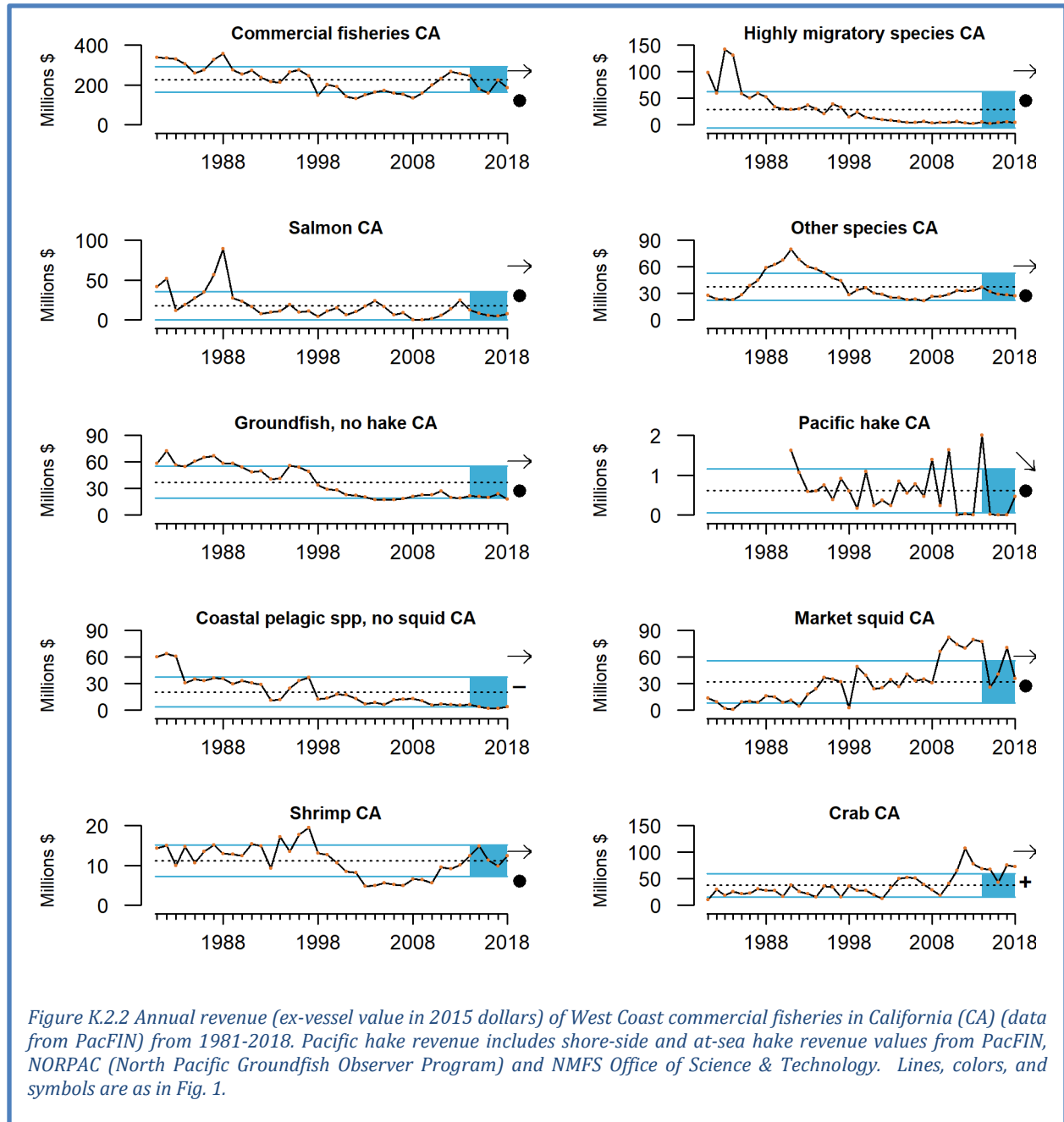
Figure K.1.3 Annual landings of West Coast commercial (data from PacFIN) and recreational (data from RecFIN) fisheries, including total landings across all fisheries from 1981-2018 in Washington (WA). Lines, colors, and symbols as in Fig. 1.

K.2 COMMERCIAL FISHERY REVENUES

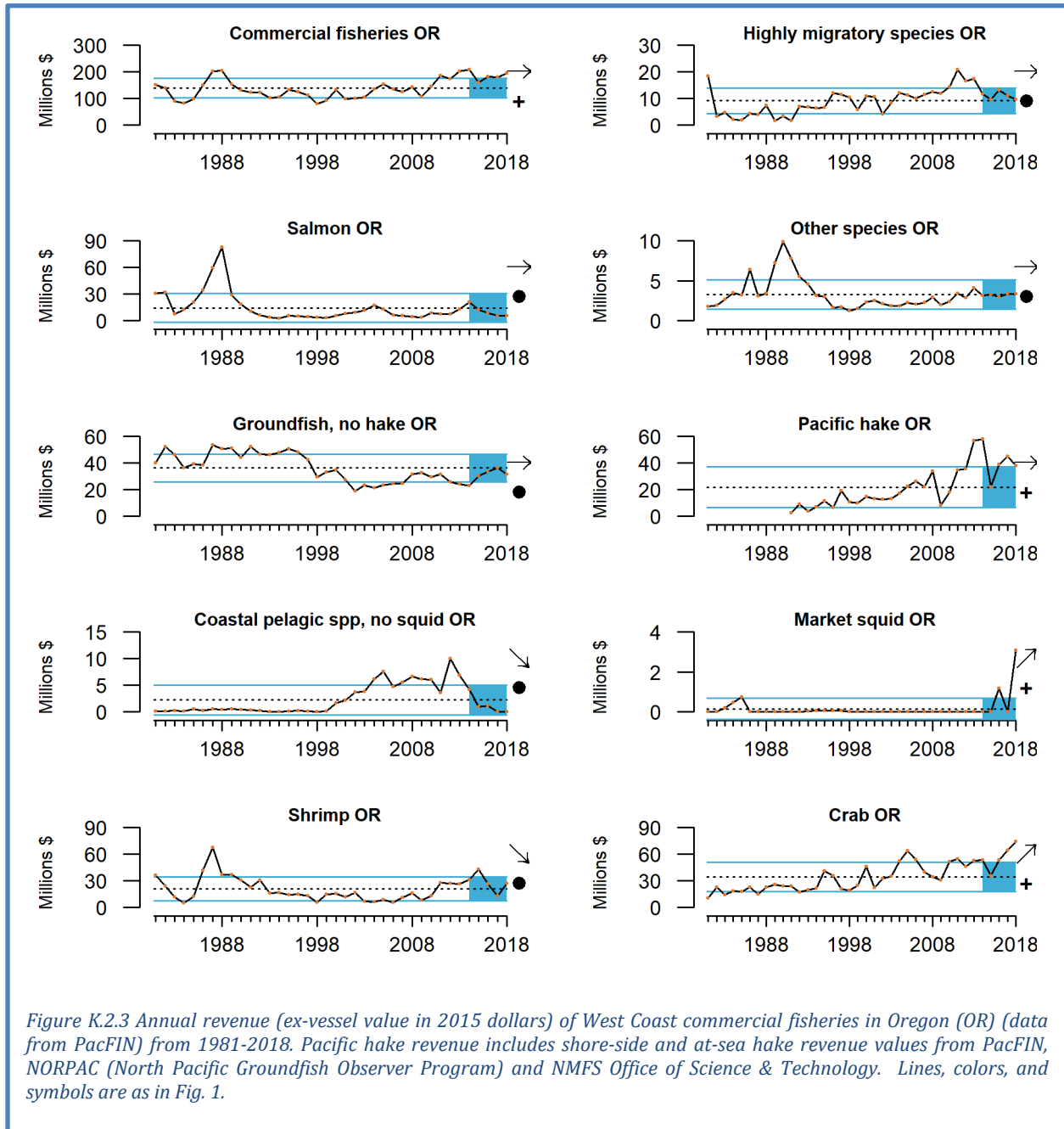
Total revenue across West Coast commercial fisheries from 2014–2018 has been near the upper range of the observed time series (Figure K.2.1). Recent patterns were driven primarily by interactions between high revenue from Pacific hake, market squid and crab fisheries, and decreasing revenue in the shrimp fishery over the last 5 years. Revenue from CPS finfish was >1 s.d. below long-term averages from 2014–2018. Revenue from HMS species, commercial salmon, Other species and groundfish (excluding hake) were relatively unchanged and within 1 s.d. of long-term averages over the last 5 years.



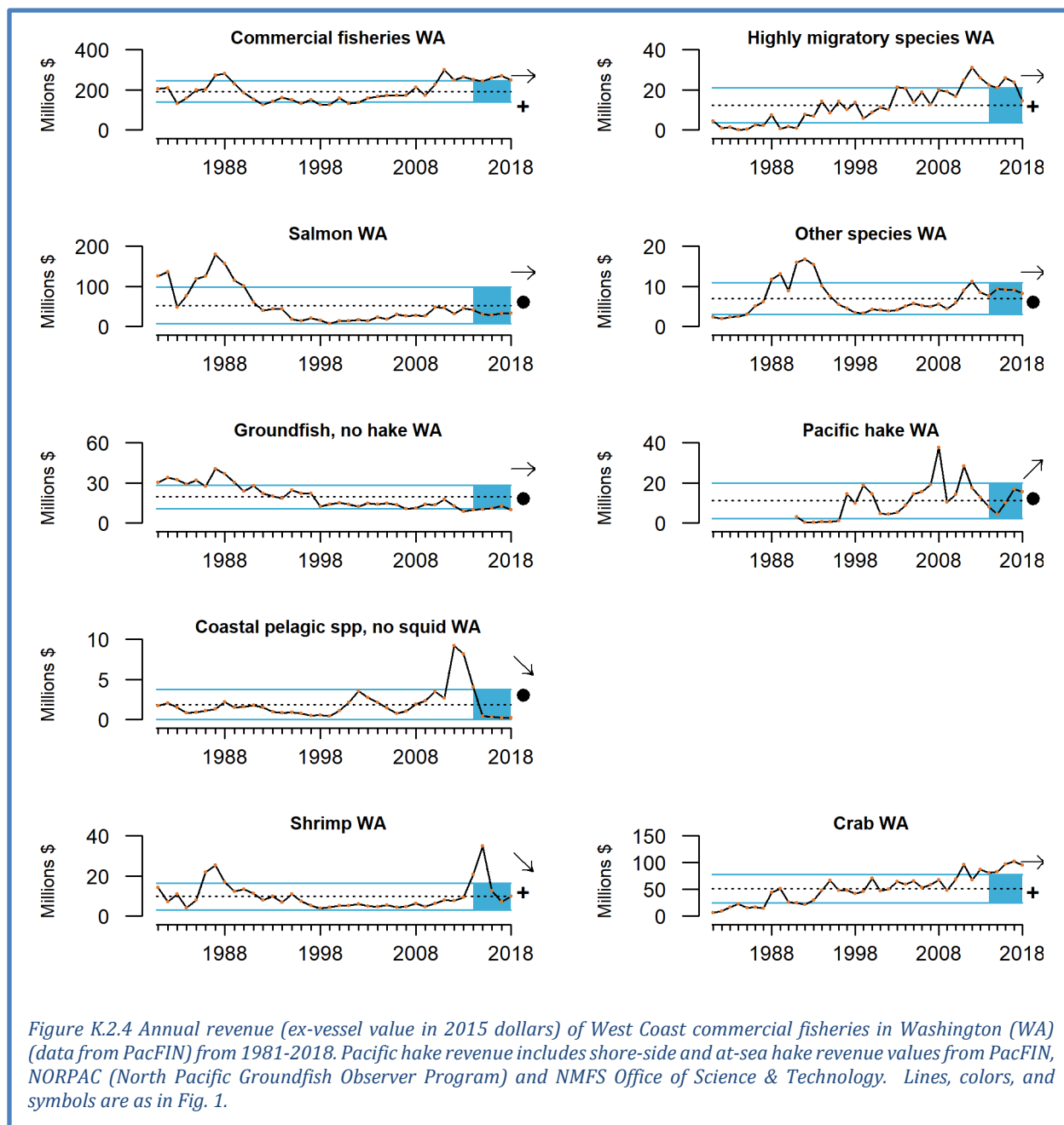
Total revenue across commercial fisheries in California varied within ± 1 s.d. of the time series average from 2014–2018 (Figure K.2.2). Revenue from crab fisheries is the most lucrative and was >1 s.d. above long-term averages, while CPS finfish revenue was >1 s.d. below long-term averages in recent years. Pacific hake revenue decreased, but this fishery accounts for a very small portion of total revenue in California. Revenue from HMS species, commercial salmon, Other species, groundfish (excluding hake), market squid and shrimp showed no recent trends and varied within historical averages over the last five years.



Total revenue across commercial fisheries in Oregon was near the upper range of the time series in 2014–2018 (Figure K.2.3). This was driven by higher than average revenues for Pacific hake and crab, along with increases in revenue from groundfish fisheries. CPS finfish and shrimp revenue declined over the last 5 years. Market squid showed a large increase in revenue in 2016 and another in 2018 that may be related to unusual oceanographic conditions that have pushed market squid north in the system. All other fisheries revenues in Oregon showed no trends and were within ± 1 s.d. of long-term averages over the last 5 years.



Total revenue across commercial fisheries in Washington remained relatively unchanged and above the long-term average from 2014–2018 (Figure K.2.4). This was a similar pattern to that observed in Oregon over the same time period (Figure K.2.3). The pattern in Washington is primarily driven by the relatively consistent and above-average levels of revenue for crab and HMS, the increasing trend in hake, and the peak in revenue in the shrimp fisheries observed in 2015. Revenue for CPS finfish decreased from 2014-2018 and is near zero. Revenue of non-hake groundfish remained near the lower range of the time series from 2014-2018, while revenue from salmon and Other species showed no significant trends and were within 1 s.d. of long-term averages over the last 5 years.



Appendix L FISHING GEAR CONTACT WITH SEAFLOOR HABITAT

In Section 5.2 of the report, we presented a spatial representation of the status and trends of gear contact with the seafloor as a function of distances trawled. We used estimates of coastwide distances exposed to bottom trawl fishing gear along the ocean bottom from 1999–2018. We calculated trawling distances based on set and haul-back locations. Data come from logbooks analyzed by the Northwest Fisheries Science Center’s West Coast Groundfish Observer Program. Here, we present time series of the data at a coastwide scale and broken out by ecoregion (Northern, north of Cape Mendocino; Central, Cape Mendocino to Point Conception; and Southern, south of Point Conception), substrate type (hard, mixed, soft) and depth zone (shelf, upper slope, lower slope).

At the scale of the entire coast, bottom trawl gear contact with seafloor habitat remained consistently at historically low levels from 2014–2018 (Figure L.1, top). During this period, the vast majority of bottom trawl gear contact occurred in soft, upper slope and soft, shelf habitats (Figure L.1, bottom). The Northern ecoregion has seen the most bottom trawl fishing gear contact with seafloor habitat with nearly five times the magnitude as observed in the central ecoregion in soft, upper slope habitat. Very little to no bottom trawling has occurred in the Southern ecoregion within the time series. A shift in trawling effort from shelf to upper slope habitats was observed during the mid-2000’s, which in part corresponded to depth-related spatial closures implemented by the Council. With new spatial closures and openings beginning in 2020, this indicator will be of interest to monitor over the next few years for changes in bottom trawl fishing effort. Reduced bottom trawl gear contact may not coincide with recovery times of habitat depending on how fast recovery happens, which is likely to differ among habitat types (e.g., hard and mixed habitats will take longer to recover than soft habitat).

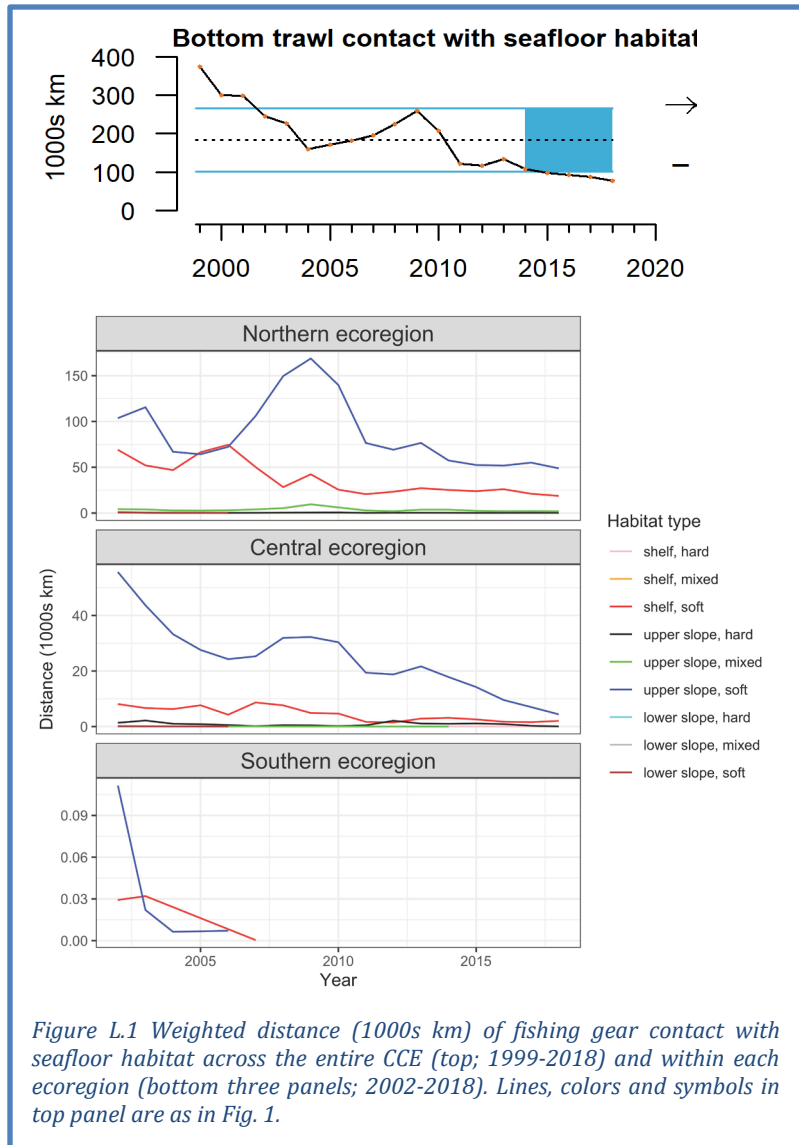
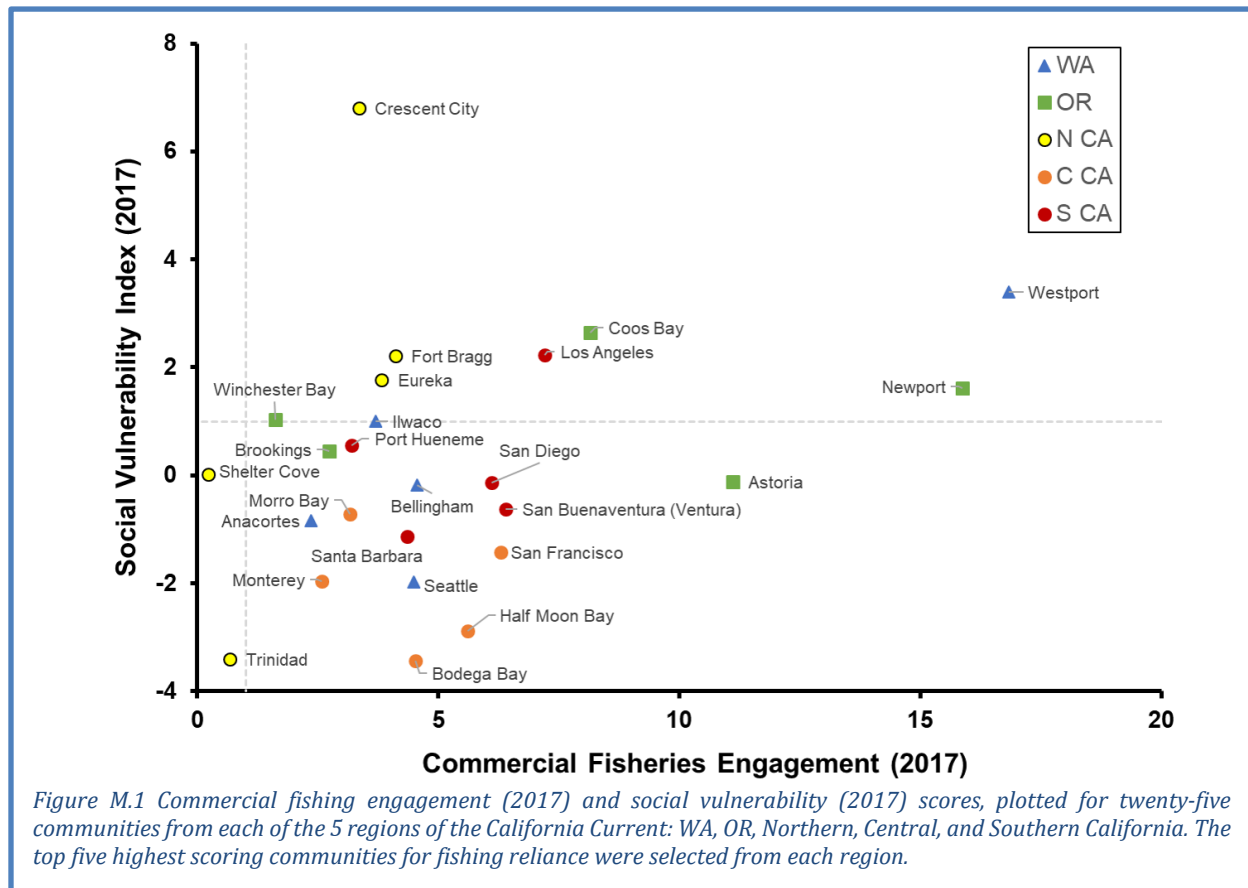


Figure L.1 Weighted distance (1000s km) of fishing gear contact with seafloor habitat across the entire CCE (top; 1999-2018) and within each ecoregion (bottom three panels; 2002-2018). Lines, colors and symbols in top panel are as in Fig. 1.

Appendix M SOCIAL VULNERABILITY OF FISHING-DEPENDENT COMMUNITIES

In Section 6.1 of the main report, we present information on the Community Social Vulnerability Index (CSVI) as an indicator of social vulnerability in coastal communities that are dependent upon commercial fishing. Fishery *dependence* can be expressed by two terms, or by a composite of both. Those terms are engagement and reliance. *Engagement* refers to the total extent of fishing activity in a community; engagement can be expressed in terms of commercial activity (e.g., landings, revenues, permits, processing, etc.) or recreational activity (e.g., number of boat launches, number of charter boat and fishing guide license holders, number of charter boat trips, number of bait and tackle shops, etc.). *Reliance* is the per capita engagement of a community; thus, in two communities with equal engagement, the community with the smaller population would have a higher reliance on its fisheries activities.

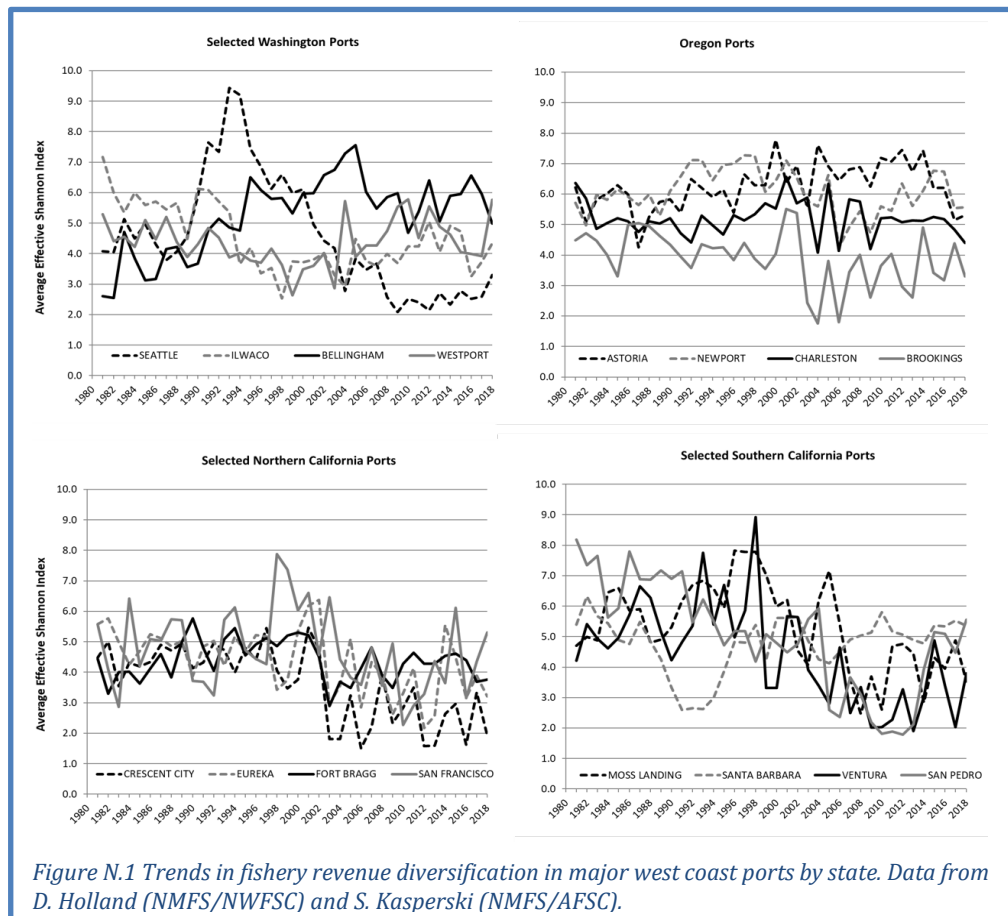
In the main body of the report, Figure 6.1.1 plots CSVI in 2017 against commercial reliance for the five most dependent communities in each sector from each of five regions of the CCE. Here, we present a similar plot of CSVI relative to commercial fishing engagement scores from 2017. Figure M.1 shows commercial fishing-engaged communities and their corresponding social vulnerability results. Communities above and to the right of the dashed lines are at least 1 s.d. above the coastwide averages of both indices. Of note are fishing-oriented communities like Westport, Crescent City, Coos Bay, Newport, Fort Bragg, Eureka, and Winchester Bay, which have relatively high commercial fishing engagement results and also a high CSVI composite result.



Appendix N FLEET DIVERSIFICATION INDICATORS FOR MAJOR WEST COAST PORTS

Catches and prices from many fisheries exhibit high interannual variability, leading to high variability in fishermen’s revenue, but variability can be reduced by diversifying activities across multiple fisheries or regions (Kasperski and Holland 2013). It should be noted that there may be good reasons for individuals to specialize, including reduced costs or greater efficiency; thus while diversification may reduce income variation, it does not necessarily promote higher average profitability. Kasperski (AFSC) and Holland (NWFSC) examined diversification of fishing revenue for more than 28,000 vessels fishing off the West Coast and Alaska over the last 38 years. As a measure of diversification, we use the effective Shannon index (ESI). ESI increases as revenues are spread across *more* fisheries, and as revenues are spread more *evenly* across fisheries; ESI = 1 when a vessel’s revenues are from a single species group and region; ESI = 2 if revenues are spread evenly across 2 fisheries; ESI = 3 if revenues are spread evenly across 3 fisheries; and so on. If revenue is not evenly distributed across fisheries, then the ESI value is lower than the number of fisheries a vessel enters.

As is true with individual vessels, the variability of landed value at the port level is reduced with greater diversification of landings. Diversification of fishing revenue has declined over the last several decades for some ports (Figure N.1). Examples include Seattle and most but not all ports in Southern Oregon and California. However, a few ports have become more diversified including Bellingham Bay and Westport in Washington. Diversification of Astoria, in Oregon, had been increasing but has decreased in recent years while Brookings has had an erratic increasing trend. Diversification scores are highly variable year-to-year for some ports, particularly those in Southern Oregon and Northern California that depend heavily on the Dungeness crab fishery, which has highly variable landings. Some ports saw a decrease in diversification between 2017 and 2018, but others saw an increase.



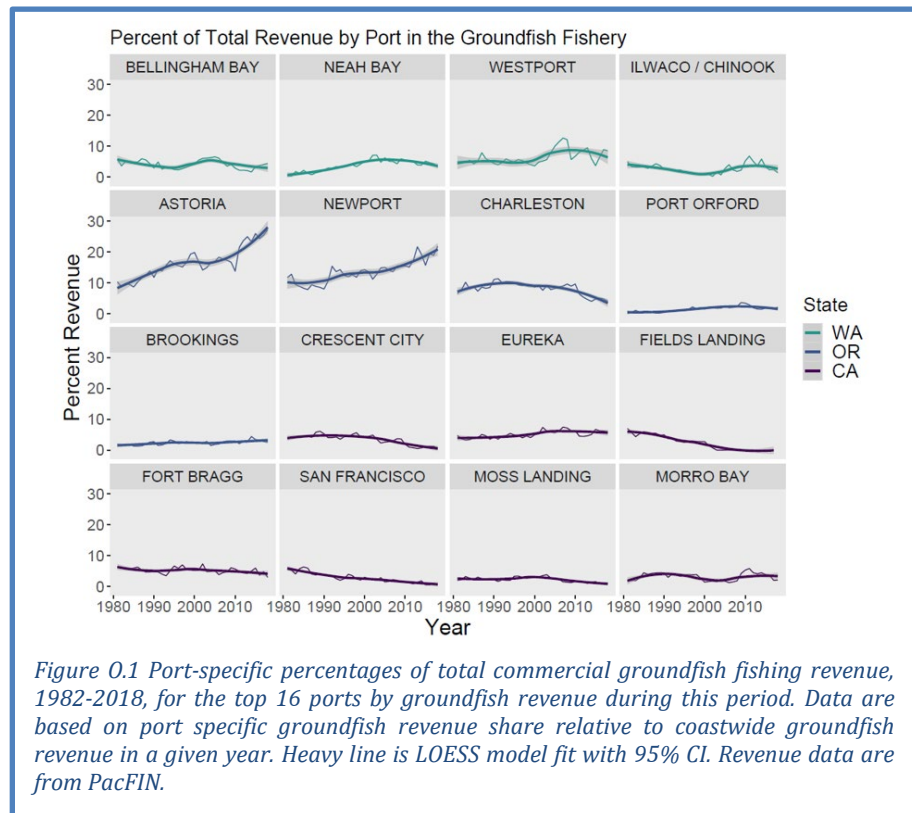
Appendix O REVENUE CONSOLIDATION BY FISHERY MANAGEMENT PLAN

At the request of the Ecosystem Advisory Subpanel, we are working to develop indicators relevant to National Standard 8 (NS-8) of the Magnuson-Stevens Act. NS-8 states that: “Conservation and management measures shall, consistent with the conservation requirements of this Act (including the prevention of overfishing and rebuilding of overfished stocks), take into account the importance of fishery resources to fishing communities by utilizing economic and social data that meet the requirement of paragraph (2) [i.e., National Standard 2], in order to (a) provide for the sustained participation of such communities, and (b) to the extent practicable, minimize adverse economic impacts on such communities.” (NS-2 states that “Conservation and management measures shall be based upon the best scientific information available.”)

Following initial discussions with economists in the NOAA IEA network, we chose to examine ex-vessel revenue as a potential indicator of progress toward NS-8. In particular, we are looking at how the proportion of revenues taken in by commercial fishing operations by different ports has changed over time. Consolidation of revenue into a smaller number of ports may indicate that fishery access opportunities are changing and potentially constraining some communities (Kuriyama et al. 2019).

Methods: Total revenue per year was calculated annually for ports in Washington, Oregon and California from 1982 to 2018, and compared to the cumulative revenue for all ports by year generating percent revenue share by port. Revenue was calculated in cpi-adjusted dollars reported by port. FMP-specific fishery revenues were calculated by aggregating revenues based on management species groups and comparing them to the coast-wide cumulative annual revenues. Salmon, HMS, CPS, and groundfish fisheries were all considered; we evaluated groundfish both with and without Pacific hake. For space considerations, we present only the 16 ports with the highest revenue proportions over the full time series (except for CPS, for which only 12 ports were frequent participants). The proportional revenue represented the revenue share for a single port’s landings compared to cumulative revenue by all ports with landings that matched the given fishery type. A LOESS model was applied to estimate a smoothing curve with a 95% confidence interval.

Results: For all groundfish, revenue has become more concentrated in a few ports since 1982, most notably Astoria and Newport (Figure O.1). Several other ports have had small increases on average over the full time period (Neah Bay, Port Orford, Brookings, Eureka) while others have had increases since ~2000 (Westport, Ilwaco/Chinook, Morro Bay). Other ports in this top-16 list saw declines



in percent of total groundfish revenue, some gradually over the full time series (e.g., Fields Landing, Fort Bragg, San Francisco) and others more recently (Charleston, Crescent City, Moss Landing).

When we excluded hake revenue from this analysis, the list of top-16 ports did not change, but patterns changed for some ports (Figure 0.2). Westport saw a downturn in non-hake groundfish revenue, dating to the 1990s, in contrast to the relative increase that Westport experienced in the 2000s when hake are included (Figure 0.1). Also, the increasing trend for Astoria was more gradual in non-hake groundfish. Otherwise, changes were minor, likely reflecting that many of these communities do not have hake landings.

For CPS, only 12 ports were regular-enough recipients of CPS landings to be included in the analysis. Patterns of CPS revenue percentage were highly dynamic for most ports, both from year to year and over the long term (Figure 0.3). Ventura experienced a long-term increase, as did Moss Landing and Half Moon Bay, although not to the extent of Ventura. Sausalito, San Francisco and Terminal Island all declined. Monterey had been declining until an increase that began prior to 2010, while Port Hueneme increased for the first half of

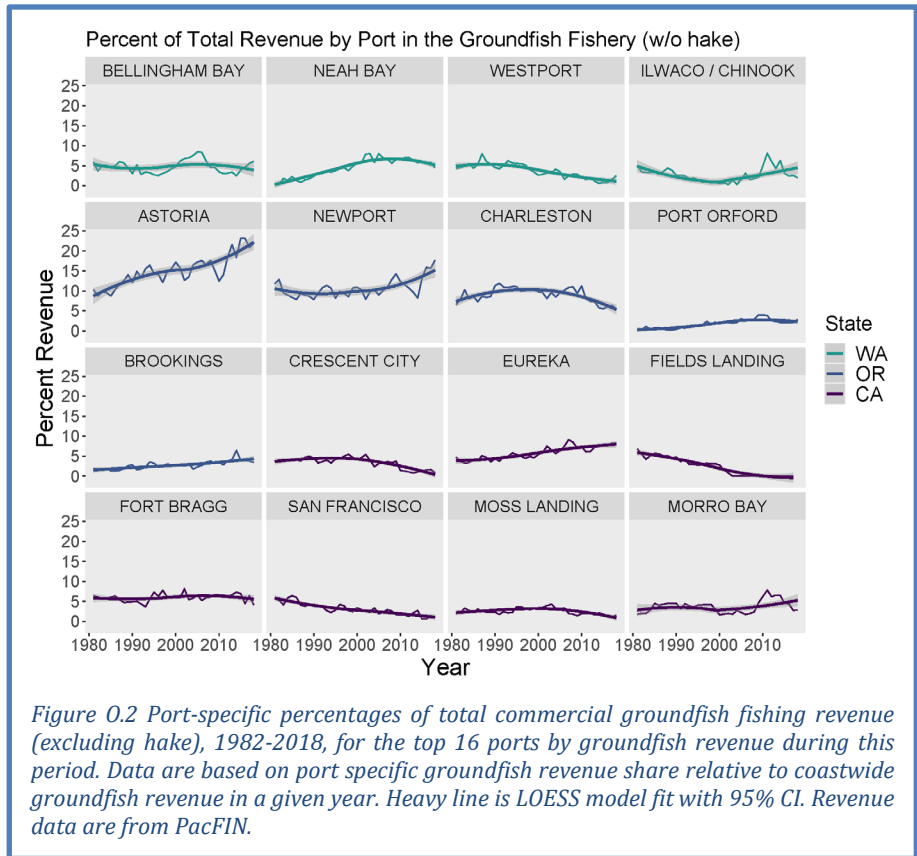


Figure 0.2 Port-specific percentages of total commercial groundfish fishing revenue (excluding hake), 1982-2018, for the top 16 ports by groundfish revenue during this period. Data are based on port specific groundfish revenue share relative to coastwide groundfish revenue in a given year. Heavy line is LOESS model fit with 95% CI. Revenue data are from PacFIN.

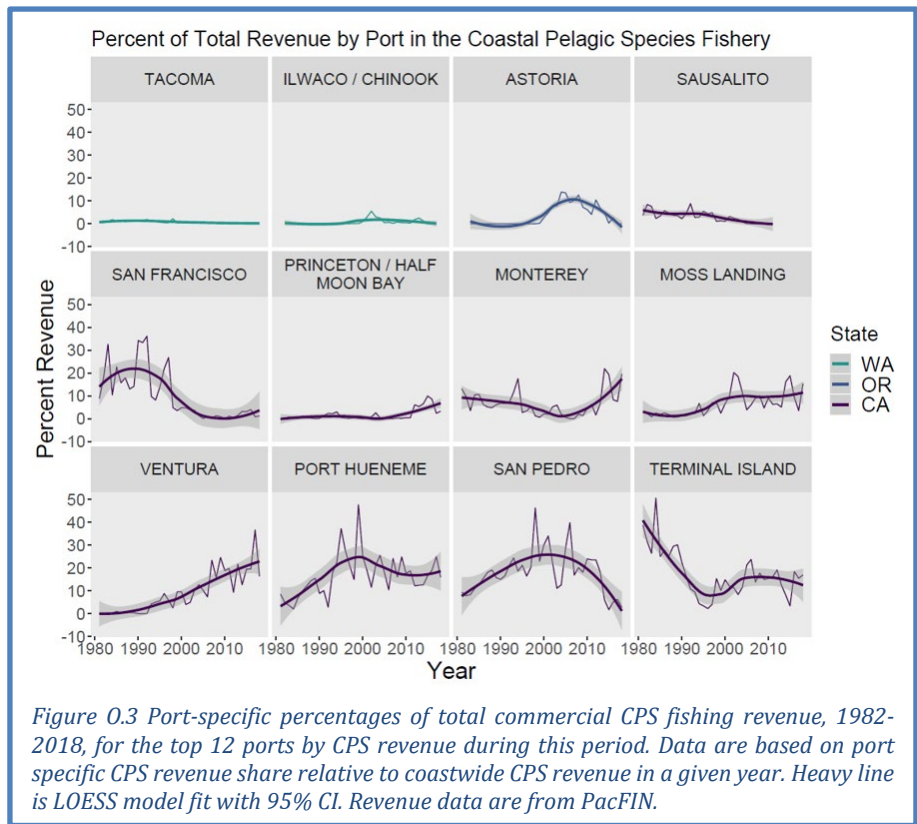


Figure 0.3 Port-specific percentages of total commercial CPS fishing revenue, 1982-2018, for the top 12 ports by CPS revenue during this period. Data are based on port specific CPS revenue share relative to coastwide CPS revenue in a given year. Heavy line is LOESS model fit with 95% CI. Revenue data are from PacFIN.

the time series then leveled off. Astoria and San Pedro had dome-shaped patterns. Very little CPS revenue came from Washington.

The list of top-16 commercial salmon ports was very different, and half were located in the Salish Sea (Puget Sound and the Strait of Juan de Fuca). Most patterns showed high interannual variability and several long-term trends (Figure 0.4). Several ports in the Salish Sea experienced long-term declines in revenue percentage (Blaine, Bellingham, La Conner, Port Angeles) while others generally had long-term increases (Neah Bay, Shelton). Aggregated ports along the Washington outer coast and in the Columbia River also saw increases. Top commercial salmon ports in coastal Oregon and California typically experienced long-term oscillating patterns, and it is difficult to discern any clear long-term trends over the full course of the time series.

The list of top-16 commercial HMS ports is again different from the other FMPs, and the trends from these ports show dramatic changes (Figure 0.5), primarily an increase in commercial HMS revenue percentage for several northern ports where albacore are landed (Westport, Ilwaco/Chinook, Newport, Charleston) and declines in southern ports (San

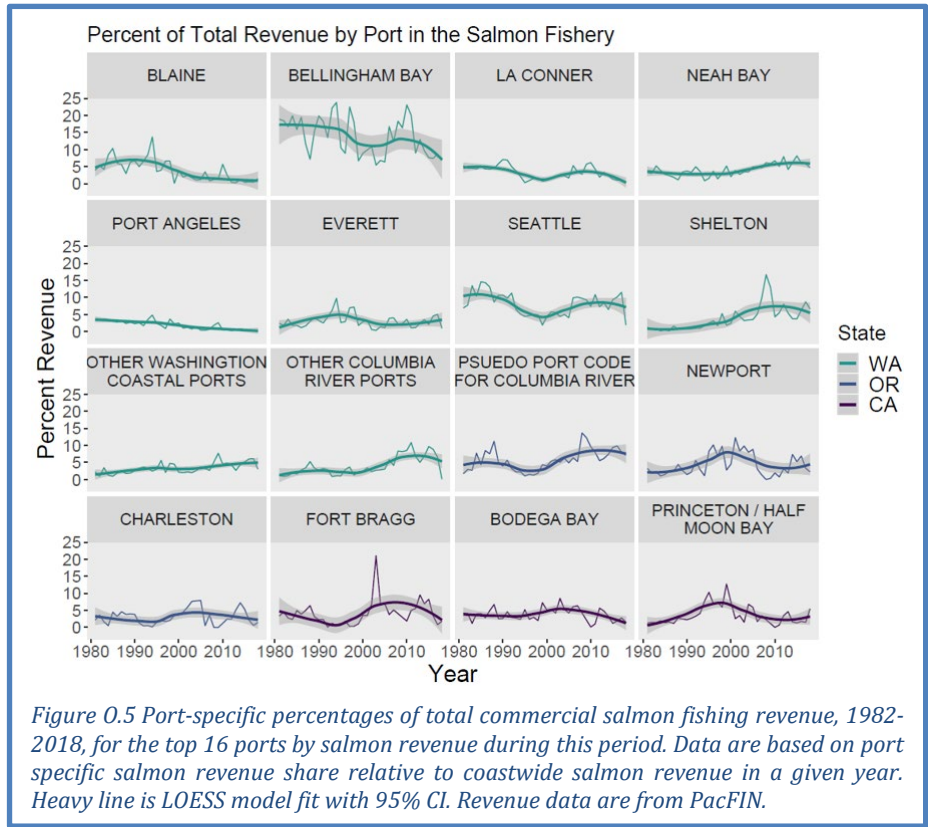


Figure 0.5 Port-specific percentages of total commercial salmon fishing revenue, 1982-2018, for the top 16 ports by salmon revenue during this period. Data are based on port specific salmon revenue share relative to coastwide salmon revenue in a given year. Heavy line is LOESS model fit with 95% CI. Revenue data are from PacFIN.

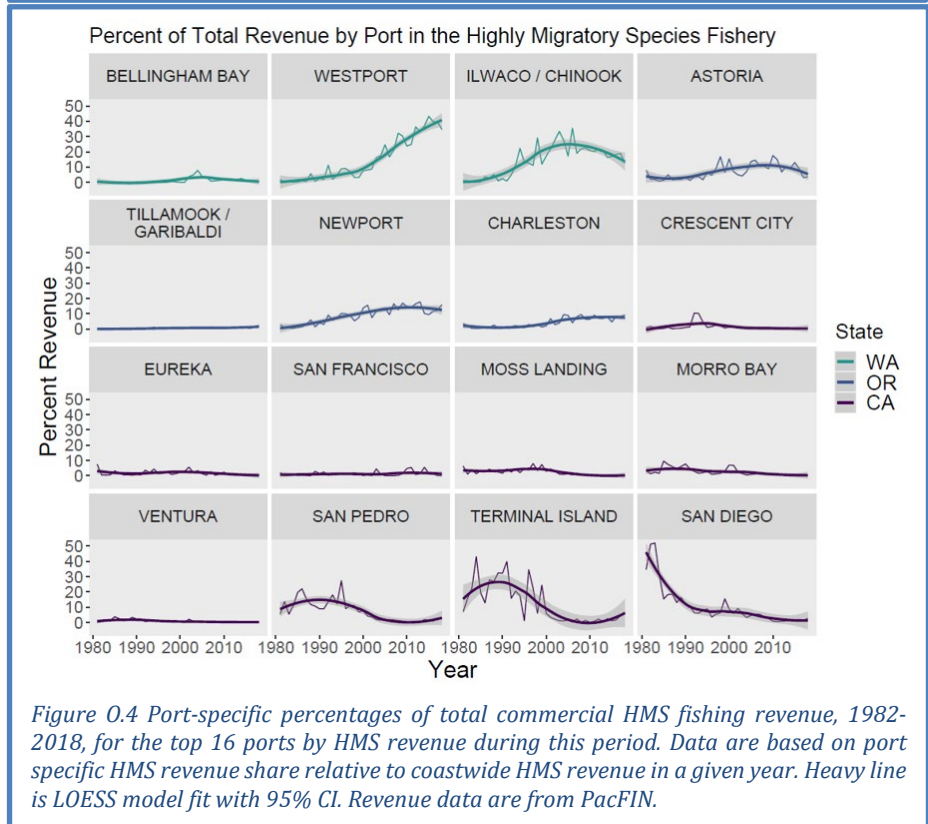


Figure 0.4 Port-specific percentages of total commercial HMS fishing revenue, 1982-2018, for the top 16 ports by HMS revenue during this period. Data are based on port specific HMS revenue share relative to coastwide HMS revenue in a given year. Heavy line is LOESS model fit with 95% CI. Revenue data are from PacFIN.

Pedro, Terminal Island, and San Diego). For most of the other ports, the percentage of commercial HMS revenue was quite low.

We must stress several key points regarding these analyses:

- The analyses are preliminary, and we will be doing subsequent work internally and ideally with the PFMC SSC to ensure the analyses are appropriate. For example, as of the briefing book deadline, we have not determined if communities that are experiencing negative trends in percent revenue are also experiencing net decreases in revenue, an important consideration for making judgments about impacts.
- We also have made no effort yet to attribute changes in revenue percentage with management actions, environmental changes, food web changes, or changes within coastal communities. It is therefore premature to link any of these changes explicitly to revenue consolidation as a measure of community-level economies or opportunities in the context of NS-8. We will work with the Council and advisory bodies on how to best approach such interpretation so that this indicator is evaluated for its usefulness.
- The analyses only consider a subset of communities with relatively high revenues for each FMP, and NS-8 is not meant to be selective in that manner. We will thus work to identify ways to classify changes in revenue across a wider range of communities, if this indicator proves to be useful. Because port communities have different levels of coastal community vulnerability (see Section 6.1), they likely experience changes in revenue in different contexts.

Appendix P REFERENCES

- Abell, R., *et al.* 2008. Freshwater ecoregions of the world: A new map of biogeographic units for freshwater biodiversity conservation. *BioScience* 58:403-414.
- Bednaršek, N., *et al.* 2020. Exoskeleton dissolution with mechanoreceptor damage in larval Dungeness crab related to severity of present-day ocean acidification vertical gradients. *Science of the Total Environment*, article no. 136610.
- Burke, B.J., *et al.* 2013. Multivariate models of adult Pacific salmon returns. *PLoS One* 8:e54134.
- Chan, F., *et al.* 2008. Emergence of anoxia in the California current large marine ecosystem. *Science* 319:920-920.
- Dyson, K., Huppert, D.D. 2010. Regional economic impacts of razor clam beach closures due to harmful algal blooms (HABs) on the Pacific coast of Washington. *Harmful Algae* 9: 264-271.
- Feely, R.A., *et al.* 2008. Evidence for upwelling of corrosive "acidified" water onto the continental shelf. *Science* 320:1490-1492.
- Fisher, J.L., *et al.* 2015. The impact of El Niño events on the pelagic food chain in the northern California Current. *Global Change Biology* 21:4401-4414.
- Friedman, W.R., *et al.* 2019. Modeling composite effects of marine and freshwater processes on migratory species. *Ecosphere* 10:e02743.
- Hobday, A.J., *et al.* 2016. A hierarchical approach to defining marine heatwaves. *Progress in Oceanography* 141:227-238.
- Jacox, M.G., *et al.* 2016. Impacts of the 2015–16 El Niño on the California Current System: Early assessments and comparison to past events. *Geophysical Research Letters* 43:7072–7080.
- Jacox, M.G., *et al.* 2018. Coastal upwelling revisited: Ekman, Bakun, and improved upwelling indices for the U.S. west coast. *Journal of Geophysical Research: Oceans* 123:7332-7350.
- Jepson, M. and L.L. Colburn. 2013. Development of social indicators of fishing community vulnerability and resilience in the U.S. Southeast and Northeast Regions. NOAA Tech. Memo. NMFS-F/SPO-129.

- Kasperski, S., and D.S. Holland. 2013. Income diversification and risk for fishermen. *Proceedings of the National Academy of Sciences of the United States of America* 110:2076-2081.
- Keister, J.E., *et al.* 2011. Zooplankton species composition is linked to ocean transport in the Northern California Current. *Global Change Biology* 17:2498-2511.
- Kuriyama, P.T., *et al.* 2019. Catch shares drive fleet consolidation and increased targeting but not spatial effort concentration nor changes in location choice in a multispecies trawl fishery. *Canadian Journal of Fisheries and Aquatic Sciences* 76:2377-2389.
- Lefebvre, K.A., *et al.* From sanddabs to blue whales: the pervasiveness of domoic acid. *Toxicon* 40:971-977.
- Leising, A.W., in prep. Marine heatwaves of the North East Pacific from 1982-2019: a Blobtrospective. For submission to *Journal of Geophysical Research: Oceans*.
- Lindgren, F., and H. Rue. 2015. Bayesian spatial modelling with R-INLA. *Journal of Statistical Software* 63(19):1-25.
- McCabe, R.M., *et al.* 2016. An unprecedented coastwide toxic algal bloom linked to anomalous ocean conditions. *Geophysical Research Letters* 43:10366-10376.
- McKibben, M., *et al.* 2017. Climatic regulation of the neurotoxin domoic acid. *Proceedings of the National Academy of Sciences* 114:239-244.
- Melin, S.R., *et al.* 2012. California sea lions: an indicator for integrated ecosystem assessment of the California Current system. *CalCOFI Reports* 53:140-152.
- Miller, R.R., *et al.* 2019. Distribution of pelagic thaliaceans, *Thetys vagina* and *Pyrosoma atlanticum*, during a period of mass occurrence within the California Current. *CalCOFI Reports* 60:xx-xx.
- Peterson, W.T., *et al.* 2014. Applied fisheries oceanography ecosystem indicators of ocean condition inform fisheries management in the California Current. *Oceanography* 27:80-89.
- Reynolds, R.W., *et al.* 2007. Daily high-resolution-blended analyses for sea surface temperature. *Journal of Climate* 20:5473-5496.
- Ritzman, J., *et al.* 2018. Economic and sociocultural impacts of fisheries closures in two fishing-dependent communities following the massive 2015 US West Coast harmful algal bloom. *Harmful Algae* 80:35-45.
- Santora, J.A., *et al.* 2020. Habitat compression and ecosystem shifts as potential links between marine heatwave and record whale entanglements. *Nature Communications* 11:536.
- Thompson, A.R., *et al.* 2019a. Indicators of pelagic forage community shifts in the California Current Large Marine Ecosystem, 1998-2016. *Ecological Indicators* 105:215-228.
- Thompson, A.R., *et al.* 2019b. State of the California Current 2018-19: a novel anchovy regime and a new marine heatwave? *CalCOFI Reports* 60:xx-xx.
- Waples, R.S. 1995. Evolutionarily significant units and the conservation of biological diversity under the Endangered Species Act. *American Fisheries Science Symposium* 17:8-27.